HIGH PERFORMANCE BIOLOGICAL SENSORS BASED ON ORGANIC ELECTROCHEMICAL TRANSISTORS (OECTS)

LIAO CAIZHI

M.Phil

The Hong Kong Polytechnic University

2014

The Hong Kong Polytechnic University
Department of Applied Physics

High Performance Biological Sensors Based on Organic Electrochemical Transistors (OECTs)

LIAO Caizhi

A thesis submitted in partial fulfillment of the requirements

for the degree of Master of Philosophy

May 2014

CERTIFICATE OF ORIGINALITY

I hereby declare that this thesis is my own work and that, to the best of my knowledge and belief, it reproduces no material previously published or written, nor material that has been accepted for the award of any other degree or diploma, except where due acknowledgement has been made in the text.

_____ (Signed)

LIAO Caizhi (Name of student)

Abstract

Owing to its desirable properties, including flexible, solution-processable, low cost and versatility, organic thin film transistors (OTFTs) have emerged as a viable platform for high performance chemical and biological sensors. As an important type of OTFTs, organic electrochemical transistors (OECTs) have attracted a great deal of interest during the last few years, which could be attributed to its high stability in aqueous electrolytes and low operation voltage affordable for biological applications. OECTs based on PEDOT:PSS have shown extensive applications in chemical and biological sensors, including pH, bacteria, ions, glucose, dopamine, DNA, lactate, proteins, and cells, etc.

In this thesis, the performance of OECT based glucose sensor has been systematically investigated. It was found that the sensitivity of OECT glucose sensor could be significantly improved by co-modifying gate electrodes with graphene nano-materials (graphene or reduced graphene oxide (rGO)) and the enzyme glucose oxidase. The low detection limit of the functionalized device to glucose was down to 10 nM, which was two orders of magnitude better than that of devices without graphene modification. The optimized devices showed a linear response to a wide range glucose concentration from 10 nM to 1 mM, covering the physiological glucose range in human saliva. In addition, the selectivity of OECT glucose sensors was systematically studied for the first time. The selectivity of OECT glucose sensors could be dramatically improved by modifying the gate electrodes with

biocompatible polymers (Chitosan and Nafion). These modified polymers served as effective block layers to minimize the interfering effect from uric acid and L-ascorbic acid. Therefore, the sensitivity and selectivity of the OECT-based glucose sensors could be simultaneously improved by modifying gate electrodes.

High-performance OECT-based dopamine(DA) sensors have also been successfully fabricated. To improve the selectivity of DA sensor, the gate electrodes of OECT devices were modified with biocompatible polymers, such as Nafion and Chitosan. Additionally, the sensitivity of OECT based DA sensors could be further improved by the modification of graphene nanomaterials(graphene and reduced graphene oxide (rGO)) on the gate electrodes. The DA sensors functionalized with Nafion and graphene materials showed a detection limit down to 5 nM, and a wide linear region from 5 nM to 1 mM with a good selectivity. Therefore, the OECT-based DA sensors hold great potential for the disposable and low-cost sensing applications in the near future.

In addition, OECT based uric acid(UA) sensors with high sensitivity and selectivity were successfully fabricated for the first time. The OECT UA sensors modified with enzyme(UOx), polyaniline (PANI) and graphene-based nano-materials(graphene sheets and reduced graphene oxide (rGO)) showed a high selectivity to UA additions. The sensors with UOx-rGO /PANI/ graphene flakes/Pt gate electrode can detect UA down to 10 nM, which was approximately 4 orders of magnitude better than that of conventional electrochemical UA sensors using the similar enzyme

electrodes. Interestingly, the devices demonstrated an excellent linear response in the range of 100 nM to 500 μM, covering the normal uric acid level in human body. Interference signals from co-existed bio-active intereferents(e.g. glucose, dopamine and ascorbic acid) were effectively blocked because of the modified polymer layers. Owing to the versatility of modification techniques, OECT devices can be further explored for various kinds of biological applications, including DNA, cells, bacteria, protein and antigen/antibody.

List of Publications

1. **Caizhi Liao**, Feng Yan, et al, Multilayer layer functionalized enzyme electrode for the high performance uric acid sensor based organic electrochemical transistors. To be submitted.
2. **Caizhi Liao**, Zhang Meng, Feng Yan. Flexible organic electronics in biology: Materials and devices. *Adv. Mater.* (Invited review, submitted)
3. **Caizhi Liao**, Feng Yan, Organic semiconductors in organic thin-film transistor-based chemical and biological sensors, *Polymer Reviews*, 53, 352-406 (2013)
4. **Caizhi Liao**, Meng Zhang, Liyong Niu, Zijian Zheng and Feng Yan, Highly selective and sensitive glucose sensors based on organic electrochemical transistors with graphene-modified gate electrodes, *J. Mater. Chem. B*, 1, 3820-3829 (2013)
5. **Caizhi Liao**, Meng Zhang, Liyong Niu, Zijian Zheng and Feng Yan, Organic electrochemical transistors with graphene-modified gate electrodes for highly sensitive and selective dopamine sensors, *J. Mater. Chem. B.* 2, 191-200 (2014)
6. Meng Zhang, **Caizhi Liao**, Yanli Yao, Zhike Liu, Fengfei Gong and Feng Yan, High-Performance Dopamine Sensors Based on Whole-Graphene Solution-Gated Transistors, *Adv. Funct. Mater*. 24, 978–985 (2014)
7. Yan, Feng, **Liao Caizhi**. Plastic fiber based organic transistor for high performance chemical and biological sensors.*US Patent.* Pending.

Acknowledgments

My study life at PolyU is full of wonderful memories. The work presented in this thesis would not have been accomplished without help and support from many people.

First of all, I would like to express my sincere gratitude to my chief supervisor Dr. YAN Feng for giving me such a wonderful opportunity to study and work on the most cutting-edge research area during the past two years. He indeed does me a great favor when I encounter problems both in work and life by providing some in-time advices. More importantly, my study would not be so smooth without his patience, encouragement, and support.

I am also grateful to the group members in the Dr YAN's group. Sincere thanks to Miss. ZHANG Meng, Mr. LIU Zhike, Mr. LIU Shenghua, Dr. YAO Yanli, Dr. LI Jinhua, Mr. YOU Peng, for their generous help and inspiring discussions. Many thanks to Mr Willy Yip, for his excellent Labview programs designed for this work and Mr. Yeung, for his hard work on the mask design and sputtering work. I would also thanks Mr. BU Chenghao and Mr. ZHU Hongwei, exchange students from Wu Han University, for their kind help and helpful discussion.

I also greatly appreciate for the useful help Dr. Albert Choy and Dr WONG Tai Lun, Terence from our department. Many sincere thanks to my colleagues, Dr XIE Yizhu,

Dr CHAI Yang, Mr ZHAO Yuda, for their useful help and discussions. I would also express my heartfelt gratitude to my roommates, for their in-time suggestions and help.

Finally, I would express my deepest gratitude to my family, for their forever love and support. Without them, I would not be able to live such wonderful life and have the choice to do what I like. It would be a great pleasure to dedicate this thesis to my family.

Table of Contents

List of Figures

List of Tables

Chapter 1 Introduction

1.1 Background

Analytical methods for the detection of specific chemical and biological species have attracted significant attention in the last few decades, a large number of high-performance sensors have emerged to shape the area of sensing technology [1]. Basically, a sensor is a device that can response to a specific quantity of targets and convert it into a readable signal which can be directly observed or recorded by an external device. Interestingly, medical diagnostics and environmental control have become the research hub of chemical sensors and biological sensors [2]. By definition, a chemical sensor normally consists of a chemically sensitive layer that unveils information of its ambient environment and a physical transducer that transforms the signal into a readable form, while a biological sensor typically incorporates with biological probe molecules, including protein, ssDNA, antibody/antigen, bacteria, etc., as the biological elements for sensing particular analytes [3].

Research on OTFT-based sensors increased rapidly in the last few years, covering a broad range of applications in chemical and biological sensing, ranging from environmental monitoring, food safety detection [4] and artificial skin[5], to biological warfare agents [3] , medical diagnostics [6] and drug delivery [7], among

which some applications are now excitingly stepping close to the real life. These distinguished sensors afford to detect extremely low concentrations of target analytes with enhanced sensitivity and selectivity, by simply manipulating the molecular structure and morphology of organic active materials. Furthermore, active materials used could be covalently integrated with recognition elements, providing highly specific interactions with given analytes [8].

OTFTs can be divided into two primary categories, i.e., organic field-effect transistors (OFETs) and organic electrochemical transistors (OECTs) (Figure 1.1), principally based on the difference in device structure and operation principles [9]. The performance of OFET device is significantly affected by the features of dielectric/insulator interface and grain boundaries in semiconductors. Consequently, OFET-based sensors are able to detect the target analytes according to the chemical/physical changes of organic semiconducting layer induced by the external stimulis [10]. The functionalities of OFET-based sensors can be readily tailored via surface engineering [11]. Different from the OFET-based sensors, OECT sensors show some desirable properties. Firstly, OECTs normally operate with a much lower working voltages (typically less than 1 V), which could effectively prohibit the hydrolysis of electrolyte during operation. More importantly, OECT-based sensors can be operated in aqueous electrolytes that are essential for the practical real-time chemical and biological sensing applications [12]. In addition, the fabrication process of OECTs is much easier due to its simple structure, in which the active layers and gate electrodes could be separately fabricated in different substrates

[13]. The above properties make OECTs to be easily integrated with complex systems, such as high throughput sensor arrays or microfluidic channels. Therefore, OECT devices hold great potential for the high performance detection of biological elements.

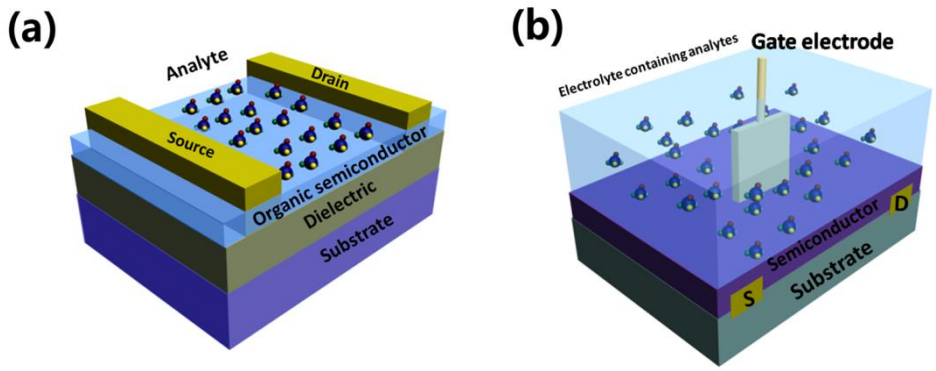

Figure 1.1 Schematic structures of (a) an OFET-based sensor and (b) an OECT-based sensor [14].

1.2 Objectives of Research

Although several different methods have been developed for particular sensing applications, such as spectroscopy, cyclic voltammetry, chromatography, etc., the testing is either laborious or expensive. Due to its high sensitivity, versatility and small size, thin film transistors (TFTs) based sensing methods have attracted increasing interest and emerged as a feasible tool for sensor technology. Organic thin

film transistors(OTFTs), which can be conveniently prepared by cost-effective solution processes, far outweigh its counterparts based on silicon, carbon nanotube, graphene, or oxide semiconductors. More interestingly, OECT-based sensors can exhibit extremely high sensitivity and selectivity toward target analytes by the proper modification of working electrodes and interfaces. Therefore, OECT based devices serve as a promising platform for the disposable and high-performance sensors [15].

There are two major objectives in this thesis:

1. To optimize the performance of already existed OECT based biological sensors, i.e,. glucose sensor and dopamine (DA) sensor. The sensitivity and selectivity of OECT based sensors are expected to be simultaneously improved by co-modifying the gate electrodes with enzymes, biocompatible polymers and graphene materials.

2. To explore the novel applications of OECT based devices in biological sensing applications. The OECT devices with UOx-GO /PANI/ graphene flakes/Pt multilayer gate electrode hold great potential for high performance uric acid detection, which has not been reported previously.

1.3 Outline of Thesis

The chapters of this thesis are organized as follows:

Chapter 1: Introduction. In this chapter, the background of OTFT based biological sensors is firstly introduced. Then the objectives and outline of this thesis are introduced.

Chapter 2: Overview of organic electrochemcial transistor (OECT) based chemical and biological sensors. In this chapter, the work on OTFT sensors are systematically reviewed and classified according to sensor types.

Chapter 3: Highly selective and sensitive glucose sensors based on organic electrochemical transistors with graphene-modified gate electrodes. In this chapter, the sensitivity and selectivity of PEDOT:PSS based OECTs glucose sensors are systematically studied using the biocompatible polymers, graphene materials (graphene or reduced graphene oxide (rGO)) and glucose oxidase co-modified gate electrodes.

Chapter 4: Organic electrochemical transistors with graphene-modified gate electrodes for highly sensitive and selective dopamine sensors. In this chapter, high-performance OECT-based dopamine(DA) sensors have also been successfully fabricated using the Nafion and graphene flakes co-modified electrode.

Chapter 5: Multilayer functionalized enzyme electrode for high performance uric acid sensor based organic electrochemical transistors. In this chapter, PEDOT:PSS based OECT devices with enzyme, polyaniline and graphene-based materials modified on the surface of Pt gate electrode demonstrated high performance for UA sensing .

Chapter 6: Conclusions and future outlook. In this chapter, this thesis is summarized and personal perspective for the future of OECT based devices is proposed.

Chapter 2 Overview of Organic Electrochemical Transistors based Chemical and Biological Sensors

2.1 Introduction

In this chapter, we will review the chemical and biological sensors based on OECTs. The first part of this review is devoted to a brief introduction on the materials used in the OECT devices, then sensors based on OECTs grouped by their specific applications are discussed in details. Older seminal work shapes the development of this field are also reviewed. The chapter is mainly focusing on the OECT based chemical and biological sensors. Therefore, most of previously inspiring works on gas sensors, chemical vapor sensors, optical sensors, etc., will not be reviewed in this paper.

2.2 Materials of OECTs based Sensors

Since the ground-breaking discovery in highly conductive polyacetylene in 1970s [16], conductive organic semiconductors develop rapidly in the last few decades and has already become the versatile “rising-star” material both for academic and industry. As the futuristic materials for the manufacturing of emerging organic electronics, organic semiconductors have emerged as a promising competitive

material for conventional inorganic semiconductors such as silicon. One particular feature distinct from inorganic-based semiconducting material, the chemical and physical properties of organic semiconducting material could be easily manipulated by the adoption of differentiated molecular structures(either/both in molecular backbone or/and functional groups) or just tailoring the physical parameters of processing(film thickness, annealing temperature and time, etc.), to meet the specific requirements of particular application [17]. Owing to the versatility of organic semiconductors, this kind candidate material serves as a brand new essential element for the further development of electronic devices. Significant effects are made by chemists to create a large family of π-conjugated conducting materials, most typically including polypyrrole, polyaniline and polythiophene, etc,. (Figure 2.1) More interestingly, such kind organic semiconducting materials have successfully been used in the state-of-art organic electronics, ranging from organic photovoltaic devices (OPVs) [18], organic light-emitting diodes (OLEDs) [19], to organic thin-film transistors (OTFTs) [20].

Compared with their inorganic counterparts, organic semiconductors (normally including polymer semiconductors and small molecule organic semiconductors) can be easily prepared via low-cost conventional processing conditions. Most inorganic semiconductors based electronic devices require stringent and strictly controlled environments. Normally, high-purity crystalline substrates should be processed in a ultraclean room equipped with expensive facilities, including magnetic sputtering system, inductively coupled plasma (ICP) etching system and reactive ion

etching (RIE), etc,. In contrast, organic electronics can be readily prepared by solution-processable techniques (polymer semiconductors) or thermal evaporation (small molecule organic semiconductors) at low temperatures, which enables the use of wide range of low-cost substrates, including normal glass, flexible plastics, metal foils, clothing and even papers [21]. As one kind of most studied alkyl-substituted polythiophenes, poly(3-hexylthiophene) (P3HT) demonstrates excellent solubility in a variety of organic solvents, enabling the ease fabrication process by conventional solution processable techniques, including spin coating, screen printing and inkjet printing, etc,. [22]

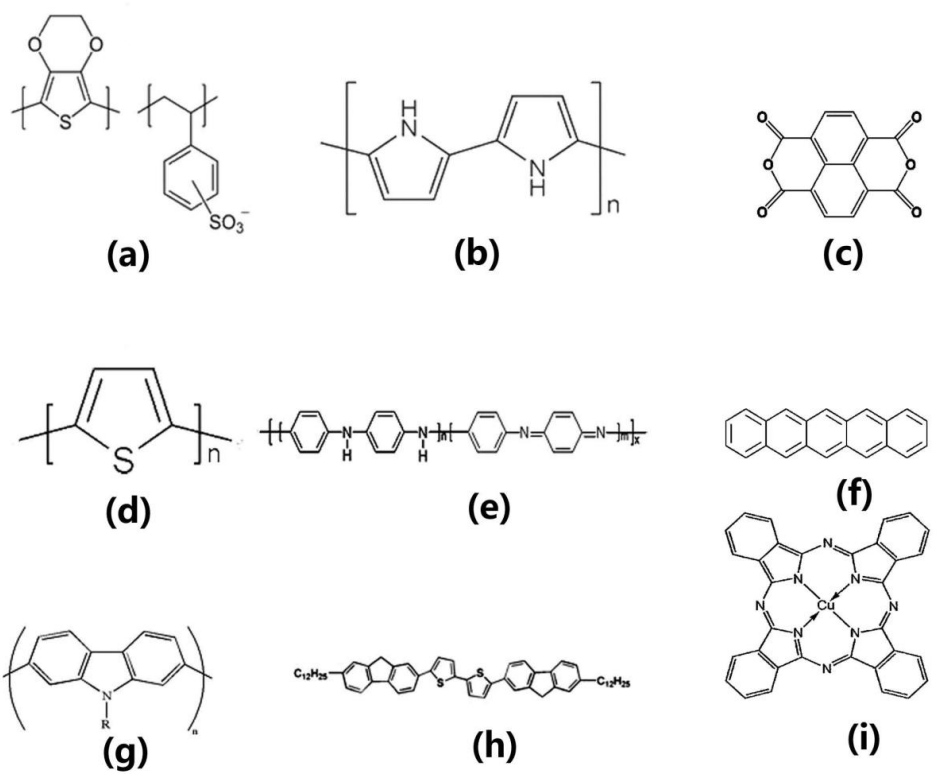

Figure 2.1 Chemical structures of the organic semiconductors commonly used inOTFT-based sensors.(a) Poly(3,4-ethylenedioxythiophene):poly(styrene sulfonic acid) (PEDOT:PSS). (b) Polypyrrole.(c) 1,4,5,8-naphthalene-tetracarboxylicdianhydride (NTCDA). (d) Poly(3-hexylthiophene) (P3HT).(e) Polyaniline. (f) Pentacene.

(g) Polycarbazole. (h) 5,5_-bis-(7-dodecyl-9H-fluoren-2-yl)-2,2'-bithiophene (DDFTTF). (i) Copper phthalocyanine (CuPc).

Organic semiconductors normally can be divided into two types: p-type semiconductors with electron-donating groups involving the high highest occupied molecular orbital (HOMO) levels and n-type semiconductors with electron-accepting ones involving the HOMO levels. Both type semiconducting materials are mostly in conjugated molecular structures and exhibit similar electronic and optical properties to that of inorganic semiconductors [23]. Also, organic semiconductors can be classified as two major families: polymer semiconductors and small molecule organic semiconductors, based on the molecular backbones and structures. Polymer semiconductors contain a long π- conjugated backbone with side chains that could increase the solubility in solvents. Therefore, semiconducting polymer-based devices can usually fabricated by solution processable processes. Primarily due to their extremely high electrical conductivity, some kind of conjugated polymers are also referred as "synthetic metal" [24]. Small molecule organic semiconductors can normally form ordered crystal structures, leading to a carrier mobility comparable to or even higher than that of amorphous silicon [25]. Small molecule based organic devices can be fabricated by thermal evaporation at low temperature and thus enable the high throughout fabrication processes [26]. Distinct from their polymer counterparts, small molecule organic semiconductors exhibit some distinguished features, such as high purity, strictly controlled molecular structure and well-defined molecular-weight [27]. However, for the electronics associated with the interfacing world of biology, conducting polymers are far more utilized than small organic

molecules. Biological system is an aqueous environment in which ion flux carries significant amount of information and regulates the life processes. The mixed ionic and electronic transport ability makes conducting polymers the ideal communication channel bridges the worlds of electronics and biology [28]. Therefore, the afterward-mentioned organic semiconductor materials and organic bioelectronics are mostly refereed to the conducting polymers. The most-commonly used polymers in OECT devices are concluded as follows:

2.2.1 PEDOT

One of the most studied conjugated polymers is the p type poly(3,4-ethylenedi oxythiophene) (PEDOT). PEDOT material exhibits extremely high conductivity, excellent stability in a wide range of pH and commercially available in the market [29], all of which make it the candidate material for numerous applications, such as TFTs [30],sensors [31], memories [32], displays [33], etc. As pristine PEDOT is insoluble, high-molecular-weight counter-ion, including poly(styrene-sulfonate) (PSS) and p-toluenesulfonate (TOS), are usually used to achieve a stable solution-processable dispersion of PEDOT. The conductivity of PEDOT was ranged from 1 to 300 S/cm, depending on the doping level and the counter-ion used [34].

2.2.2 Polyaniline

Primarily due to its high electrical conductivity, excellent biocompatibility and good stability in electrolytes, polyaniline(PANI) has attracted the great attention of the research community [35]. Normally, polyaniline materials consist of three idealized

oxidation states as shown in Figure 2.2, including leucoemeraldine, emeraldine and (per)nigraniline, among which emeraldine base demonstrate the highest conductivtity at room temperature and is regarded as the most important type of polyaniline for practical sensing applications. Importantly, the conductivity of polyaniline for a specific application could be easily obtained by fine tuning the chemical states of the material. In addition, polyaniline has desirable processing properties, making it possible to be processed by the inexpensive and conventional solution processable methods. The potential utilization of polyaniline is in transparent conductors, electrochromic coatings and chemical/ biological sensors, etc.

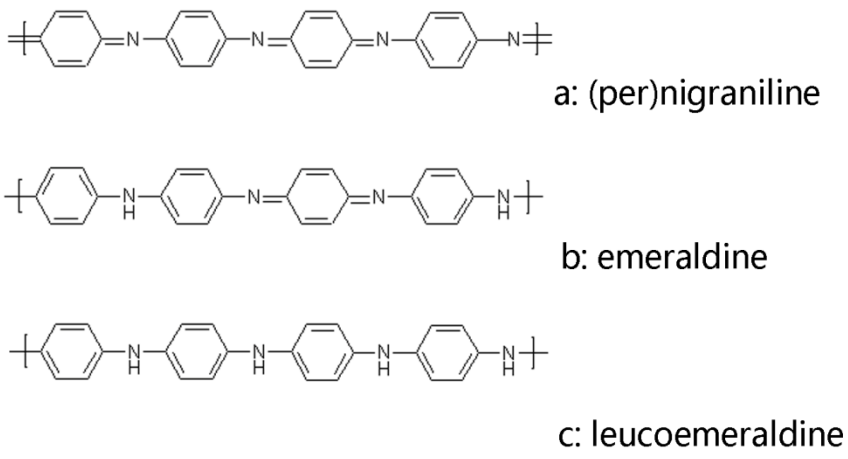

Figure 2.2 Three oxidized states of polyaniline.

2.2.3 Other type semiconductors

Polypyrroles: Basically being a polyacetylene derivative, polypyrroles are rigid-rod polymer show high conductivity. The so-called organic electrochemical

transistor (OECT) using polypyrroles as the active material of transistor could be traced back to the early 80s by Wrighton et al. [36]

Poly(3-methylthiophene): As a type of polythiophene material, poly(3-methylthiophene) was extensively studied and used in organic electronics [37]. Compared with polythiophene, conductivity was increased by 3 to 4 orders of magnitude when a methyl group was introduced into the backone.

Polycarbazole: As an aromatic conjugated polymer material containing nitrogen atom, polycarbazole shows some potential for biological sensing applications, due to its relatively high conductivity approximately 1.4×10^{-4}S/cm.

2.3 Sensors Based on OECTs

2.3.1 Working Principle of OECTs

The operation mechanism of PEDOT:PSS was systematically investigated by Bernards et al. [38].Cations in electrolyte could be injected into PEDOT:PSS layer to de-dope the semiconductor when a positive gate voltage was applied, resulting in a decreased channel current. To further elucidate the underlying transient behavior of OECT devices, OECTs were divided into two fundamental circuits, i.e., electronic circuit and ionic circuit. According to Ohm's Law, electronic transport was decided by the mobility and density of holes. The ionic transport, however, was closely related to the ionic charges existed in electrolyte. The channel current was proposed as follows[39]:

$$I_{DS} = \frac{q\mu p_0 tW}{LV_P}\left(V_P - V_g^{eff} + \frac{V_{DS}}{2}\right)V_{DS} \qquad |V_{DS}| << |V_P - V_g^{eff}|$$

$$V_P = qp_0 t / C_i$$

$$V_g^{eff} = V_G + V_{offset}$$

Among which V_p is pinch-off voltage, V_g^{eff} is effective gate voltage, q is electric charge, μ is hole mobility, p_0 is the initial hole density in the conducting polymer film without any gate voltage applied. t is the thickness of active layer. W and L are the channel width and length, respectively. C_i is the effective per unit area capacitance of transistor, and V_{offset} is the parameter determined by the potential drops both at gate/electrolyte interface and electrolyte/channel interface [40].

2.3.2 Chemical Sensors

2.3.2.1 Humidity Sensors

Nafion, as one of the most commonly studied proton conducting material, has already been exploited in sensing areas [41]. Nilsson et al. [13] demonstrated a flexible OECT based humidity sensors inexpensively manufactured by printing the commercially available PEDOT:PSS on fine paper and thin polyester foils. The PEDOT:PSS active layer were patterned to act as the source, drain and gate electrodes, and active channel layer as well. Then Nafion layer as the solid-state electrolyte was deposited to cover the channel area and gate electrode. The conductivity of Nafion was closely related with the humidity level of ambient environment, therefore the variation in humidity will introduce a corresponding

change of electrolytes' conductivity up to several orders of magnitude, which in turn modifies the reduction level of PEDOT:PSS active layer when a positive gate voltage was applied. They reported that the current of OECT based humidity sensor exponentially decreased (approximately two orders of magnitude) when the tested humidity level increase from 40% to 80% (Figure 2.3). This report proved the fruitful use of OECTs as the practical humidity sensors in our daily life.

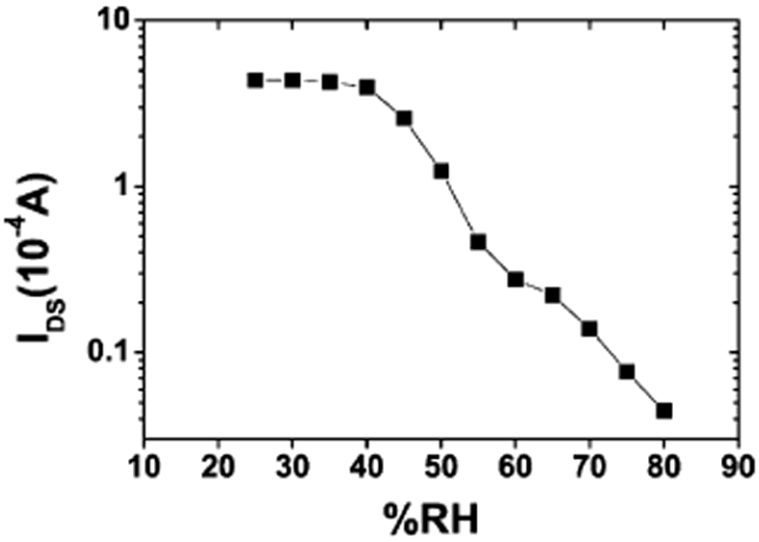

Figure 2.3 The current response of the OECT device to the variations of humidity level [13].

2.3.2.2. Ion Sensors

Rapid tracing metal analysis or determination of inorganic ions in clinical analysis is of critical importance. OECT device has emerged as a new platform for highly sensitive and selective ion sensors and shape the development of inexpensive,

disposable and high-performed devices. A high selective Ca^{2+} PEDOT:PSS based OECT sensor has been reported by Berggren et al. [42]. Upon the application of small gate voltage(V_g = 0.15V), this type Ca^{2+} sensor could be able to detect low level Ca^{2+} with a detection limit down to 10^{-4} M. The high selectivity toward Ca^{2+} detection was achieved by coating a thin layer of ionophore-based solvent polymeric membrane, which was composed of 2-nitrophenyl octyl ether, poly(vinyl chloride), potassium tetrakis(4-chlorophenyl)borate, and N,N,N,N -tetracyclohexyl-3-oxapentanediamide, onto the top of PEDOT:PSS channel.

Furthermore, Bernards et al. [43] incorporated an OECT device with biological recognition components to distinguish monovalent and divalent cations in solutions. The biological elements used in this study was a bilayer lipid membrane (BLM) coupled with Gramicidin, forming an ion-channel only permeable to monovalent cations, instead of polyvalent cations or anions. The gating effect of OECT could be significantly suppressed when the BLMs was formed, even when a gate voltage larger than 0.1 V was applied. However, the incorporation of gramicidin seemed to be able to restore the gating effect and rendered membrane the sensitivity to monovalent cations. The conductivity of PEDOT:PSS layer was significantly changed when a small gate voltage was imposed in KCl electrolyte solution. However no obvious modulation was observed when $CaCl_2$ electrolyte solution was tested. Those results further confirmed that the integration of ionophore proteins into BLMs enable the high selectivity for monovalent ion identification. This concept provides great possibilities for accurate sensing applications.

To achieve high selectivity, Mousavi et al. [44] also incorporated OECT based on PEDOT:PSS with K^+, Ca^{2+}, and Ag^+-selective ionophore-based solvent polymeric membrane. Highly selective and sensitive K^+, Ca^{2+}, and Ag^+ sensors were fabricated. The detection limits toward K^+, Ag^+, and Ca^{2+}were 10^{-4} M, 10^{-5} M, and 10^{-4} M, respectively. More interestingly, PEDOT:PSS active layer itself could served as the Ag^+-selective membrane for the detection of Ag^+ in solution, primarily due to the spontaneous oxidization of PEDOT:PSS in Ag^+ solution.

Later, Yan et al. [45] systematically study the ion-sensitive mechanism of OECT based on PEDOT:PSS (Figure 2.4). The device was characterized in several electrolyte solutions, such as like H^+, K^+, Na^+, Ca^{2+}, and Al^{3+} solutions. Similar results were achieved in different solutions. They demonstrated that the transfer curves shifted to a lower gate voltage when the cation concentration of electrolyte was increased, and a universal curve was obtained by horizontally scaling the curves, both of which could be explained by Nernstian relationships between gate voltage shifts and ion concentration. In addition, different gate electrodes, including Ag/AgCl, Pt, and Au, were further used to study the transfer characteristics of device. Interestingly, they found that the ion-sensitive properties of device were largely affected by the gate electrode. The devices with Pt or Au gate electrodes demonstrated higher ion sensitivities than the case of Ag/AgCl electrode was used. They concluded that the shift of gate voltage of OECT device with an Ag/AgCl gate electrode demonstrated Nernstian relationship to the cations concentrations, however not for the devices with Pt or Au gate electrodes. The devices could be used to detect

metal ions down to 10^{-6} M. Based on this work, enhanced OECTs could be fabricated by optimizing the physical parameters of devices.

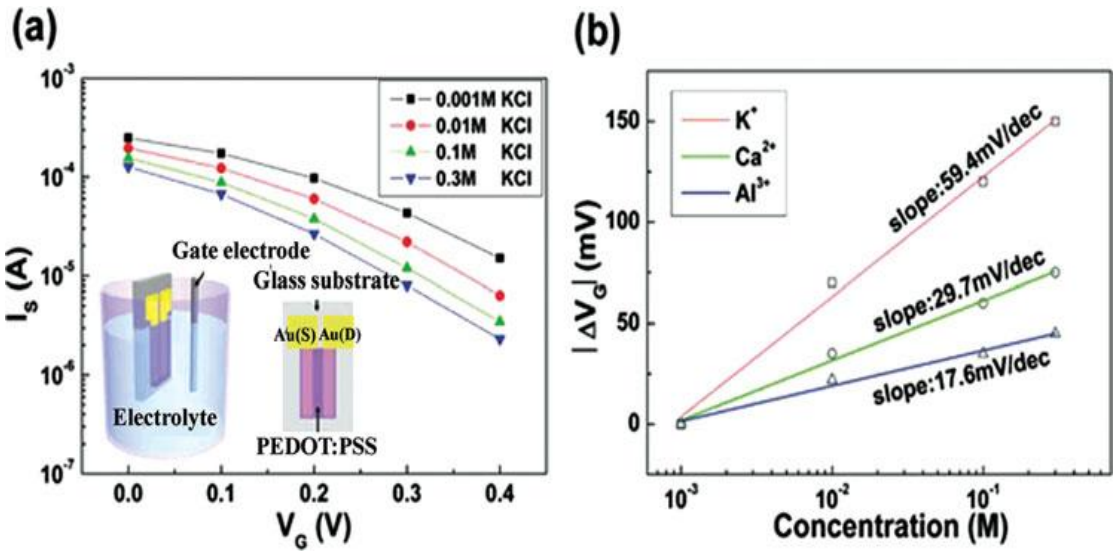

Figure 2.4 (a) Transfer characteristics of a PEDOT:PSS-based OECT measured in KCl solutions with different concentrations. Inset: schematic of the device. (b) OECT response $|\Delta V_G|$ as functions of the concentrations of metal cations in the solutions of KCl, $Ca(NO_3)_2$ and $Al_2(SO_4)_3$ [45].

Tarabella et al. [46] reported a similar result when PEDOT:PSS based OECTs with different gate electrodes were characterized. They demonstrated that the device with Ag gate can more effectively modulate the channel current than that of device with a Pt gate electrode. The distinct responses were due to the different gate electrode effects in solution. The OECT with Ag gate electrode was operated in the Faradic regime, nearly no gate voltage was dropped at the electrolyte/gate electrode interface. While for the OECTs with Pt gate electrode, the device was in operated within the no-Faradic regime, gate voltage applied on the electrolyte/semiconductor interface

was greatly reduced, leading to a smaller modulation of channel current.

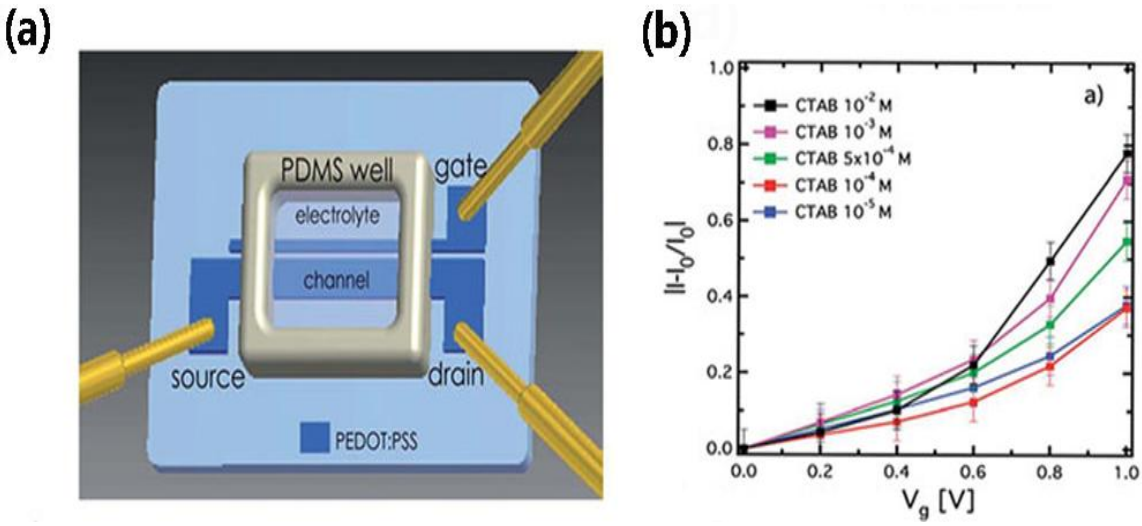

Figure 2.5 (a)Schematic of the OECT device indicating the electrical contacts. (b) Channel current response $|(I - I_0)/I_0|$ as a function of gate voltage V_g characterized in different CTAB concentrations[47].

Tarabella et al. [47]then investigated the specific effects of electrolyte on OECT performance. Planar OECTs based on PEDOT:PSS were fabricated by the lithographic patterning process. Micelle-forming cationic surfactant cetyltrimethylammonium bromide (CTAB) was used as the electrolyte for characterization. When the CTAB concentration was lower than its critical micellar concentration (CMC, approximately 10^{-3} M at 298 K), the channel current remains stable even when the CTAB level was changed, as shown in Figure 2.5. While if the CTAB concentration was higher than the CMC point, the channel current was dramatically shifted. These results clearly demonstrated that positively charged CTA^+ micelles (above CMC point) can de-dope the PEDOT:PSS layer more

effectively than that of CTA^+ dissociated ions (below CMC point). This work extended the sensing applications of OECTs by demonstrating the possibility of rapid detection of micelles formation.

More recently, Tarabella et al. [48] presented an interesting work by testing the saline in human sweat. The OECT sensors were fabricated on a single natural cotton fiber deposited with PEDOT:PSS, using a simple Ag wire as the gate electrode. Stable and reproducible results were achieved. The sensing mechanism was depended on the redox reaction between ions in solution and Ag gate electrode. The devices were competent for effective NaCl concentration detection in the range of 10^{-1}-10^{-4} M (Figure 2.6). The role of gate voltage was also investigated. Importantly, a small gate voltage as low as 0.2 V was already able to differentiate the different concentrations of NaCl. This device holds great potential for salts sensing in physiological conditions.

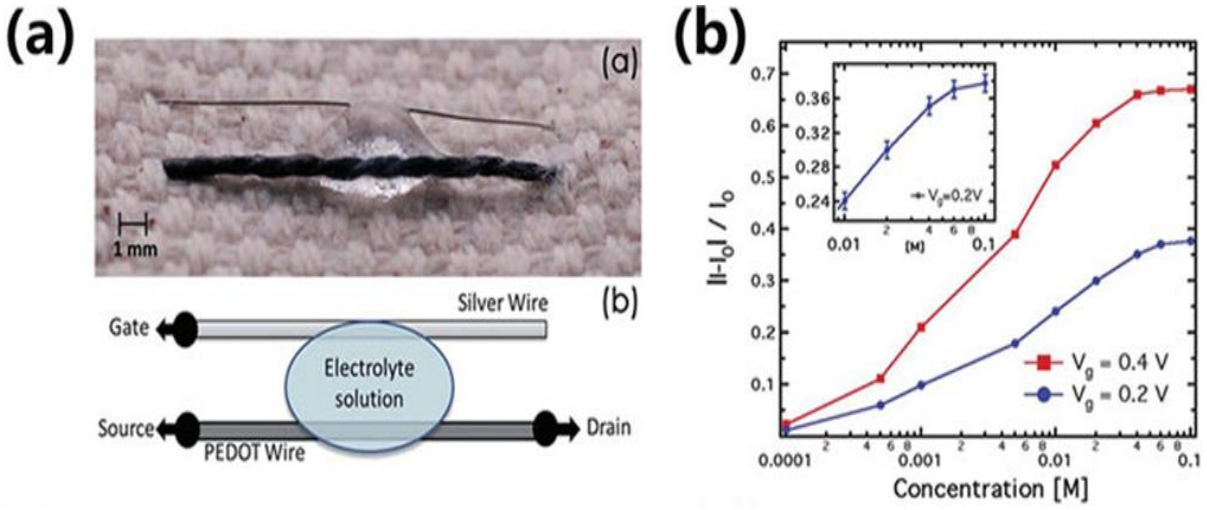

Figure 2.6 (a) Schematics of the OECT based on cotton functionalized with PEDOT. (b) Normalized transistor response $|(I - I_0)/I_0|$ as a function of the salt concentration with different gate voltages [48].

2.3.2.3. Polyelectrolyte Sensor

Polymeric material plays a pivotal role in the drug delivering system. S. Iannotta et al. [49] explored the application of OECTs in the determination of polyelectrolyte polymeric shells. OECT sensors made of PEDOT: PSS were used to detect poly (acrylic acid) (PAA) and poly (allylamine hydrochloride) (PAH), which were typically used to functionalize the nanoparticles for drug delivery systems. The detection systems were realized by means of an automatic syringe controlled by the micro-positioning system. A PDMS vessel was attached to glass slide to create a chamber. They found that the modulation of channel current was reduced upon the addition of negatively charged PAA, and increased PAA concentration will further decrease the response of sensors. While the positively charged PAH have no visible effect on the modulation of channel current. The different responses toward PAA

and PAH could be explained by the distinct interactions between the polymeric chain and the ions presented in $CaCl_2$ solutions. They further reported that gold nanoparticles (NPs) modified with PAA could also affect the performance. The devices showed a lower detection limit when gold nanoparticles was modified with PAA molecule. This result could be explained by the fact that more than one polymeric chains were attached onto a single NPs, resulting in a higher response than that of polymer alone. This idea hopefully provides us the possibilities to discriminate different polymeric shells, and more significantly, to determine the quantity of polymer shell materials already attached on the surface of nanoparticle.

2.3.3 Biological Sensors

2.3.3.1 Glucose Sensors

Malliaras's group has extensively investigated the OECT based glucose sensors, which open the door for a series of elegant studies on the successful utilization of OECTs in chemical and biological sensing. Zhu et al. [50] demonstrated that the OECT based sensors were competent for glucose sensing at neutral pH. PEDOT:PSS layer was patterned as the active channel, source, and drain electrodes by spin-coating, and Pt wire was used as the top gate electrode. The application of gate voltage will induce a small decrement of channel current, even when GOx alone was added into the solution. However, a dramatic modulation of I_{ds} was displayed upon the addition of glucose in GOx containing solution. This could be explained by the fact that the OECT devices were sensitive to the peroxide generated by GOx. The oxidation of peroxide occurred on the surface of Pt gate electrode, to maintain charge

balance, PEDOT was reduced to the neutral state, resulting in a much decreased value of channel current (Fig 2.7). Then Macaya et al. [51] demonstrated that OECTs able to detect glucose down to micromolar concentration, which was sensitive enough for the clinical determination of glucose level in human saliva. The glucose detection limit of the sensors was 1μM. They also reported that the performance of devices was greatly influenced by the gate voltage. The mechanism of sensing was related with the oxidation of H_2O_2 at the gate electrode. This work holds great potential for non invasive glucose detection technology in clinical analysis.

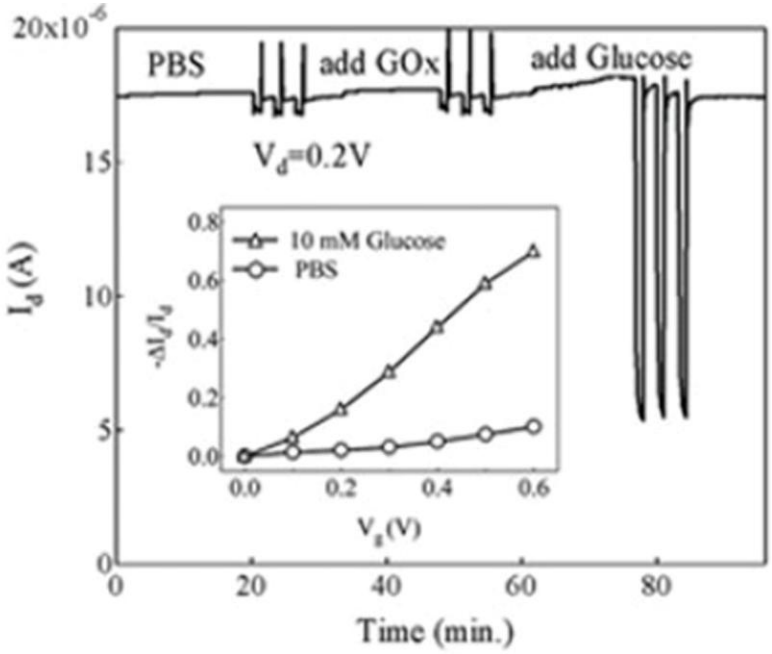

Figure 2.7 Sensing response as a function of time in PBS solution. Inset: relative changes of I_{DS} vs. V_g for two solutions [50].

To understand the underlying sensing mechanism of OECT devices, Bernards et al. [39] systematically investigated the device physics of OECT glucose sensor (Figure 2.8). A universal curve describing device operation was established. The PEDOT:PSS-based OECT with Pt gate electrode was characterized in PBS solution containing GOx. A poly(dimethylsiloxane) (PDMS) well was used to define the transistor channel and fill the electrolyte. Due to the de-doping of PEDOT:PSS, channel current decreased with applied gate voltage. The conductivity of organic semiconductor layer was dramatically decreased with the addition of glucose. The transfer curves (I_{DS} *VS* V_G) of OECTs could horizontally shift to lower gate voltages upon the introducing of glucose, which was largely dependent on the concentration of glucose. The sensing mechanism could be given by Nernst equation:

$$V_g^{eff} = V_g + (1+\gamma)\frac{kT}{2e}\ln[H_2O_2] + const$$

in which $[H_2O_2]$ is the concentration level of hydrogen peroxide in solution, Vg^{eff} is the effective gate voltage of OECT device; γ is the ratio between the capacitances of channel and gate. H_2O_2 was generated by glucose oxidization at the Pt gate electrode, inducing Faradic current flow near the interface of electrolyte/Pt-gate. The potential drop at the interface of electrolyte/Pt-gate decreased with the increase of glucose concentration due to the increased Faradic current, thus leading to a higher voltage applied on the electrolyte/PEDOT:PSS interface. The improved understanding of sensing mechanism paves the way for the rational design of OECT based enzymatic sensors.

All-plastic OECT based glucose sensor was firstly realized by Shim et al. [52] The

source, drain, and gate electrodes, as well as the active area of transistors, were all fabricated with PEDOT:PSS material. The device displayed reliable responses to glucose level in the range of 1μM-200μM, which holds great possibility for glucose level detection in human saliva. More importantly, ferrocene could facilitate the electron transfer process between gate electrode and enzyme redox centre, resulting in a dramatically increased normalized response. The simple architecture of OECT allows the use of most commonly fabrication processes.

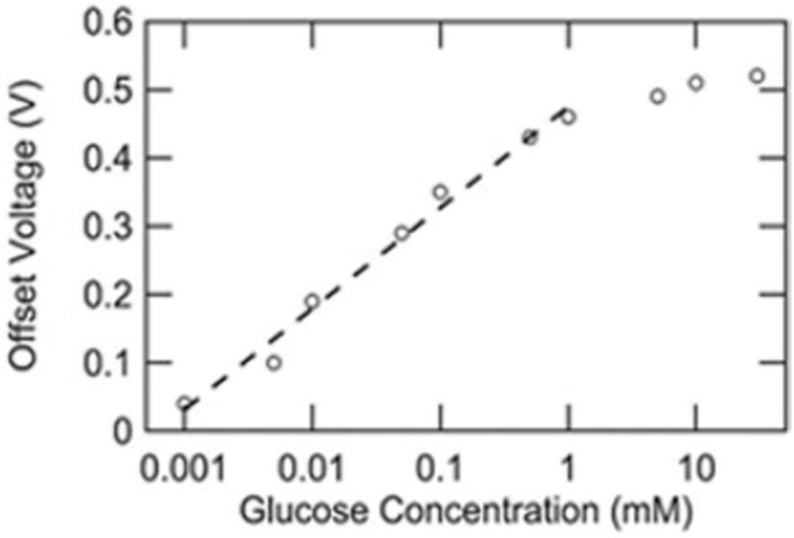

Figure 2.8 The offset voltage of an OECT *vs*. glucose concentration [39].

Cicoira et al. [40] investigated the role of geometric parameters on the PEDOT:PSS based OECT. Hydrophobic SAM perfluoro octyl trichlorosilane (FOTS) was patterned to define the electrolyte containing regions. They found that the OECT glucose sensor with smaller gate electrode demonstrated lower background signal

and higher sensitivity toward H_2O_2 detection. They concluded that most of applied gate voltage was dropped at the electrolyte/Pt gate interface when the channel/gate area ratio was set to be high, resulting in a small modulation of channel current. The modulation of channel current was tremendously improved in the presence of H_2O_2 due to Faradaic contribution. In addition, the detection limits (both minimum and maximum) of analyte seem to be insensitive to the channel/gate area ratio. The report implicated that optimized physics geometry of devices could significantly enhanced the sensing performance.

Kanakamedala et al. [53] also studied the physical properties of device by presenting an OECT fabricated by one step process using the inexpensive xurography technique. All the electrodes and channel areas were made with PEDOT: PSS. Polymer wells were attached onto substrate to accommodate solution. The proper geometric design of gate electrode and channel dimensions guaranteed a decent response for glucose detection. The device showed a pronounced I_{ds} modulation for sensing the glucose in the 1–200 mM concentration range, without incorporating any electron mediator to the active layer or solution.

Yang et al. [54] demonstrated that room temperature ionic liquid could used as the effective immobilization medium for enzyme and mediator mediator. The planar OECT device was all PEDOT:PSS based. The (tridecafluoro-1,1,2,2-tetrahydrooctyl) trichlorosilane (FOTS) monolayer was then deposited to served as the hydrophilic "virtual wells" to define electrolyte area. To functionalize the device, room

temperature ionic liquids (RTILs) containing the mediator ferrocene [bis(n5-cyclopentandienyl)iron] and enzyme glucose oxidase (GOx) was placed onto the device. During testing, glucose PBS solution was added into electrolyte. The OECT glucose sensor show enough sensitivity in a wide range of glucose levels(from $10^{-7}$to 10^{-1} M), as shown in Figure 2.9.

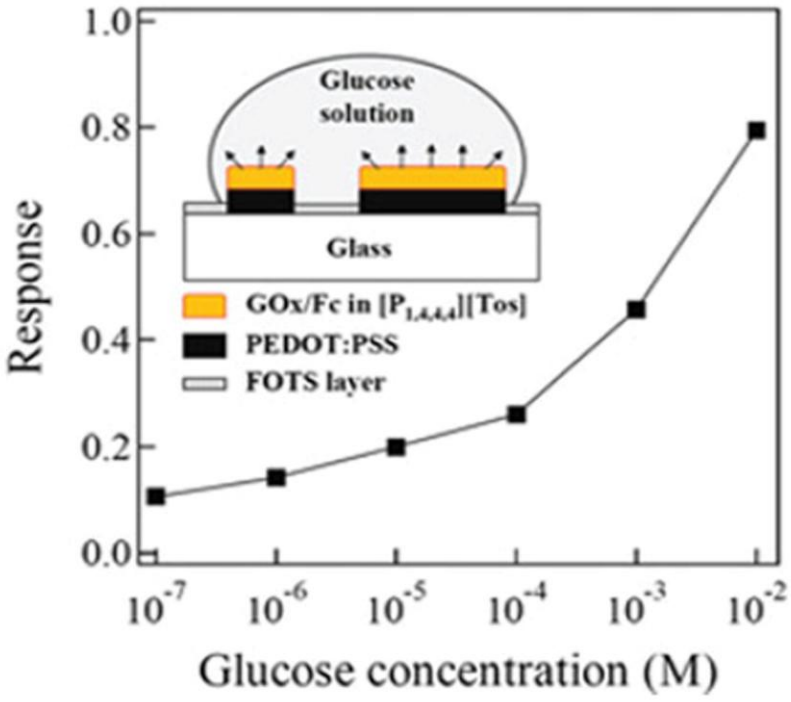

Figure 2.9 Sensing response of the OECT sensor as a function of glucose concentration [54].

Integrating OECTs with complex microfluidic systems demonstrate great possibilities for microfluidic-based chemical and biological sensors. Mabeck et al [55]. fabricated an OECT device integrated with microfluidic channel, in which the PDMS microfluidic channel was patterned on the top of PEDOT:PSS layer. The microfluidic channel not only affords to control the flowing of small sample volumes

in the system, but also serves as the gate electrode of devices. When +1 V operation voltage was applied, the channel current significantly changed up to two orders of magnitude with 10 mM Tris(hydroxymethyl)aminomethane hydrochloride (Tris-Cl) buffer solution flowing through the microfluidic channel at 0.1μL/min.

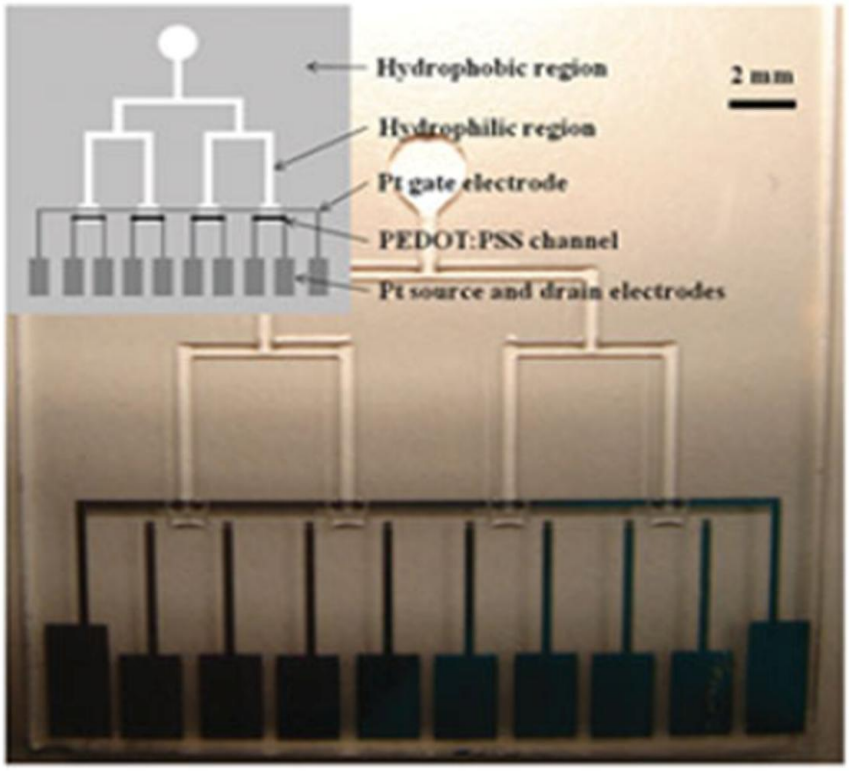

Figure 2.10 Photograph of the OECT array integrated with a surface-directed microfluidic system [56].

Yang et al. [56] also reported that the OECTs integrated with surface-directed microfluidic system could sensitively detect multiple analytes simultaneously. The sample was firstly placed on the top reservoir and began to flow along the hydrophilic channels spontaneously, finally reached the measurement reservoir

(Figure 2.10). Glucose and lactate were successfully identified and differentiated from the same sample solution by modifying the PEDOT: PSS channels with corresponded enzymes. Utilizing the same approaches, more analytes could be selectively detected simultaneously by adding several more measurement reservoirs.

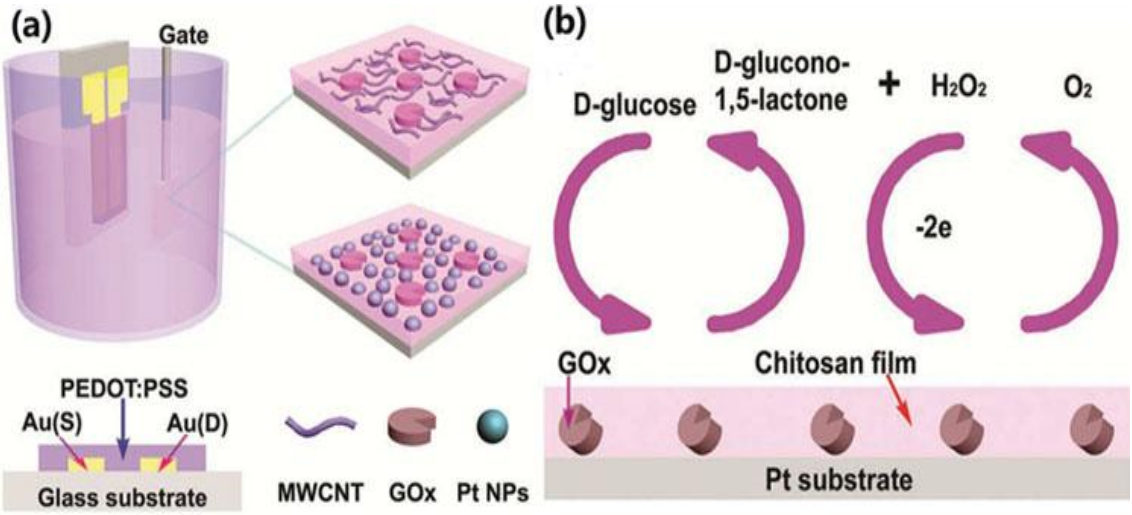

Figure 2.11 (a) The schematic of the PEDOT:PSS based OECT glucose sensor. (b) The enzymatic reaction cycle essential for the determination of glucose by PEDOT:PSS-based OECTs [57].

Most recently, our group demonstrated a highly sensitive OECT-based glucose sensor by modifying the gate electrode [57], as shown in Figure 2.11. Chitosan (CHIT), a kind of biocompatible polymers was used to immobilize GOx onto Pt gate electrode. Nanomaterials, including Pt nanoparticles (Pt-NPs) and multi-wall carbon nanotubes (MWCNTs), were also used to modify the gate electrode to improve the sensitivity of glucose sensors. The device displayed an obvious response to an

addition of 5 n M H_2O_2 using the Pt-NPs/Pt gate electrode. The enhanced sensitivity toward H_2O_2 could be attributed to the excellent electrocatalytic activity of modified Pt-NPs. More interestingly, the devices with CHIT/GOx/Pt-NPs/Pt gate electrodes exhibited a pronounced response to the addition of 5 nM glucose, which were three orders of magnitudes better than the devices without nanoparticles modified on the Pt gate. In addition, the fabricated OECT glucose sensors delivered a much better performance in comparison with conventional amperometric methods. Based on the same modifying techniques, other types of highly sensitive enzymatic sensors could be realized.

2.3.3.2 Cell Sensors

Thin film transistors(TFT) based cell sensors have attracted great amount of interests in the last few decades, with regard to its advantages in terms of high sensitivity, fabrication ease and low cost. Transistors fabricated with silicone have already been successfully used for the detection of various cells [58]. However, the essential complex facilities required for inorganic based transistors fabrication procedure strictly prohibit the development of inorganic TFT based cell based biosensors for the disposable *in vitro/in vivo* measurements. New techniques are in great needed for practical cell detection. OECT based cell sensors using PEDOT: PSS as the active layers were firstly demonstrated by Yan et al. [59] (Figure 2.12). They reported that the PEDOT: PSS based OECTs showed excellent biocompatibility and stability in culture medium. To functionalize OECT device, OECTs was firstly integrated with human esophageal squamous epithelial cancer cell

lines (KYSE30) and fibroblast cell lines (HFF1) in cell culture medium. The shifts of sensor responses could be attributed to the electrostatic interaction between cells and active transducing layer of OECT, making those devices sensitive to the changes related to the surface charge and morphology of attached cells. Due to the inherent negative charge on the surface of cells, the transfer characteristic of devices with cells attached would shift to a more positive gate voltage. They further investigated the influence of cell detachment on the performance of devices. Cancer cells could quickly detach from PEDOT: PSS layers by the treatment of Trypsin treatment. The transfer curve of device shifted to lower gate voltage for about 150 mV after the treatment (Figure 2.13). A similar phenomenon was observed using the devices integrated with fibroblast cells. More practically, the effects of retinoic acid (anti-cancer drug) on the activity of the cells were also carefully monitored. A lower value of gate voltage was obtained after the retinoic acid treatment, which could be attributed to the sensing mechanism explained above. This work developed a new transistor-based platform for the measurements of cell activities.

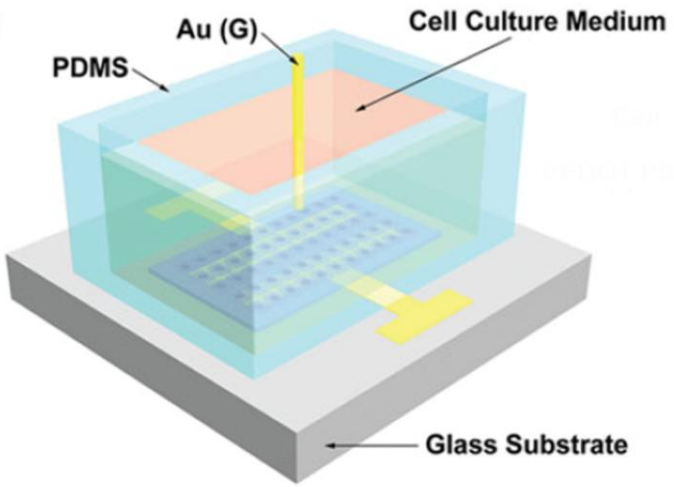

Figure 2.12 Schematic of an OECT cell sensor using PEDOT:PSS as the active layer [59].

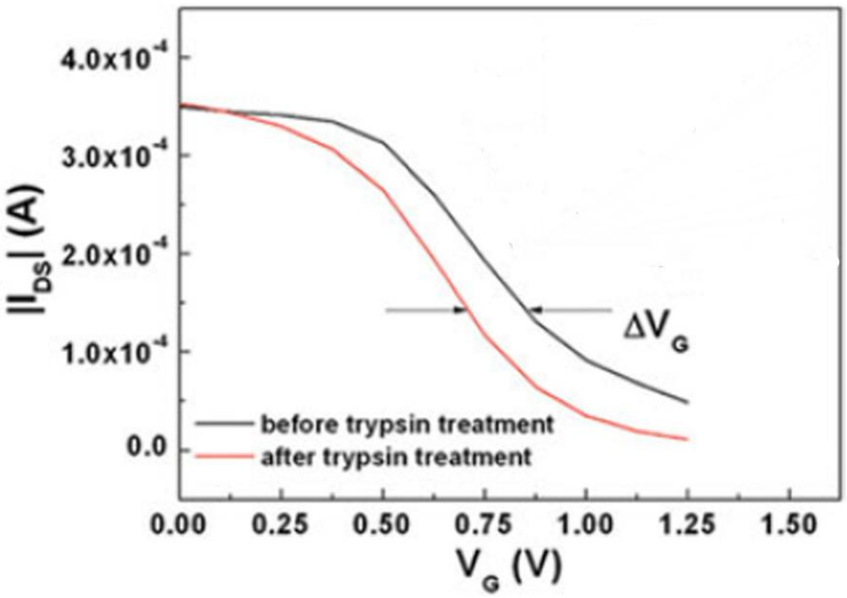

Figure 2.13 Transfer curves of the OECT with attached cancer cells before and after trypsin treatment. Inset: output characteristics of the OECT before and after trypsin treatment [59].

OECTs are suitable for miniaturization process and super-high density array integrated by the most-common solution processes, e.g, spin-coating, inject printing, et al, making them a prime candidate for the high throughout, disposable and low cost sensing applications. Microarray technology has become a candidate tool to shape the development of rapid determination of multi-analytes in the diagnostic analysis. Therefore, microarray biosensors using OECT platform are expected to play a significant role in the practical sensing applications. Recently, Yan et al.[60] fabricated the micro dimensional OECT arrays based on PEDOT:PSS. The device was fabricated by photolithography technique. In order to avoid the damages caused by the organic solvents in fabrication process, a new processing technique-physical delamination was employed to pattern the device. Compared with the conventional millimeter-sized OECTs, these micro OECTs showed faster responsibility and better stability in aqueous solution. Human hepatoma ($HepG_2$) cancer cells lines trapped by the poly(ethylene glycol) (PEG) microwells were successfully cultivated on the surface of OECTs, providing a great deal of possibilities for the cell analysis application**.**

Barrier tissues, as the essential functional interfaces in the multicellular organisms, play a significant role in the regulation of biological activities by controlling the ions concentration, nutrients, and biomolecules. The malfunction or disruption of barrier tissues in organism essential indicate the disease states [61]. Typically, permeability of a cell layer was monitored to assess the integrity of barrier tissue, which normally reveals a wealth of information about the barrier tissue function. However, present

technologies for the measurement are expensive and time-consuming. To alleviate the problems, R. M. Owens and coworkers [62] presented the OECT based devices for sensing in situ barrier tissue integrity in a more cost-effective way, as shown in Figure 2.14. The Caco-2 cells layer was firstly cultivated on Transwell membrane and incorporated into the OECT device before characterization. To improve the ion-transportation process in the tissue cell layer, H_2O_2 or ethanol was introduced to disrupt the barrier tissue integrity, which in turn resulted in a faster response of the cell sensor. They demonstrated that the sample assays showed no obvious change of the apparent permeability up to 50 mM H_2O_2 exposure and the detection limit of H_2O_2 was 1 mM. While the barrier properties began to be disrupted after a 20% ethanol (EtOH) exposure, indicating the higher sensitivity of OECTs for ethanol detection. Most recently, the same group [63] further demonstrated the capability of OECTs in barrier tissue integrity assessment. This kind work offers a new avenue for barrier tissue cell layers assessment by utilizing the OECTs based devices.

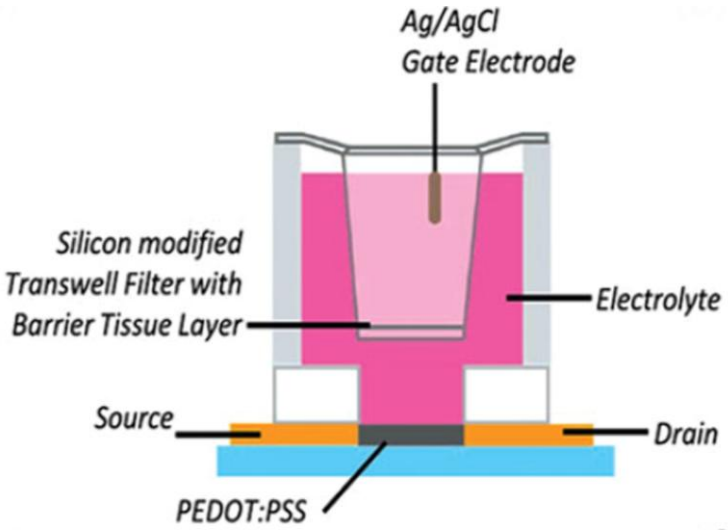

Figure 2.14 Schematic of an OECT integrated with barrier tissue [62].

Due to its excellent electrical properties, biocompatibility and processing simplicity, PEDOT doped tosylate(TOS) also offers a huge amount of possibilities for appropriate applications in biological sensing areas,. Berggrens group [64] demonstrated that OECT based device could effectively control the cell-density gradients on the surface of active channel. The Madin–Darby canine kidney (MDCK) cells were cultured on the surface of active PEDOT: TOS layer of transistor. The cell-density gradients could be precisely controlled by setting the source and gate voltages. This work is of utmost importance and paves the way for exact control of cell-density gradient characteristics in research studies.

2.3.3.3 DNA Sensors

Label-free OECT DNA sensor was firstly proposed by Krishnamoorthy and coworkers [65]. Using the same principle of antibody-antigen sensor demonstrated

by Kanungo et al. [66], they proposed that the specific coupling effect between single stranded DNA probe to its complementary DNA will form a double stranded DNA, which in turn induces a morphology change to the PEDOT layer. Since the channel current was overwhelmingly dominated by the morphological changes of transducing layer, OECT device functionalized with DNA probe show high sensitivity to its correspond complementary DNA . Single-strand probe DNA was incorporated onto the active layer during the electro-polymerization process of PEDOT. Sigmoidal response was observed when the OECT devices were exposed to the complementary ssDNA, while no detectable response was displayed when the OECT devices were exposed to the non-complementary ssDNA. The duplex formation between the probe ssDNA and complementary ssDNA was further confirmed by the fluorescence spectroscopy. The OECT DNA sensor shows a low limit down to 80 ng mL^{-1} complementary ssDNA in PBS solution. More interestingly, the sensitivity as well as the linear range of detection could be enhanced by increasing length of the ssDNA probe embedded in the PEDOT active layer.

Yan et al. [67] also developed a platform for labeling-free DNA detection based on the PEDOT: PSS type OECT devices. Interestingly, the devices were fabricated on the mechanical flexible polyethylene terephthalate (PET) substrates and incorporated with the microfluidic system, which highlight the practical sensing technique concept -“Lab on a chip”. The single strand probe DNA was immobilized on the Au gate electrode. The work function of Au gate electrode could be modulated by the

surface dipole formed by the inherent negative charge of DNA molecules, which in turn change the channel current. More importantly, no obvious differentiation in the performance of devices was observed when flexible devices bent into both sides, providing a great deal of possibility for the real point-of-care health application. Those high performance label-free DNA sensors were able to detect complementary target DNA down to 1 nM. To enhance the hybridization of DNA on gate electrode, a controlled electric field was applied and the detection limit could be further extended to 10 pM (Figure 2.15). They concluded that the controlled electric field plays an important role in regulating and assisting the immobilization and hybridization of DNA. Therefore, OECT sensors integrated in flexible microfluidic systems is a promising platform for various applications, particularly the cost-effective, high sensitive, disposable chemical and biological sensors.

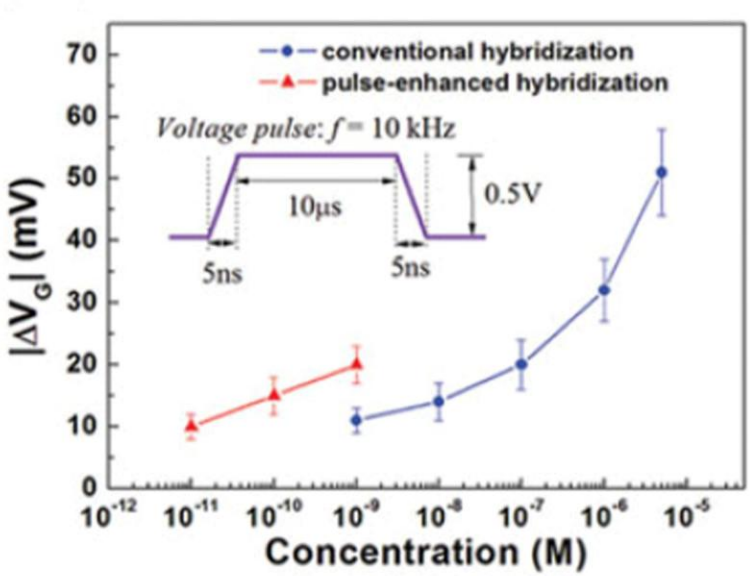

Figure 2.15 $|\Delta V_G|$ *vs.* the concentration of DNA targets in PBS solutions. Inset: the voltage pulse applied on the gate to facilitate the hybridization of DNA [67].

2.3.3.4 Antibody Sensors

OECT based sensors can potentially be used to sense analytes-receptor binding events. Owing to the physical conformation change of active organic semiconducting layer upon the coupling of analytes and receptor, the conductivity of active layer is significantly modulated, which could be simply detected by the common measurements [68].

Most enzymatic OECT sensors, like the glucose OECT based sensor detailed above, require the electron transfer process between the electrode and analytes to shift the OFF and ON states of OECT devices. In the late 1990s, Contractor et al. [68] proposed that morphology /conformation change of the active layer could also modulate the electronic conductivity of organic semiconductor. Typically the so called host-guest systems, in which one acts as a detector for the other part, were introduced to change the morphology of active layer. Depended on the specific condition, host (guest) could be either covalently modified onto the conjugated polymers (in most cases) or merely physically entrapped by the active layer. Because of the bio-specificity of binding effects in system, this kind devices display extremely high selectivity toward the target analytes. One of the most interesting binding systems is the antigen-antibody binding, which lays the foundation for the design of the effective immunosensors. In 2002, Contractor and co-workers [66] reported that antigen-antibody binding effects has been successfully used to fabricate the first reagentless OECT based immunosensor. They used PEDOT as the immobilization matrix, which was produced by electropolymerization process.

During the fabrication of those devices, different amount of goat antirabbit IgG (probe for goat antigen rabbit IgG detection) were added in the electropolymerization solution. The maximum response was achieved when the gate potential was −0.8V. They found that the increase load of goat antirabbit IgG antibody in the polymer matrix could induce an improved sensitivity of immunosensors. A detection limit down to 1×10^{-10} g/mL antigen was achieved within a response time of 3 minutes. Furthermore, they analyzed the responses of devices fabricated by physical adsorption of goat antirabbit IgG antibody via the post-polymerization process. The experiment indicated that physical entrapment of antibody in the polymer layer lead to a very weak response when the sensors were exposed to antigen analyte.

Kim et al. [69] successfully demonstrated an OECT based immunosensor for the specific detection of prostate antigen/1-antichymotrypsin (PSA-ACT) complex. In order to fabricate immunosensor, PEDOT: PSS active layer was firstly functionalized with 3-aminopropyldiethoxymethylsilane (APTMS), then treated with ProLinker molecules, PSA monoclonal antibody (PSA mAb) as the probe was finally immobilized on its surface. The detection limit to the prostate specific antigen (PSA) was down to 100 pg/mL. Negative surface charge of PSA-ACT complex will reduced de-doping effect in the PEDOT: PSS channel layer, which in turn modified the channel current. I_{DS} shifted to larger value upon the adding of PSA-ACT complex. In addition, the detection limit of PSA could be tremendously improved (up to 1 pg/mL) by the use of gold nanoparticles (AuNPs) conjugated with PSA

polyclonal antibody (PSA pAb).The electron transfer from the AuNPs-PSA pAb to the PSA-ACT complex/PSA mAb was greatly facilitated and result in a higher sensitivity to analyte, presumably due to the larger effective surface area of the AuNPs.

2.3.3.5. Bacterial Sensors

Bacterial pathogens identification plays an important role in our health condition. Conventional techniques for the bacterial pathogens analysis, *e.g*, polymerase chain reaction or enzyme linked immunosorbent assays, normally are labor-consuming and always require complicated electric equipment systems [70]. Therefore, novel techniques enable the rapid detection of bacterial pathogens are in great need. Yan et al. [71] proposed the disposable bacterial sensor based on the OECT devices for the first time (Figure 2.16). Enterohemorrhagic Escherichia coli (E. coli) O157:H7, the widespread foodborne pathogen, was tested in this work. The OECTs were fabricated on glass substrates, PEDOT: PSS conducting films were patterned on the Cr/Au (10 nm/100 nm) source and drain electrodes. Before the immobilization of the antibodies on the surface of active layer, PEDOT:PSS active layers were firstly treated with oxygen plasma and 3-glycidoxypropyl- trimethoxysilane (GPMS) toluene solution. The transfer curves of the OECT were shifted to higher gate voltage after the immobilization of E. coli O157:H7. This result could be explained by the fact that a higher gate voltage was needed to compensate the influence of negative charge from the surface of bacteria, similar to the electrostatic interaction between the cells and OECTs reported previously. Furthermore, they explicated the influence

of ionic strength of KCl on the transfer characteristics of bacteria devices. Larger transfer curve shifts were observed in the low concentrations of KCl, while no voltage shift could be observed in 10 mM KCl solutions. The device could detect bacteria concentrations down to 10^3 cfu mL^{-1} in the optimized condition. In summary, this pioneering work opens the door for extending OECTs based sensors' application to the bacterial detection area.

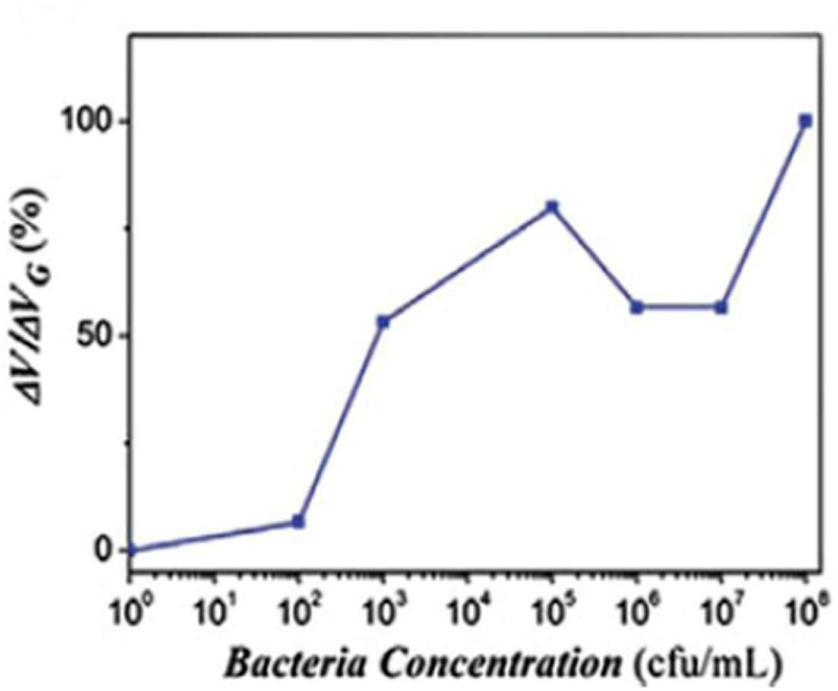

Figure 2.16 Relative gate voltage shifts of an OECT vs. bacteria concentrations [71].

2.3.3.6. Dopamine Sensors

As one kind of neurotransmitter, dopamine is of utmost importance in the whole body system. Notorious example of so-called neurodegenerative disorders is the Parkinson's disease, which is predominately caused by the dys-function of the

dopaminergic neuron process. Based on the fact that OECT devices could be operated in aqueous solutions with a high stability and a low voltage, YAN et al. [72] described an OECT based sensors for the detection of dopamine in solution for the first time. Different gate electrodes, including graphite, Au and Pt electrode, etc, were adopted for the PEDOT: PSS based OECTs. They clearly demonstrated that the gate electrode materials have a huge impact on the responses of the device to dopamine. The devices characterized at 0.6 V gate voltage using the pure Pt gate electrode showed the highest sensitivity. The detection limit of OECT sensor devices to dopamine was lower than 5 nM, as shown in Figure 2.17. Due to the electro-oxidation occurred at gate electrode upon the addition of dopamine, the effective gate voltage shifted to a higher value. Compared with the conventional electrochemical method using a similar working electrode, the detection limit was improved about two orders of magnitude. Therefore, dopamine sensors based on OECE is a viable tool for the rapid determination of dopamine in clinical studies.

2.3.3.7. Other Sensors

Lactate is an essential element for the anaerobic metabolism. Khodagholy, et al. [73]demonstrated that OECT device using the room temperature ionic liquids (RTILs) as a solid-state electrolyte able to detect the lactate. More importantly, this type sensor could be fabricated on the flexible substrates. The sensing mechanism of the PEDOT:PSS based OECTs was similar to that of previously reported OECT-based glucose sensors. The device showed an effective response to lactate in the

range of 10–100 mM, covering the normal physiological ranges of lactate presented in human body fluids.

Liposome-based structures plays an important role in the drug delivery areas [74]. Real-time monitoring of liposome provides great amount of information on the drug delivery process. Tarabella et al. [75] reported an OECT device was sensitive enough to detect liposome-based nanoparticles down to 10^{-7}mg/ml. When a positive gate voltage was applied, channel current of devices could be effectively modulated upon the addition of liposome-based nanoparticles. The devices integrated in microfluidics system provide a viable solution to the cost-effective study of drug-delivery mechanisms in the pharmaceutical industry.

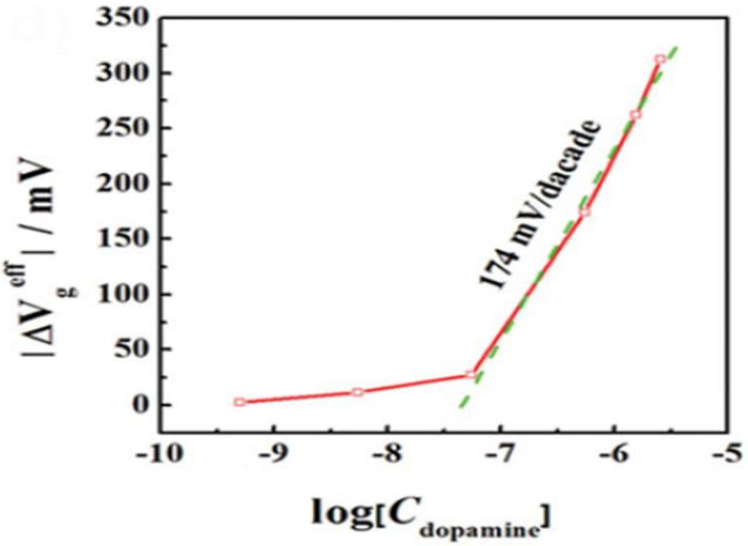

Figure 2.17 The change of the effective gate voltage (ΔV_g^{eff}) of the OECT *vs.* the concentrations of dopamine [$C_{dopamine}$] [72].

2.4 Summary

Due to its synthetic versatility, tunable electronic property, excellent biocompatibility and solution processable fabrication methods, organic semiconductors hold great potential for OTFT based sensors. Typically, polyaniline, PEDOT: PSS, poly(3-methylthiophene) and polypyrrole are the most common ones for the OTFT based sensing application. OTFTs, particularly the OECTs, have been exhaustible investigated for the applications both in chemical and biological sensing. It is worthwhile to note that OECT based sensors able to show a stable performance in aqueous environments, making it suitable for the real in-situ detection. Promisingly, a large number of high performance sensors, such as ion, pH, DNA, glucose and dopamine sensors, etc, have already been explored and demonstrated.

In the last few decades, various novel types of semiconducting polymers with high carrier mobility and excellent stability have been reported and used in the sensing applications. To better realize the practical sensing applications, two basic strategies are proposed. The first one is to optimize the existed OECT sensors. The performance of sensor device, typically including sensitivity, selectivity, and stability, could be significantly improved by manipulating the physical geometric features of the devices or just adopting novel organic semiconductors/techniques in device fabrications. The second strategy is to develop new type of OTFT based sensors. Due to its versatility, OTFTs is a viable platform for various kinds of sensors. Surface modification and interfacial engineering methods are usually used to functionalize the device to meet specific requirements. Overall, OTFT-based

sensors have emerged as a candidate platform for the sensing both academic study as well as daily practical applications.

Chapter 3 Highly Selective and Sensitive Glucose Sensors Based on Organic Electrochemical Transistors with Graphene-modified Gate Electrodes

This chapter systematically study the organic electrochemical transistor (OECT) based glucose sensor. The sensitivity of the OECT sensor could be significantly increased by co-modifying the gate electrode with graphene materials(graphene or reduced graphene oxide (rGO)) and glucose oxidase. The functionalized device was sensitive enough to detect glucose level down to 10 nM, which was two orders of magnitude better than that of device without graphene modification. The optimized device shows a linear response to a wide range glucose concentration from 10 nM to 1 mM, covering the physiological glucose range in human saliva. The selectivity of device was systematically studied for the first time. The sensitivity of the OECTs glucose sensor could be dramatically improved by modifying the gate electrode with biocompatible polymers, including chitosan and Nafion. The interfering effect from uric acid and L-ascorbic acid was mostly blocked. High performance OECT-based glucose sensors could be realized by modifying the gate electrodes. Therefore, the OECTs devices are the promising platform for the low-cost, flexible and disposable sensing applications.

3.1 Introduction

Accurate and rapid detection of glucose level in biological environments is of critical importance to the health conditions, particular for the clinical diagnosis of diabetes mellitus [76, 77]. Therefore, the area of glucose detection has been intensively investigated in the last few decades. Due to it high sensitivity, flexibility, low-cost and easy fabrication methods, organic thin film transistors (OTFTs) have become the viable platform for chemical and biological sensing applications. As an important family of OTFTs, organic electrochemical transistors (OECTs) have emerged as a versatile candidates for the state of art sensor platforms [7, 9, 78] The very first OECTs device was fabricated by the conjugated polymer polypyrrole in 1984 [79] which shapes the direction in the development of OTFTs. Owing to its high conductivity and stability, poly(3,4-ethylenedioxythiophene): poly(styrenesulfonate) (PEDOT:PSS), a highly doped p-type organic semiconductor, has been widely used in organic electronics [80]. Importantly, PEDOT:PSS based OECTs have demonstrated extensive applications in chemical and biological sensors, ranging from pH [81], bacteria [71], ions [45], and glucose [50, 56, 57], to dopamine [72], DNA [67], lactate [73], proteins [69], and cells [59], etc.

Recently, glucose sensors based on OECTs have been reported by many groups. Zhu et al. [50] reported the OECT-based glucose sensors for the first time. The device able to detect glucose level down to several mM, which was sensitive enough

to measure the normal range of glucose levels in human saliva. Then our group demonstrated that the sensitivity of OECT glucose sensors could be remarkably improved by modifying the gate electrodes with nanomaterials (multi-wall carbon nanotubes or Pt nanoparticles), chitosan (CHIT) and the enzyme glucose oxidase (GOx) [57]. The low detection limit of sensor could be extended to 5 nM when the gate electrode was electrochemical deposited with Pt nanoparticles. Therefore, optimized gate modification could enhance the sensitivity. However, the OECTs device had low selectivity toward specific glucose detection, which may become a drawback for real applications.

Graphene flakes have been used to the sensitivities in electrochemical glucose sensors [82]. Kang et al. fabricated the high performance electrochemical glucose sensors by modifying the electrode with CHIT–graphene and GOx [83]. Owing to the high conductivity and large surface area to volume ratio of graphene, the sensitivity was greatly improved. The excellent biocompatibility of CHIT guarantees the success immobilization of enzyme on the electrode.

Wu et al. reported that device with CHIT–graphene/Pt nanoparticle composite films show good reproducibility as well as long-term stability and could detect glucose level down to 0.6 μM [84]. Shan et al. fabricated the glucose sensors using the CHIT–graphene/Au nanoparticle composite films [85]. Due to the synergy effect of graphene and Au nanoparticles, the device exhibited good amperometric response to glucose in the linear range of 2–10 mM. Zhou et al.investigated the glucose sensing

of Nafion–graphene/Au nanoparticle composite films with a detection limit of 5 mM [86]. Graphene oxide (GO) also play an important role in electrode modification process because of its unique chemical and electronic and features [87, 88]. Compared with Pt nanoparticles and graphene flakes, GO is easier to access and cheaper. To our best acknowledge, graphene-based materials have not been used in the modification of OECT based devices, and are expected to show pronounced effects on improving the performance.

Equally important as the sensitivity, selectivity of device is also a key parameter for the real sensing applications. However, to our best knowledge, no systematic work has been done before on the selectivity of OECT-based glucose sensors, which prohibits the development of this promising technology. Electro-active interference compounds [89], such as L-ascorbic acid (AA) and uric acid (UA), are commonly co-exist in physiological samples, which may cause errors in the accurate detection of glucose. Due to the electrochemical reaction of glucose at gate electrode, the effective gate voltage applied on OECTs could be shifted. Interestingly, the selectivity feature of device is similar to that of conventional electrochemical glucose sensor using a similar electrode. The selectivity of electrochemical glucose sensors can be improved by modifying the electrodes with biocompatible polymers, such as Nafion and CHIT [90-92]. Owing to its desirable properties, including excellent biocompatibility and film-forming ability, CHIT has been widely used to immobilize the functional biological molecules on electrode [82, 85]. Similarly, Nafion, a commercial available sulfonated copolymer firstly discovered by DuPont,

has become a candidate material for enzyme immobilization [90]. Therefore, the selectivity of OECT-based glucose sensor is expected to be improved by modifying the gate electrode with CHIT or Nafion.

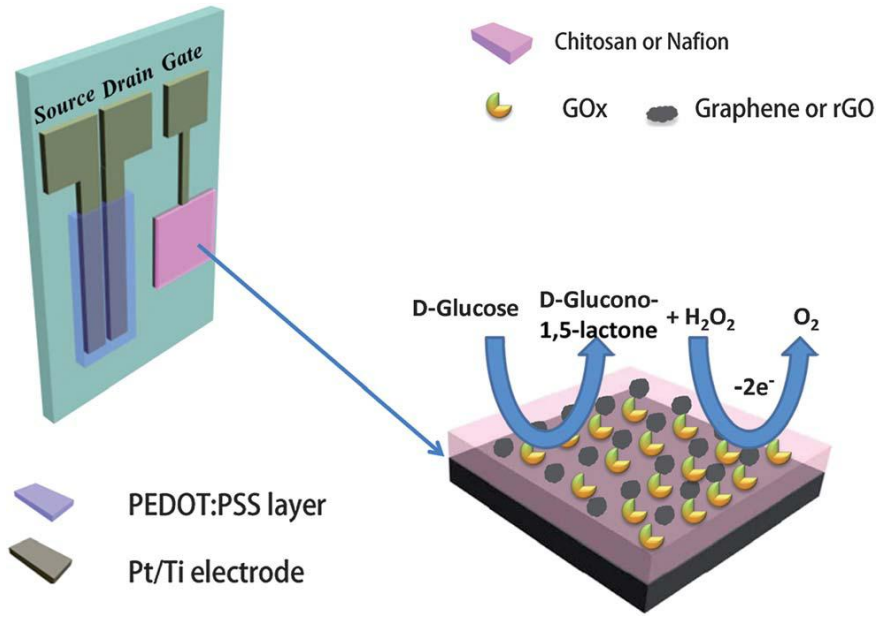

Figure 3.1 Schematic diagram of an OECT-based glucose sensor modified with GOx, CHIT (Nafion) and graphene (rGO) flakes.

In this chapter, we demonstrate the high-performance OECT-based glucose sensors prepared by a facile solution process. To simultaneously improve the sensitivity and selectivity of OECT glucose sensor, the gate electrode of OECTs was co-modified with a biocompatible polymer (Chitosan/Nafion), graphene materials(graphene flakes/reduced graphene oxide (rGO)), and enzyme GOx, as shown in Figure 3.1 The device with the CHIT, graphene and GOx modified gate electrode showed the best performance among all fabricated devices. This type OECT sensor was sensitive

enough to detect glucose level down to 10 nM and showed a broad linear response range from 10 nM to 1 mM. Therefore, the OECTs are promising transducers for high sensitive, specific, low-cost and disposable glucose sensors.

3.2 Fabrication and Electrical Measurements of OECTs

3.2.1. Materials

PEDOT:PSS aqueous solution were purchased from Sigma-Aldrich Co. and stored at 4℃. Phosphate buffered saline (PBS) solution (pH 7.4) and Nafion were also purchased from Sigma-Aldrich Co. CHIT was purchased from Advanced Technology & Industrial Co., Ltd and used as received. Glucose oxidase (GOx) (50 kU g^{-1}) was obtained from Aladdin Reagent Database Inc. and stored at-20 ℃. AA and UA power were also purchased from Sigma-Aldrich Co. Micrometers-sized graphene flakes were prepared by ultrasonic exfoliation from graphite in chemical solutions [93]. rGO was produced by the in situ reduction of graphite with the aid of sodium dodecylbenzene sulfonate as the stabilizing agent [94, 95]. Solution-based graphene and rGO dispersions were store in room-temperature environment for the future use. Figure 3.2a and b demonstrate atomic force microscopy (AFM) images of the graphene and rGO flakes on SiO_2/Si substrates.

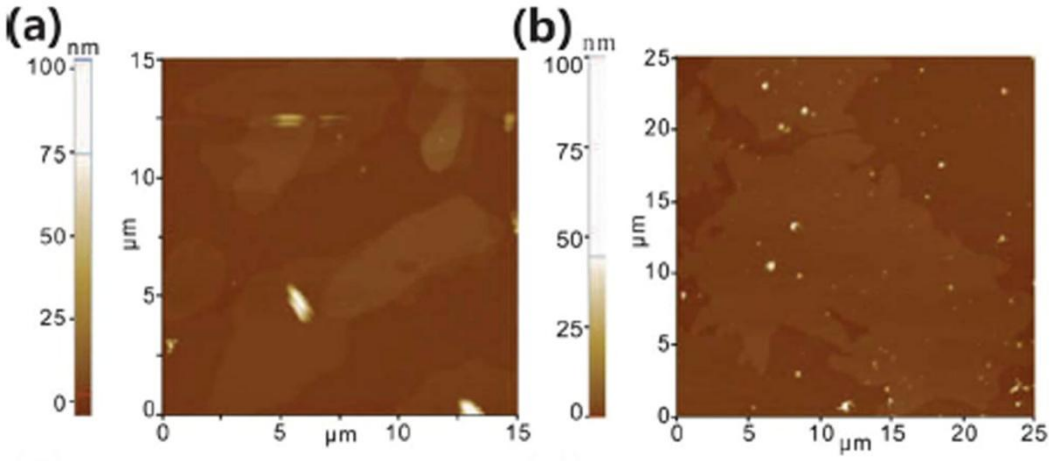

Figure 3.2 AFM images of (a) graphene and (b) reduced graphene oxide rGO.

3.2.2 Device Fabrication

Figure 3.1 demonstrates the schematic diagram of OECT-based glucose sensor fabricated on a glass substrate. Firstly, Ti/Pt source, drain and gate electrodes were patterned through a shadow mask on glass substrates by rf magnetron sputtering. The thin layer of Ti (thickness: ～10 nm) serves as a adhesion layer for Pt thin film (thickness: ～100 nm). The length and width of channel on the OECT devices were 0.2 mm and 6.0 mm, respectively. In device preparation, the surfaces of samples were firstly treated with 5 mins oxygen plasma, PEDOT:PSS solution was spin-coated (3500 rpm) onto the channel area. Then the devices were transferred into a glove box filled with high purity N_2 and annealed at 200 ℃ for 1 h [95]. To functionalize the device, the gate electrodes of OECTs were co-modified with biocompatible polymers, graphene and enzyme. In the preparation of CHIT/GOx/ Pt based gate electrodes, 10 mL GOx PBS solution was firstly drop coated on the surfaces of Pt gate electrodes and stored in 4 ℃. Then 10 mL CHIT acetic acid

solution (CHIT 5mg/mL) was dropped on the surface of the GOx/Pt modified electrodes to immobilize the GOx molecules. When the CHIT film was solidified, the enzyme electrodes were immersed in PBS solution and stored at 4 ℃ for future testing. Similarly, in the preparation of CHIT–graphene/GOx/Pt gate electrodes, CHIT–graphene uniform mixture was obtained by mixing together equal amount volume of these two type solutions. The mixture solution was dropped onto the surface of GOx/Pt gate electrodes to immobilize the enzyme. The rest types of enzyme electrodes, including CHIT–rGO/GOx/Pt gate electrodes, Nafion (0.5%, 1.0%, 2.5%)/GOx/Pt gate electrodes, Nafion (0.5%, 1.0%, 2.5%)–graphene/GOx/Pt gate electrodes and Nafion(0.5%, 1.0%, 2.5%)–rGO/GOx/Pt gate electrodes were fabricated using the same method mentioned above. Figure 3.3a and b show SEM images of the gate electrodes modified with CHIT/GOx and Nafion/GOx composite, respectively.

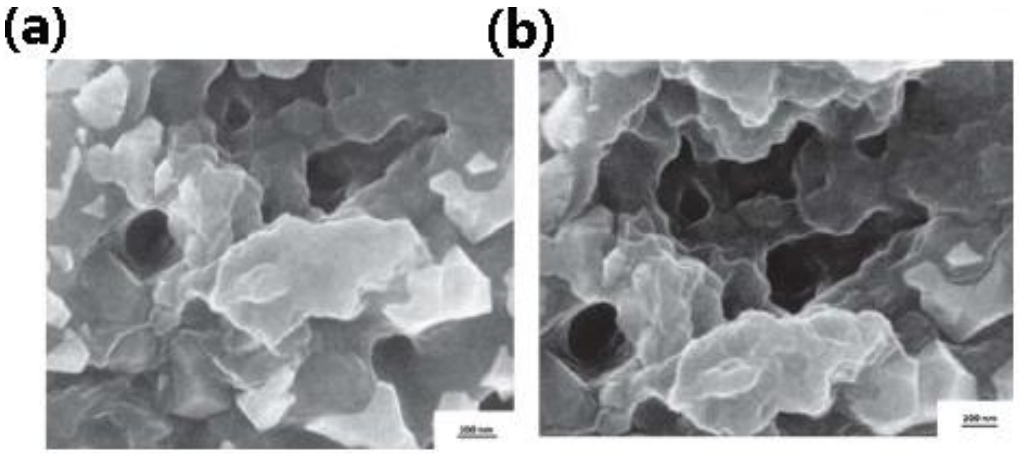

Figure 3.3 SEM images of (a) CHIT/GOx film and (b) Nafion/GOx film on Pt electrode.

3.2.3 Device Characterization

Modified gate electrodes were thoroughly rinsed with PBS solution to remove undesired residue left on the electrodes before characterization. The testing environment was performed with a beaker filled with 10 mL PBS solution. Then designed amount of glucose solution was consecutively added into PBS solution to obtain different glucose levels. The source, drain and gate electrodes of OECT device were connected to two combined Keithley source meters (Keithley 2400). The gate voltages (V_G) and source–drain voltages (V_{DS}) were controlled by a Labview program in a computer. For transfer characteristics, the channel current (I_{DS}) between source and drain was measured as a function of V_G with a fixed V_{DS} (= 0.05 V). For the real-time investigation of glucose level, V_G (=0.4 V) and V_{DS} (= 0.05 V) were set at a constant value.

3.2.4 Working Principle of OECT-based Glucose Sensors

The sensing mechanism of the OECT-based glucose sensor is based on the enzymatic reaction involved with the elecro-oxidation of glucose, producing D-glucono-1,5-lactone and H_2O_2. Then, H_2O_2 is oxidized at the gate electrode and induce electron transfer (Faradic current) to the gate electrode, which in turn modify the effective gate voltage applied on the transistor and thus the conductivity of channel [39]. The immobilized enzyme GOx makes the bio-reaction particularly sensitive and selective to glucose.

$$D-Glu\cos e \xrightarrow{Enzyme(GO_X)} \mathrm{D-glucono-1,5-lactone} + H_2O_2$$

$$2H_2O_2 \xrightarrow{-2e^-} O_2 + 2H_2O$$

The channel current of OECT could be given by:

$$I_{DS} = \frac{q\mu p_0 tW}{LV_p}(V_p - V_G^{eff} + \frac{V_{DS}}{2})V_{DS}, \quad (\text{when } |V_{DS}| << |V_p - V_G^{eff}|)$$
$$V_p = qp_0 t / c_i, \tag{3.1}$$
$$V_G^{eff} = V_G + V_{offset},$$

where q is electron charge; m and p_0 are the hole mobility and the initial hole density, respectively; t is the thickness of the organic semiconducting layer, Vp and V_G^{eff} are the pinch-off voltage and the effective gate voltage, respectively; V_{offset} is an offset voltage at interfaces; W and L are the width and length of the OECT glucose sensor, respectively; c_i is the per unit area effective gate capacitance of transistor. The oxidation reaction of H_2O_2 at gate voltage can change the offset voltage V_{offset} ,which in turn modify the effective gate voltage V_G^{eff} of transistor given by [39, 40]:

$$V_G^{eff} = V_G + (1+\gamma)\frac{kT}{2q}\ln[H_2O_2] + \text{constant} \tag{3.2}$$

in which g is the capacitances ratio between the electrolyte/channel interface and the electrolyte/gate interface; k is Boltzmann's constant; T is the temperature and $[H_2O_2]$ represents the concentration of produced H_2O_2. As the concentration of H_2O_2 was increased, the transfer curve (I_{DS} *vs* V_G) of transistor shifted to a lower gate voltage. Therefore, when the device was characterized with fixed gate and source-drain voltages, the channel current would decrease with the increase of $[H_2O_2]$. Since the H_2O_2 concentration increases proportionally with the increase of glucose concentration before reaching the saturation regime, the changes in channel current would unveil the information on the added glucose concentration.

The effective gate voltage of OECT in determined by the glucose level as follows:

$$V_G^{eff} = \alpha_{Glu} \ln[Glu] + \text{constant} \quad (3.3)$$

where [Glu] is the concentration of glucose. However, the produced H_2O_2 level is greatly influence by the electrocatalytic activity of gate electrode. In order to improve electrocatalytic ability of the device and the performance of OECT-based glucose sensors, it is critical to perform the surface modification (e.g.enzyme, polymers and nanomaterials,etc,) on the gate electrode. By optimizing the modification techniques, the detection limit and selectivity could be simultaneously enhanced.

The responses of OECT toward UA and AA addition could be attributed to the direct electro-oxidation of UA(AA) on the surface of Pt gate electrode and induces a sensing response similar to that of glucose sensor:

$$V_G^{eff} = \alpha_{AA} \ln[AA] + \text{constant} \quad (3.4)$$

$$V_G^{eff} = \alpha_{UA} \ln[UA] + \text{constant} \quad (3.5)$$

where α_{AA} and α_{UA} are the constant values representing the responsibility of the device to AA and UA, respectively.

3.3 High Performance of OECT-based Glucose Sensors

3.3.1 OECTs with Pt Gate Electrodes

Figure 3.4 shows the current response of unmodified device to the additions of glucose. Due to the non-enzymatic electrochemical reaction of glucose near Pt gate electrode, the OECT device still show observable channel current response to the glucose addition even when no was modified on the gate electrode. According to the direct electro-oxidation reaction of glucose, the sole product of D-glucono-1,5-lactone was produced near Pt gate electrode [96]. Based on the similar sensing mechanism, AA or UA molecules could also been electro-oxidized at Pt gate electrode and subsequently change the channel current, which is determined by the changes in the effective gate voltage given by eqn (3.1), as shown in Figure 3.5 and Figure 3.6..

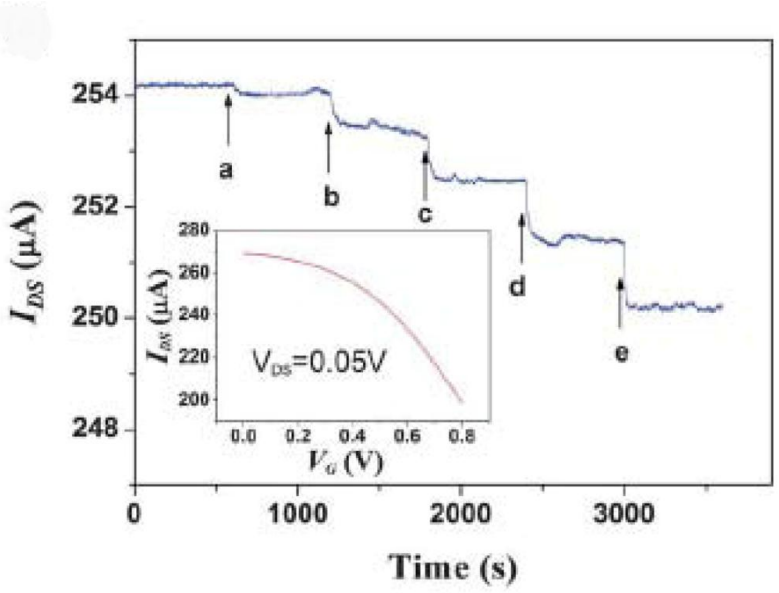

Figure 3.4 Channel current response of an OECT with a Pt gate to additions of glucose in PBS solution. From a–e, the concentrations of glucose are 1, 5, 10, 50 and 100 μM, respectively. Inset: transfer curve (I_{DS} *vs.* V_G) of the OECT.

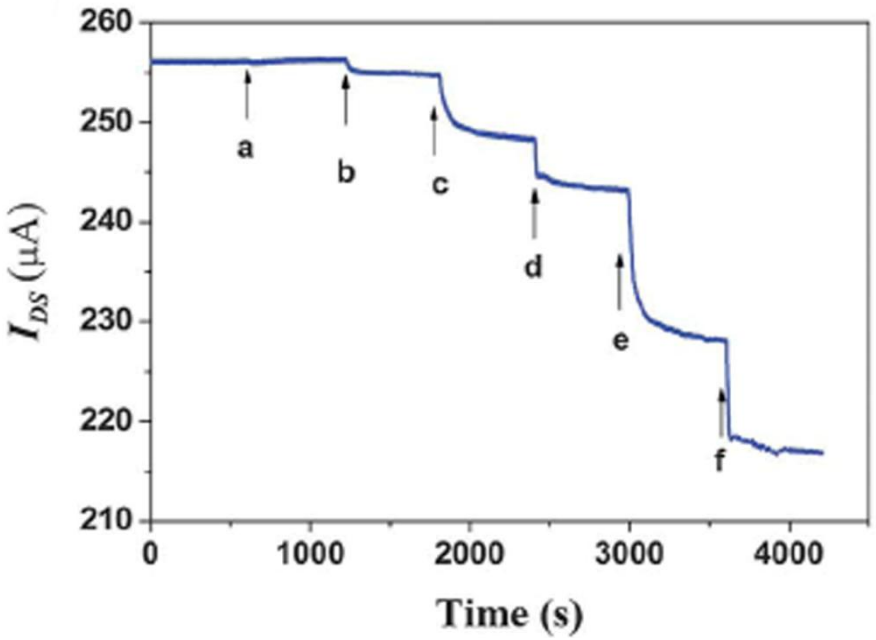

Figure 3.5 Response of the OECT to additions of AA. From a–f, the concentrations of AA are 0.1, 1, 5, 10, 50 and 100 μM, respectively.

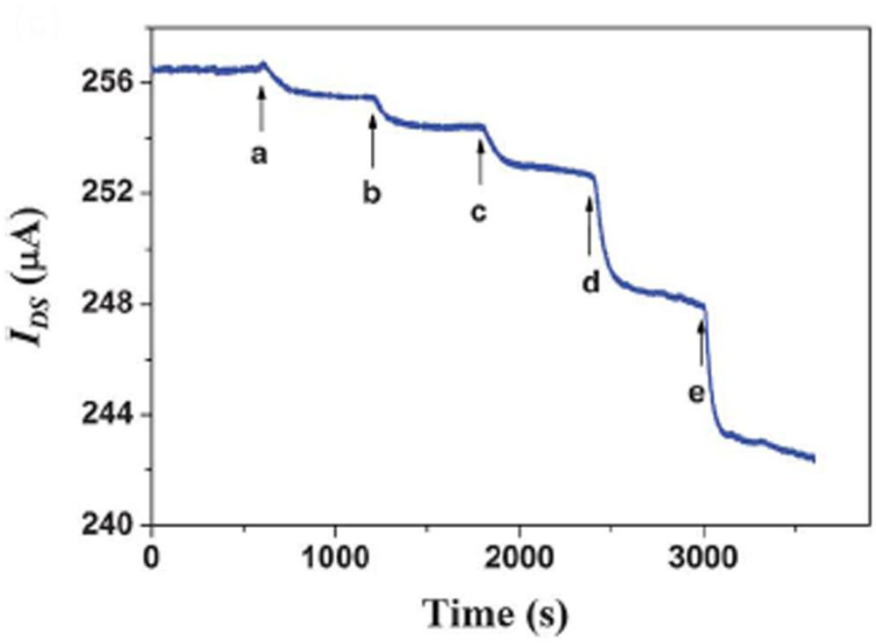

Figure 3.6 Response of the device to additions of UA. From a–e, the concentrations of UA are 1, 5, 10, 20 and 50 μM, respectively.

The relationship between effective voltage and different channel currents can be obtained from the transfer curve (I_{DS} vs. V_G) of the OECT shown in the inset of Figure 3.1. Normally, the change of effective gate voltage is defined as the difference between the gate voltages before and after addition of analyte) [72]. Therefore, the response of OECT sensors to analytes can be wirtten as changes of V_G^{eff} as functions of concentrations. Figure 3.7 shows the changes of V_G^{eff} of unmodified device to three analytes, among which glucose shows the lowest sensitivity. The glucose sensor exhibits low sensitivity and poor selectivity due to the lack of immobilized GOx. R is the correlation coefficient for linear fitting. Table 1 shows the detection limit and responsibility of all fabricated OECT glucose sensor.

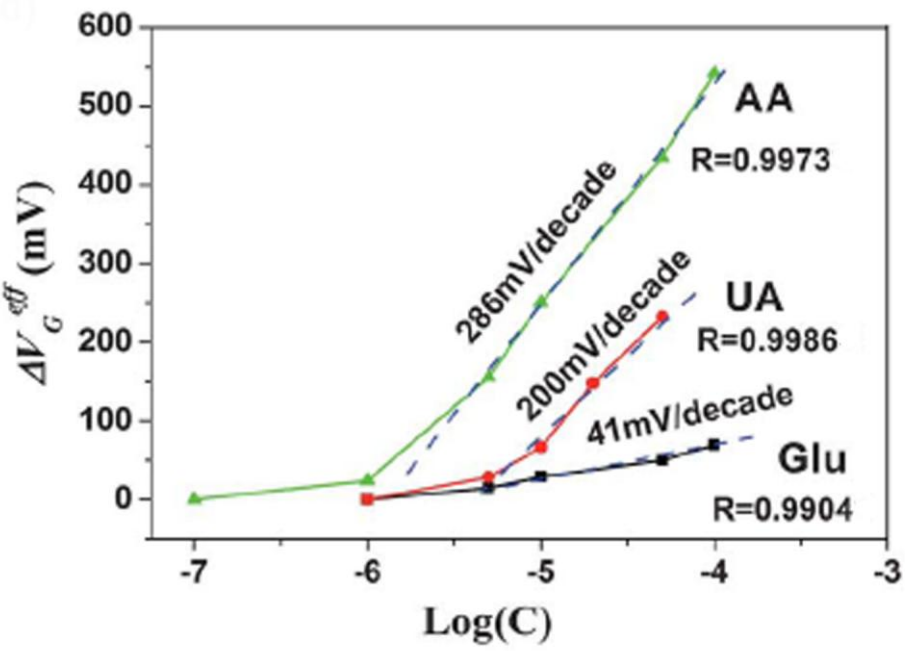

Figure 3.7 The changes of the effective gate voltage of device as functions of analyte concentrations. R is the correlation coefficient for the linear fitting with a dashed line.

3.3.2 OECTs with GOx and CHIT /Nafion

To simultaneously improve the sensitivity and selectivity of device to glucose, the pure Pt gate electrode was modified with CHIT and GOx. Analytes can easily pass through these holes(hole diameter ranging from 100 to 200 nm) to reach reactive sites on the surface of Pt electrode and induce corresponding responses. In practical application, detection limit is usually used as an important parameter for the assessment of device performance. The low detection limit of a device is defined as the minimum amount of analytes needed to produce a stable and reproducible response with the corresponding signal to noise ratio (S/N) larger than 3. Figure 3.8 shows the response of device to different glucose concentrations. The detection limit is about 100 nM, which is one order of magnitude lower than that of device without any modification on the gate electrode. More significantly, the selectivity of OECT glucose sensor was dramatically improved by modification. Figure 3.9 and Figure 3.10 demonstrate the responses of device to AA and UA addition, respectively. The device shows no observable response until 10mM AA was added, which is two orders of magnitude higher than that to glucose addition. The device shows no response to UA even when high concentration(100 mM) of UA is used. Regarding the much lower levels of these interfering substances (e.g. UA ～ 0.02 mM, AA～ 0.1mM in blood) in the normal human body fluids, this type of OECT glucose (e.g. 3.6–7.5mM in blood) sensor would show excellent selectivity for practical sensing applications. Figure 3.11 shows the changes of effective voltages as functions of concentrations of the added analytes. The gate voltage change of device shifted about 327 mV when the glucose is changed for one decade, which is much larger

than that of the device with pure Pt gate electrode(41.0 mV per decade). More importantly, the CHIT –GOx modified device shows much lower sensitivity to AA(58mM/decade), which could be attributed to the desirable properties of CHIT material. Owing to its excellent film-forming ability and biocompatibility, CHIT has been widely used as an immobilization material for the electrode modification. The GOx can be effectively immobilized on the surface of Pt electrode by CHIT primarily due to the electrostatic effects [97]. When the CHIT-GOx/Pt modified gate electrode is immersed in PBS solution (pH 7.4) for the glucose detection, CHIT is negatively charged, which act as the effective block layer to repel the negatively charged interference species, e.g. AA and UA. Therefore, the selectivity of OECT glucose is remarkably improved.

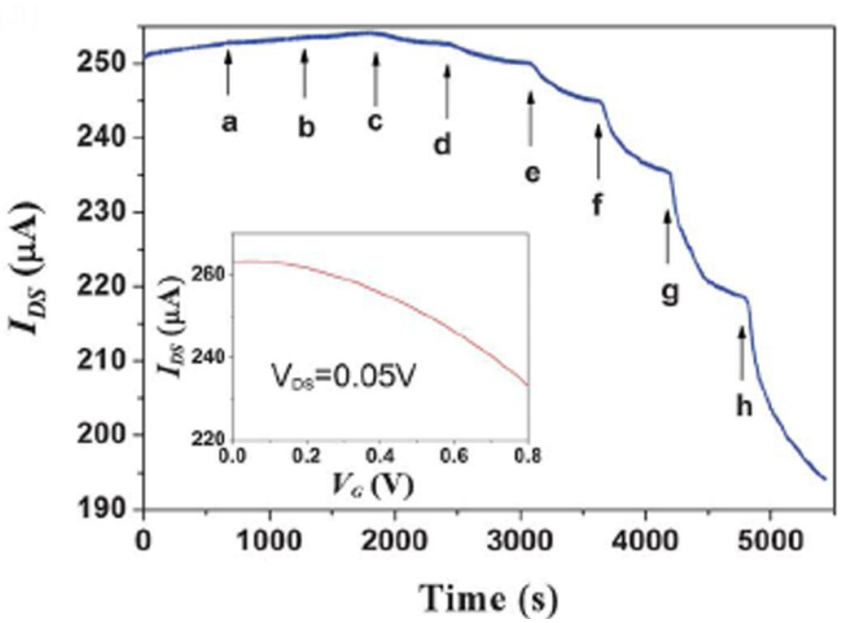

Figure 3.8 Channel current response of an OECT with the CHIT/GOx/Pt gate electrode to additions of glucose in PBS solution. From a–h, the concentrations of glucose are 10, 50, 100, 500 nM, 1, 5, 10 and 50 μM, respectively. Inset: transfer curve (I_{DS} *vs.* V_G) of the OECT.

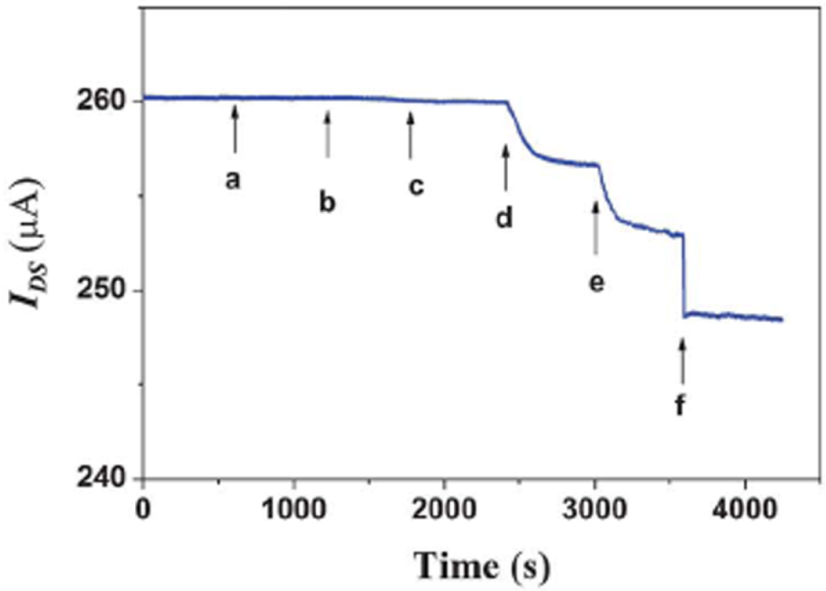

Figure 3.9 Response of the OECT to additions of AA. From a–f, the concentrations of AA are 0.1, 1, 5, 10, 50 and 100 μM, respectively.

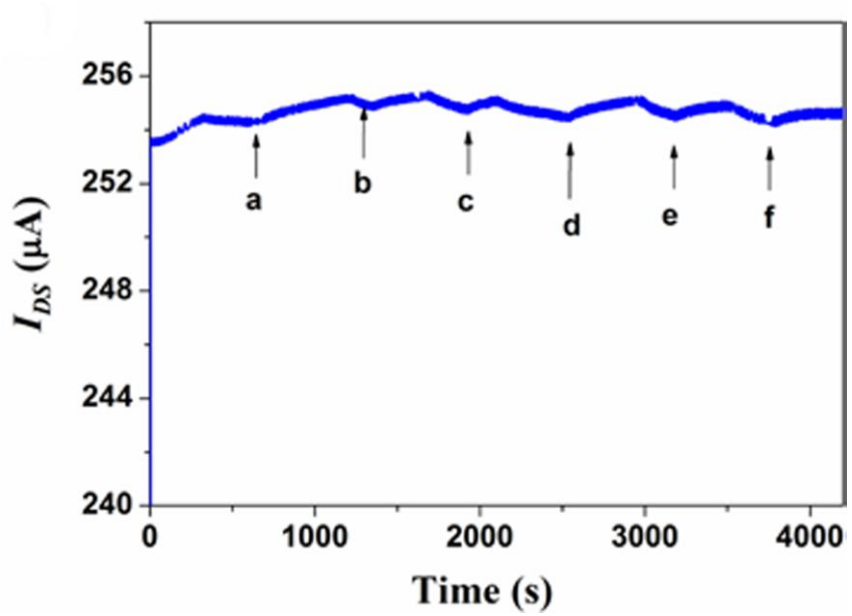

Figure 3.10 Response of the OECT to additions of UA. From a–f, the concentrations of UA are 0.1, 1, 5, 10, 50 and 100 μM, respectively.

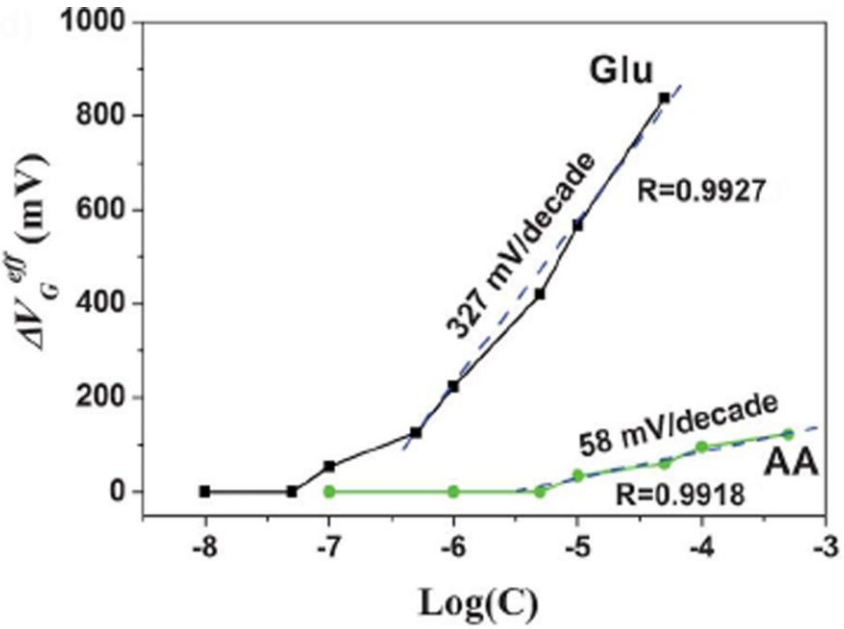

Figure 3.11 The changes of the effective gate voltage (ΔV_G^{eff}) as functions of analyte concentrations.

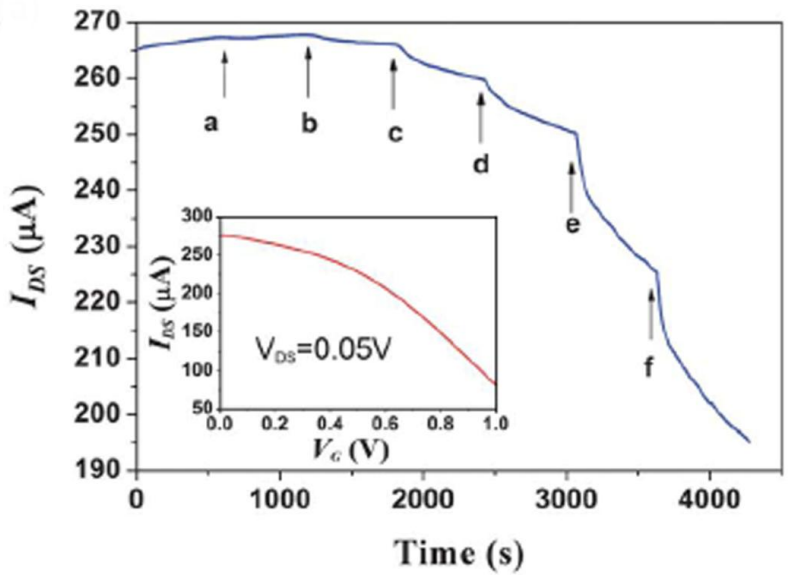

Figure 3.12 Channel current response of an OECT with the Nafion/GOx/Pt gate electrode to additions of glucose in PBS solution. From a–f, the concentrations of glucose are 50, 100, 500 nM, 1, 5 and 10μM, respectively. Inset: transfer curve (I_{DS} vs. V_G) of the OECT.

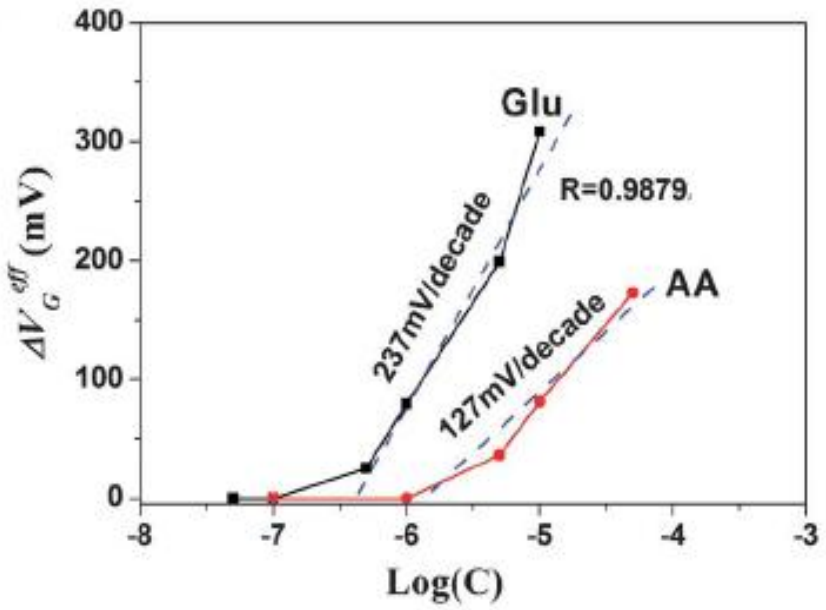

Figure 3.13 The changes of effective gate voltage (ΔV_G^{eff}) as functions of analyte concentrations.

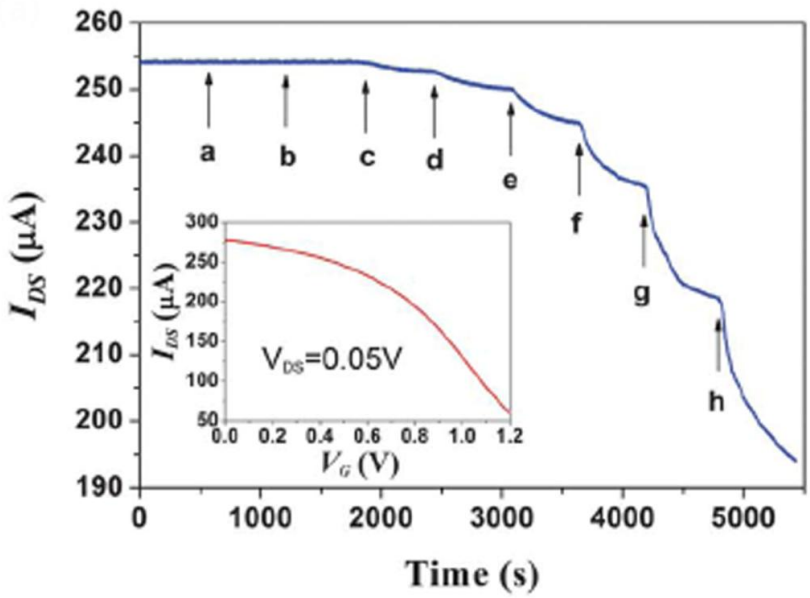

Figure 3.14 Channel current response of an OECT with the CHIT–graphene/GOx/Pt gate electrode to additions of glucose in PBS solution. From a–h, the concentrations of glucose are 10, 50, 100, 500 nM, 1, 5, 10 and 50μM, respectively. Inset: transfer curve (I_{DS} *vs.* V_G) of the OECT.

Nafion, a sulfonated tetrafluoroethylene based polymer, has attracted considerable attention for its demonstration in ionselectivity and biocompatibility. Similarly, Nafion could be used as the modification material for enzyme to improve the sensitivity and selectivity of device. Figure 3.12 and Figure 3.13 show the responses of the modified device to glucose, AA and UA. The detection limit to glucose of device is about 0.5 mM, which is not as sensitive as that of CHIT/GOx/Pt gate electrode. Compared with the change of effective gate voltage of device to glucose, the responses to AA and UA are smaller, which indicates the good selectivity for glucose sensor. Owing to its attractive properties, Nafion has been widely used to modify electrodes for both biological and chemical sensing applications [90]. Since Nafion is negatively charged in PBS solution, the interference from interfering substances in negatively charged states is effectively eliminated because of electrostatic interaction. Therefore, the Nafion modified devices exhibit enhanced selectivity. The concentration of Nafion solution could greatly affect the performance of device. In the work, three different concentrations (2.5%,1.0%, 0.5%) Nafion solutions are used in the experiments and the device modified with 2.5% Nafion solution demonstrated the best performance (Table 3.1).

3.3.3 OECTs with GOx, CHIT and Graphene/rGO

It has been reported that nano-scaled materials modification of working electrodes could improve the electrochemical activity and thus the sensitivity of corresponded devices [72]. In this work, we modified the gate electrode with chemical prepared graphene flakes, which is much cheaper than our previously used Pt nanoparticles.

Figure 3.14 shows the response of an OECT sensor with the CHIT–graphene/GOx/Pt modified electrode to additions of glucose. The detection limit to glucose is 10 nM, which is similar to that of the OECT glucose sensor based on the modified electrode with Pt nanoparticles. Figure 3.15 shows the changes of the effective gate voltage of device induced by the three type analytes. The device changed 370 mV per decade to glucose addition, which is the highest value in all the fabricated types of glucose sensors in this work. In addition, the sensor shows a good linearity (correlation coefficient (R)=0.99742) in a wide range of glucose concentration. It is notable that the linearity of modified glucose sensor is much better than that with Pt nanoparticles modified reported by our group before. Owing to its desirable properties, such as the large surface area to volume ratio of modifying composite film that can increase the load of enzyme and the high conductivity of graphene that can facilitate charge transfer during the reaction, the sensitivity of the graphene modified OECT glucose sensor is significantly improved. The device show no current response until 1 mM AA or 10 mM UA is added into PBS solution. Compared with the device with CHIT/GOx/Pt electrode, the effective gate voltage changes caused by AA(237 mV per decade) and UA (120 mV per decade)are increased. Since graphene is electrocatalytically active, UA or AA molecules could directly react on the surfaces of the graphene flake and correspondingly increase the response to UA or AA .On the other hand, CHIT sometimes cannot cover the graphene flakes completely, AA and UA may react on the surface of graphene directly without passing through the CHIT layer to the reactive sites. Nevertheless, the device shows a much higher sensitivity to glucose than that to UA and AA,

which holds great potential for real applications. Since all fabricated device could be used for more than 3 times with a similar performance, the OECT based sensor platform is promising for disposable applications. The linear response of OECT sensor to glucose level ranged from 10 nM to 1 mM, which is wide enough for sensing the normal and abnormal glucose levels in human body fluid and blood.

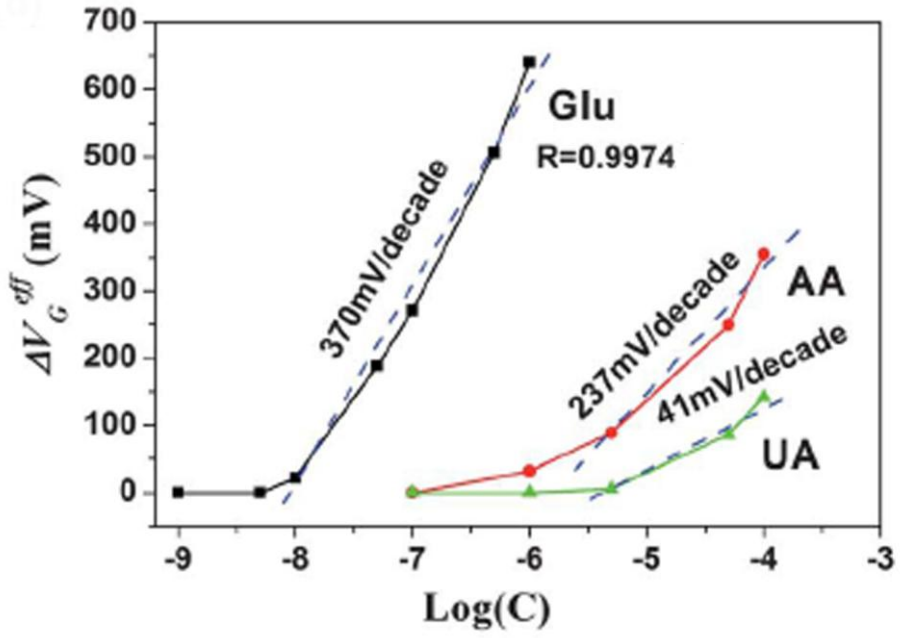

Figure 3.15 The changes of effective gate voltage (ΔV_G^{eff}) as functions of analyte concentrations.

To characterize the glucose level, the sample (body fluid or blood) is necessary to be diluted. For instance, the normal human saliva glucose level is between 3 mM and 210 mM [98], saliva needs to be diluted to the concentration of about 1% by adding PBS solution and mixed throughoutly before testing. Therefore the OECT sensor can be used to detect all the possible glucose levels in saliva. It has been reported that proteins mixed with graphene oxide (GO) can still retain their biological activity,

indicating the promising applications of GO in the electrode modification for the biosensors. Since plentiful reactive sites(typical oxygen-containing groups) are provided by the GO sheets, GO has become a candidate material for enzyme immobilization [99]. The device modified with rGO is characterized using the same conditions. Figure 3.16 shows the responses of device to glucose, AA and UA. The device shows no response until 100 nm glucose is added, which is not as sensitivity as the device with graphene flakes modified. The reduced sensitivity to glucose could be explained by the decreased conductivity of rGO sheets. However, the selectivity of device to glucose is good and the interference effects from UA and AA are negligible for practical applications.

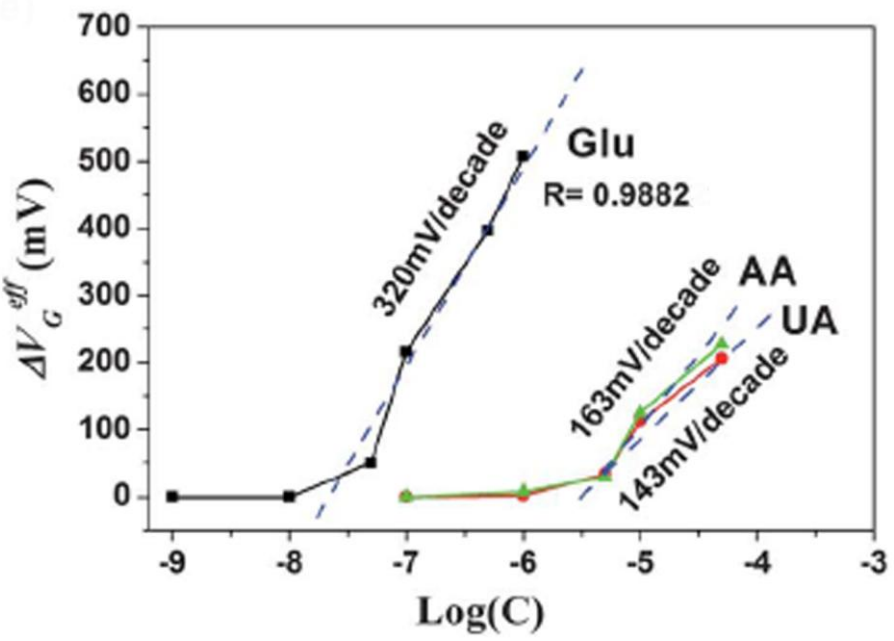

Figure 3.16 The changes of effective gate voltage (ΔV_G^{eff}) of the OECT with the CHIT–rGO/GOx/Pt gate electrode corresponding to different analytes.

3.3.4 OECTs with GOx, Nafion and Graphene/rGO

We systematically investigate the performance of device with Nafion (2.5%, 1.0%, 0.5%), graphene and GOx co-modified electrodes. The concentration of Nafion solution is critical for the performance of device. Figure 3.17 show the responses of an OECT sensor with Nafion (1.0%)–graphene/GOx/Pt electrode to glucose, AA and UA, respectively. The detection limit of device for glucose is as low as 50 nM, which is more sensitive in comparison with that of device with Nafion and GOx co-modified device. The change of the effective gate voltage of device to glucose addition is about 272 mV per decade. Therefore, the graphene flakes could be used to obviously increase the sensitivity of OECT-based glucose sensor.

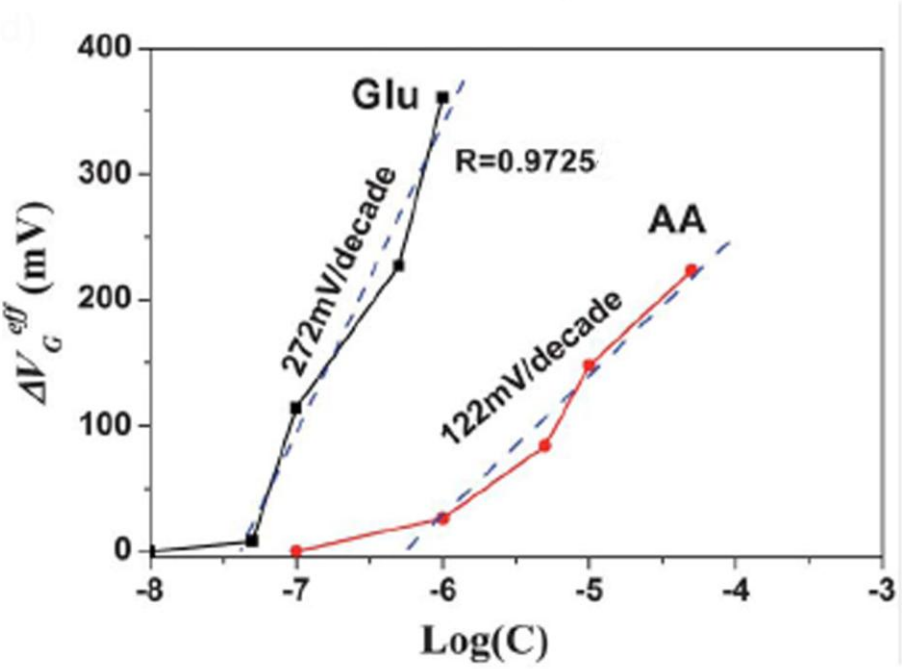

Figure 3.17 The changes of effective gate voltage (ΔV_G^{eff}) as functions of analyte concentrations.

The performances of OECT devices are strongly dependent on the Nafion concentration in the electrode modification. Table 3.1 demonstrates the performance of all devices with different Nafion concentrations. It is clearly that the device with Nafion (1.0%)–graphene/GOx/Pt modified gate electrode exhibits the best selectivity in the Nafion modified device, which could be explained by the different film thickness of the modified Nafion layer. On one hand, if the Nafion concentration is too low, the Nafion film on the electrode is too thin and can not serve as the block layer to eliminate the interference effects from other electro-active biomolecules. On the other hand, if the Nafion concentration is too much high, the formed Nafion film would be too thick, making it difficult for charge transfer process. Therefore, the concentration of Nafion should be optimized to improve the performance of glucose sensor.

Table 3.1 Detection limit and change of effective gate voltage (α) of the OECT glucose sensors.

	Glucose		AA		UA	
Gate electrodes	Detection limit (nM)	α (mV per decade)	Detection limit (nM)	α (mV per decade)	Detection limit (nM)	α (mV per decade)
Pt	1000	41.0	100	200	1000	286
CHIT/GOx/Pt	100	327	10^4	58.0	Nil	Nil
CHIT–graphene/GOx/Pt	10	370	1000	237.0	10^4	120
CHIT-GO/GOx/Pt	100	320	1000	163	1000	144
Nafion (2.5%)–GOx/Pt	500	220	10^4	128	Nil	Nil
Nafion (1.0%)–GOx/Pt	1000	204	10^4	172	1000	28.4
Nafion(0.5%)–GOx/Pt	500	111	10^4	98.6	Nil	Nil
Nafion (2.5%)–graphene/GOx/Pt	100	314	1000	215	5×10^4	Nil
Nafion (1.0%)–graphene/GOx/Pt	50	272	1000	122	Nil	Nil
Nafion (0.5%)–graphene/GOx/Pt	50	363	1000	264	5×10^3	209
Nafion (2.5%)–GO/GOx/Pt	50	224	500	120	1000	131
Nafion (1.0%)–GO/GOx/Pt	50	343	1000	170	5×10^4	110
Nafion (0.5%)–GO/GOx/Pt	500	331	1000	302	5×10^3	211

Together with Nafion and GOx, rGO is used to modify the gate electrodes of OECTs. As shown in Figure 3.18, the addition of rGO onto gate electrode can improve the sensitivity and extend the detection limit to glucose down to 50 nM. However, the device with rGO becomes more sensitive to AA and UA, which probably can be attributed to the high electrocatalytic activity of rGO for the reactions involved with AA (UA) molecules. Therefore, the selectivity of device could not be improved by rGO modification.

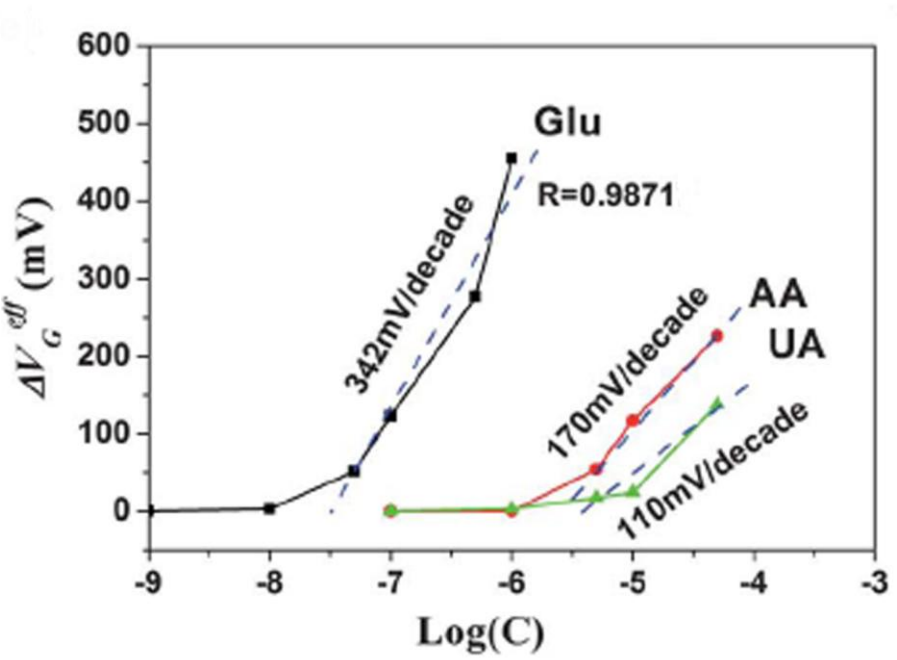

Figure 3.18 The changes of effective gate voltage of the OECT with the Nafion–rGO/GOx/Pt gate electrode to different analytes.

3.4 Summary

In conclusion, OECTs with gate electrodes co-modified with enzyme (GOx), biocompatible polymers (CHIT or Nafion) and graphene nano materials (graphene or rGO flakes) demonstrate excellent performance in glucose sensing and hold great potential for the real applications. CHIT and Nafion can be used to immobilized the enzyme GOx on the gate electrode and improve the selectivity of device. Graphene and rGO can improve the sensitivity of device because of their high conductivity and large the surface to volume ratio. Therefore, the sensitivity and selectivity of devices are simultaneously enhanced when the Pt gate electrodes are co-modified with these materials. The optimized device with the CHIT–graphene/ GOx/Pt modified gate electrode shows a detection limit down to 10 nM and a change of effective gate voltage of 370 mV per decade in the linear region from 10 nM to 1 mM. Compared with the reported OECT-based glucose sensors, the performance is significantly improved. It can be concluded that graphene based nanomaterials are very effective in improving the performance of transistor-based biosensors. Owing to its high performance, low-cost and ease of fabrication, the OECT-based glucose sensors are very promising for the disposable, flexible and high-performance future applications.

Chapter 4 Organic Electrochemical Transistors with Graphene-modified Gate Electrodes for Highly Sensitive and Selective Dopamine Sensors

In this chapter, organic electrochemical transistors (OECTs) were successfully fabricated as highly sensitive and selective dopamine sensors. The selectivity of OECT-based dopamine sensors was significantly improved by coating biocompatible polymer Nafion or Chitosan on the surface of gate electrodes. The interference induced by uric acid and ascorbic acid was effectively eliminated. In addition, the sensitivity of devices was improved by graphene flakes co-modified on gate electrodes. The detection limit of devices to dopamine was down to 5 nM, which was much lower than that of conventional electrochemical methods.

4.1 Introduction

As an important neurotransmitter mediating the transportation of messages within the nervous system [100], dopamine (DA) is a good biomarker for the neurological illnesses associated with abnormal metabolism, such as Parkinson's, Alzheimer's and Schizophrenia diseases [101-103]. However, the clinical level of DA in human body fluids is extremely low, e.g., nM level in plasma and mM level in urine [104,

105]. To effectively diagnose the nervous diseases resulting from the dysfunctional dopaminergic neurotransmission, quantitative determination with high sensitivity and selectivity is of critical importance [106]. Several characterization methods, including capillary electrophoresis [107], liquid chromatography [108], chemiluminescence [109], ultraviolet-visible spectroscopy [110] and electrochemical methods [111], have been reported for the dopamine detection, among which the electrochemical based methods are the most outstanding ones for the convenient determination of DA in clinical analysis [112]. In the last few years, organic thin film transistors (OTFTs) have attracted increasing attention for the high performance sensing applications [6, 9, 113]. OTFTs demonstrate many desirable properties in comparison with their inorganic counterparts, such as low cost ,ease of fabrication, and flexibility, are thus promising for disposable sensors devices [45, 114, 115]. As an important type of OTFTs, organic electrochemical transistors (OECTs) have been emerged as a viable platform for various sensing applications, such as H_2O_2 [40], ions [45], glucose [39, 57], cell [59, 60, 64], bacterial [71], DNA [67] and antigen–antibody sensors [66, 69]. For example, Tang et al. [72] firstly demonstrated the highly sensitive DA biosensors based on OECTs device. The highly doped p-type organic semiconductor, poly(3,4-ethylenedi-oxythiophene): poly(styrene-sulfonate) (PEDOT:PSS) [14], was spin-coated as the active layer of OECT sensors. The performance of device with different gate electrodes, including graphite, Au and Pt electrodes, were systematically investigated. They found that the device with pure Pt gate electrode showed the highest sensitivity and could detect dopamine down to 5 nM, which was two orders of magnitude lower than that of conventional

electrochemical measurements using the similar electrode. However, since the device with pure Pt gate electrode could also effectively catalyze the electrochemical reaction of many analytes in human body especially the main interferents including ascorbic acid (AA) and uric acid (UA)[116], the selectivity of device to DA was very poor and is not suitable for the real sensing applications.

It has been reported that biocompatible polymers, such as chitosan (CHIT) and Nafion, could be used to modify the gate electrode of OECT device to improve the selectivity [117, 118]. CHIT is an ideal material for electrode modification, which could be attributed to its desirable features, including excellent film-forming ability and good biocompatibility[77]. Nafion, a sulfonated copolymer, has also been exploited in the biosensors modification process [90]. As the sensing mechanism of OECT-based DA sensors associated with the electrochemical reaction of DA occurred near the gate electrodes [72], gate electrode modification with suitable polymers is expected to improve the selectivity of DA sensors, which will be systematically investigated in this chapter.

It has been reported that the sensitivity of electrochemical based DA sensors could be significantly enhanced by modifying the electrodes with graphene based materials. As the new emerging material, graphene based materials have attracted significant attentions and been extensively investigated for sensing applications [119]. Wu et al. [120] fabricated the highly sensitive electrochemical DA sensors using the porphyrin-functionalized graphene. The synergistic effects of p–p stacking between

positively charged DA and negatively charged porphyrin-modified graphene and favourable electrostatic attraction significantly facilitate electron transfer process and improve the sensitivity. Hou et al. [121] demonstrated the enhanced DA sensors by modifying the electrode with silanized graphene, which could increase active catalytic sites for the electro-oxidation of DA molecules. Liu et al. [122] reported the phenylethynyl ferrocene/graphene nanocomposite for the rapid electrochemical detection of DA . The device could detect DA as low as 50 nM and a good linearity response in a wide range DA level. Graphene oxide (GO), an important derivative material of graphene family, has also been explored in the electrode modifications to improve the performance electrochemical detection. Bao et al. [123] demonstrated that electrodes modified with graphene oxide-templated polyaniline (GO-PANI) microsheets in DA sensors showed an obvious response upon the addition of 1 mM DA.

In this chapter, high-performance OECT-based DA sensors with functionalized gate electrodes were studied. The selectivity of devices could be significantly improved by modifying the gate electrodes with biocompatible polymers (Nafion or CHIT). In addition, the sensitivity of devices could be further enhanced by the introduction of graphene nanomaterials including graphene and reduced graphene oxide (rGO). The OECT DA sensors functionalized with Nafion and graphene materials showed a detection limit down to 5 nM, a wide linear region from 5 nM to 1 mM, and good selectivity. Therefore, the OECT-based DA sensors hold great potential for disposable and low-cost sensing applications.

4.2 Fabrications and Measurements of OECTs

4.2.1. Materials

PEDOT:PSS aqueous solution, Nafion solution(5%) and phosphate buffered saline (PBS) solution (pH 7.4) were all purchased from Sigma-Aldrich Co. and stored in the refrigerator. CHIT power was obtained from Advanced Technology & Industrial Co., Ltd. Hong Kong and used as received. DA, AA and UA were also the products of Sigma-Aldrich Co. Freshly analytes solutions were prepared by dissolve designed amount of analytes into PBS and used throughout testing. Solution processable graphene flakes were prepared by surfactant assisted exfoliation of graphite oxide and chemical reduction process. Reduced graphene-oxide (rGO) was obtained by the in situ chemical reduction with the aid of sodium dodecylbenzene sulfonate [93, 94]. The purchased Nafion solution (5.0%) was diluted to 2.5%, 1.0% and 0.5% by 2-propanol for the modification. DA solutions (10^{-5} M to 10^{-1} M), AA solutions (10^{-5} M to 10^{-1} M) and UA solutions (10^{-5} M to 10^{-1} M) were prepared by adding a designed amount of these analytes into PBS solution. CHIT aqueous solution (5 mg mL^{-1}, pH= 5) was prepared by dissolving CHIT in the acetic acid solution and stored in room temperature for future use. CHIT/graphene (CHIT/rGO) hybrid aqueous suspension was prepared by adding 200 mL CHIT solution (5 mg mL^{-1}) into a 0.8 mL graphene (rGO) aqueous suspension, then sonicated for 30 mins. Nafion/graphene (Nafion/rGO) hybrid aqueous suspension was obtained by mixing

200 mL Nafion diluents (2.5%, 1.0% and 0.5%) with 0.8 mL graphene (rGO) aqueous suspension and followed by 30mins sonication.

4.2.2 Device Fabrication

Figure 4.1 demonstrates the schematic diagram of an OECTs based DA sensor. Firstly, a glass substrate was patterned with Pt (～100 nm)/Ti (～10 nm) source, drain and gate electrodes through a shadow mask by magnetron sputtering. The thin layer of Ti was deposited to improve the adhesion of Pt layer onto the glass substrate. A PEDOT:PSS layer(about 100 nm) was spin-coated(3500 rpm) onto the channel area of device after the surface of sample has been treated with 5 min O_2 plasma. The geometric length and width of the channel area were 0.2 mm and 6.0 mm, respectively. Then the fabricated devices were moved to the glove box filled with high purity of N_2 and annealed for 1 hour at 200℃.

To prepare highly sensitive and selective DA sensors, the Pt gate electrodes of OECTs were modified with biocompatible polymers (CHIT or Nafion) and graphene-based nanomaterials. In the fabrication of CHIT/Pt modified electrodes, 10 mL CHIT aqueous solution was drop-coated on the surface of Pt electrode. When the CHIT film was solidified, PBS solution was used to rinse the modified electrodes thoroughly to remove the unfixed residues. To improve the stability of device in electrolyte, the exposed regions of the source, drain and gate electrodes without PEDOT:PSS coated or modified composite film should be packaged with a layer of silicone. Other types of functionalized gate electrodes, including CHIT–graphene/Pt

electrode, CHIT–rGO/Pt electrode, Nafion (0.5%, 1.0%, 2.5%)/Pt gate electrodes, Nafion (0.5%, 1.0%, 2.5%)–graphene/Pt gate electrodes and Nafion (0.5%, 1.0%, 2.5%)–rGO/Pt gate electrodes were all prepared by a similar procedure mentioned above.

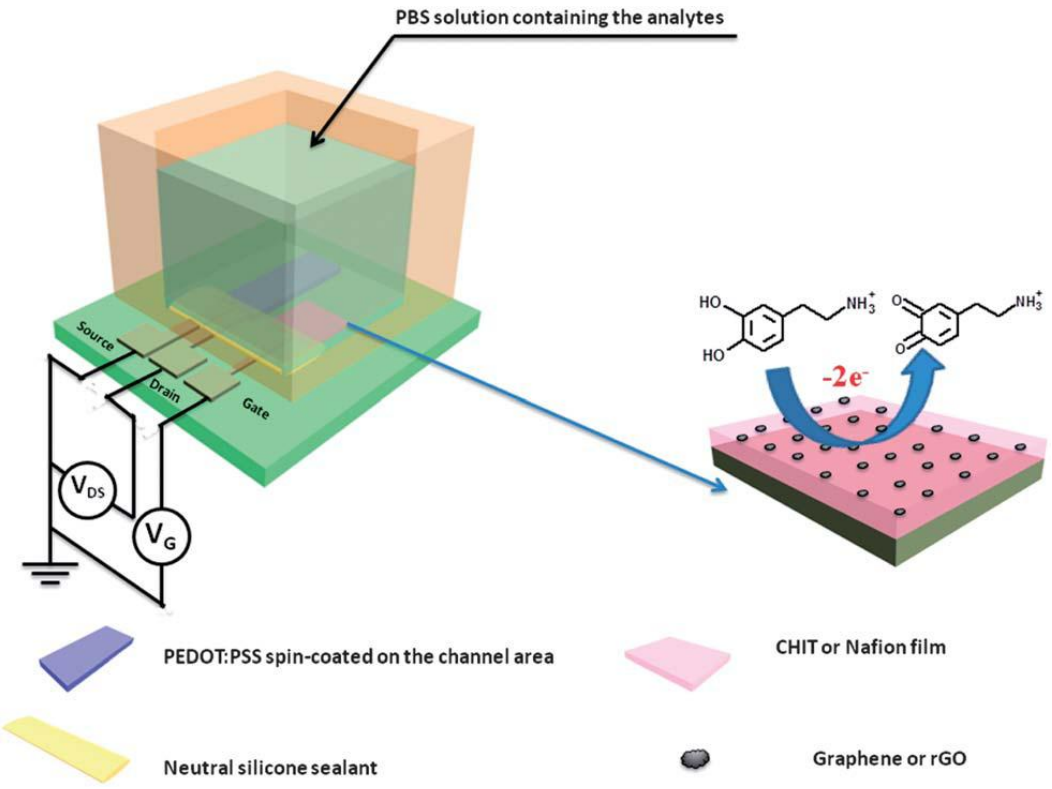

Figure 4.1 Schematic diagram of an OECT-based dopamine sensor modified with Nafion (CHIT) and graphene (rGO) flakes on the Pt gate electrode. The electro-oxidation of dopamine occurs on the surface of the gate (right figure).

4.2.3 Device Characterization

In characterization, the OECT-based sensors were immersed in measurement unit containing 10ml PBS buffer solution, as shown in Fig. 1. The source, drain and gate electrodes of devices were connected to two combined Keithley source meters

(Keithley 2400). The characterization parameters, including gate voltages (V_G) and drain voltages (V_{DS}), were automatically controlled by a Labview program installed in a computer. To obtain different concentrations of DA solutions, original prepared DA solution was diluted by adding design amount of PBS solution. The transfer characteristic, i.e. channel current as a function of gate voltage V_G at a fixed V_{DS} (= 0.05 V), was firstly measured. The gate voltage V_G was changed from 0 to 1.0 V with a sweeping rate of 0.01 V s^{-1}.Then for the real-time investigation of DA testing, the gate voltage and drain voltages were fixed(V_G=0.4 V and V_{DS}= 0.05 V). The channel current of OECT devices was corresponding shifted when the DA concentration was changed. Therefore, the relationship between channel current change and DA concentration can be obtained by performing simple calculation. The detection limit of device was defined by the observable channel current response with the condition of signal/noise > 3.

4.2.4 Working Principle of OECT-based DA Sensors

The channel current I_{DS} of an OECT is given by [39]:

$$I_{DS} = \frac{q\mu p_0 tW(V_p - V_G^{eff} + \frac{V_{DS}}{2})}{LV_p} V_{DS}, (|V_{DS}| \ll |V_p - V_G^{eff}|)$$
$$V_p = qp_0 t / c_i, \quad (4.1)$$
$$V_G^{eff} = V_G + V_{offset},$$

where q is electron charge; m is the hole mobility; p_0 is the initial hole density; t is the active layer thickness, W and L are the geometrical width and length of the channel area, respectively; V_p is the pinch-off voltage, V_G^{eff} is the effective gate

voltage applied on the electrolyte/active layer interface, V_{offset} is the offset voltage, c_i is the effective gate capacitance per unit area.

Figure 4.1 shows the electro-oxidation reaction of DA molecules occurred on the surface of Pt gate electrode of the OECT sensor, which is a two electron transfer process with the sole product o-Dopamine quinone. The sensing mechanism of the OECTs based DA sensor is similar to that of the OECT-based enzymatic sensors reported before [39]. Owing to the electro-oxidation of DA at the modified gate electrode, Faradaic current is generated and consequently potential drops at the electrolyte/gate interface decreased, which in turn increase the effective gate voltage V_G^{eff} given by [72]:

$$V_G^{eff} = V_G + (1+\gamma)\frac{kT}{2q}\ln[DA] + A = \alpha \lg[DA] + B \quad (4.2)$$

in which $\gamma = C_C/C_G$ represent the capacitances ratio between the value of channel/electrolyte interface (C_C) and gate/electrolyte interface (C_G); k is the Boltzmann constant; T is the Kelvin temperature; $[C_{DA}]$ is the molar concentration of DA in the testing environment; A is constant. Therefore, the change of channel current by DA addition could be primarily attributed to the change of effective gate voltage stated by eqn 4.1. According to eqn 4.2, when DA concentraton was increased, V_G^{eff} shifted to a larger value, which would decrease the channel current of OECT. In the selectivity tests, the current responses caused by the interferents (AA and UA) can be explained using the similar mechanisms.

4.3 High Performance of OECT-based DA sensors

4.3.1 OECT with a Pure Pt Gate

The detection limit is a paramount parameter for the assessment of sensor performance. Typically, the detection limit of an electrochemical sensor is defined as the minimum amount of target analyte required to induce an observable and reproducible response with the condition that the corresponding signal to noise ratio (S/N) is larger than 3. Figure 4.2 shows the real-time current responses of an unmodified OECT toward the continuous additions of DA. The device begins to show a current response (signal/noise > 3) when 10 nM DA is added, which is similar to the previously reported ones [72]. The modulation of channel current of device increases with the addition of DA solution. Meanwhile, Figure 4.3 and Figure 4.4 show the responses of the OECT to the additions of AA and UA. The detection limits of OECTs device to AA and UA are 100 nM and 10^3 nM(see Table 4.1), respectively.

According to eqn 4.1, the channel current change is induced by the change of effective gate voltage involved with the electrochemical reaction of analytes at gate electrodes. Based on the transfer curve of the device characterized in blank PBS solution, each different channel current corresponded effective gate voltage can be obtained by fitting the curve. Figure 4.5 shows the variation of effective gate voltage (ΔV_G^{eff}) as a function of the analyte concentrations, in which the linear slope value (a) of fitting curve represent the responses of the device toward specific analytes. The OECTs device showed a response both to AA (286 mV per decade) and UA

(200 mV per decade) within the linear response range of DA addition (242 mV per decade). As the level of AA in human body fluids is much higher than that of DA, the interference responses from AA could be even larger than that induced by DA when the device is used to test the real human samples. In similar, UA level is usually higher than that of DA in human samples, which will cause the same low selectivity problem for practical applications.

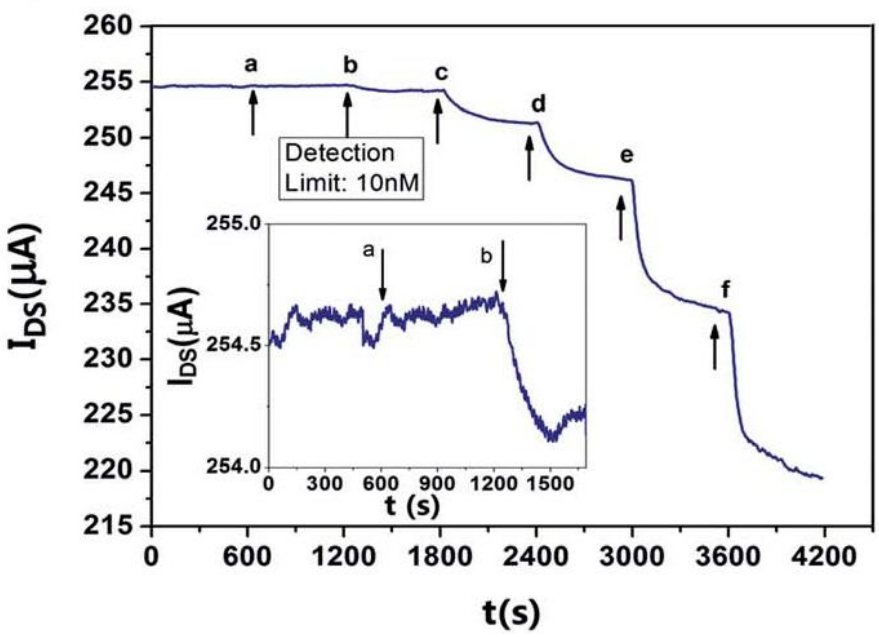

Figure 4.2 Response of the OECT with a pure Pt gate electrode to additions of dopamine in PBS solution. From (a)–(f), the concentrations of dopamine are 1, 10, 50, 100, 500 and 1000 nM, respectively. Inset: enlarged view of the device response to the additions of dopamine at low concentrations.

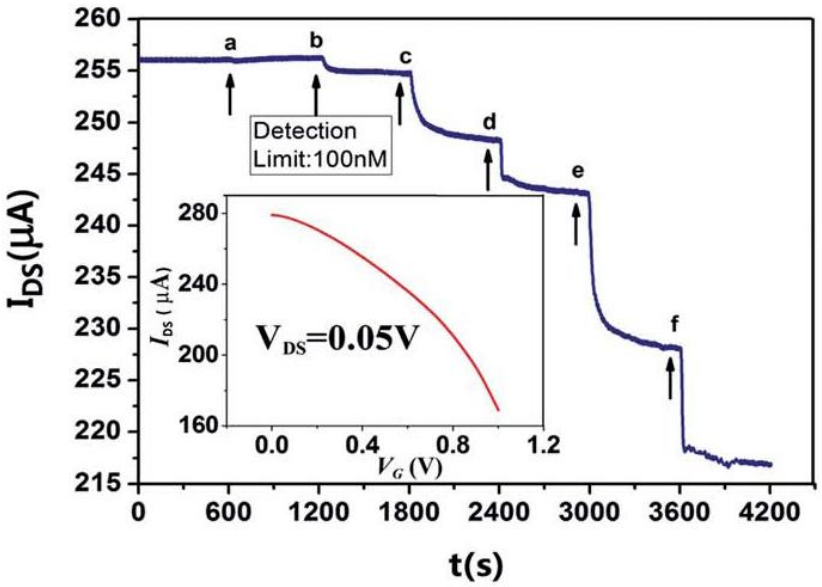

Figure 4.3 Response of the OECT to additions of AA. From (a)–(f), the concentrations of AA are 50 and 100 nM, 1, 5, 10 and 50 μM, respectively. Inset: transfer curve (I_{DS} *vs.* V_G) of the OECT.

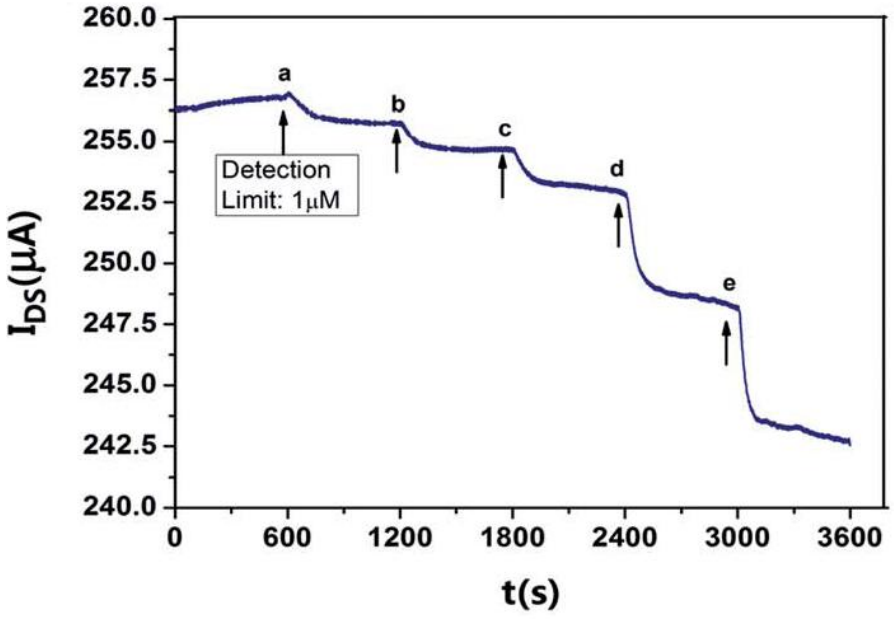

Figure 4.4 Response of the device to additions of UA. From (a)–(e), the concentrations of UA are 1, 5, 10, 50 and 100 μM, respectively.

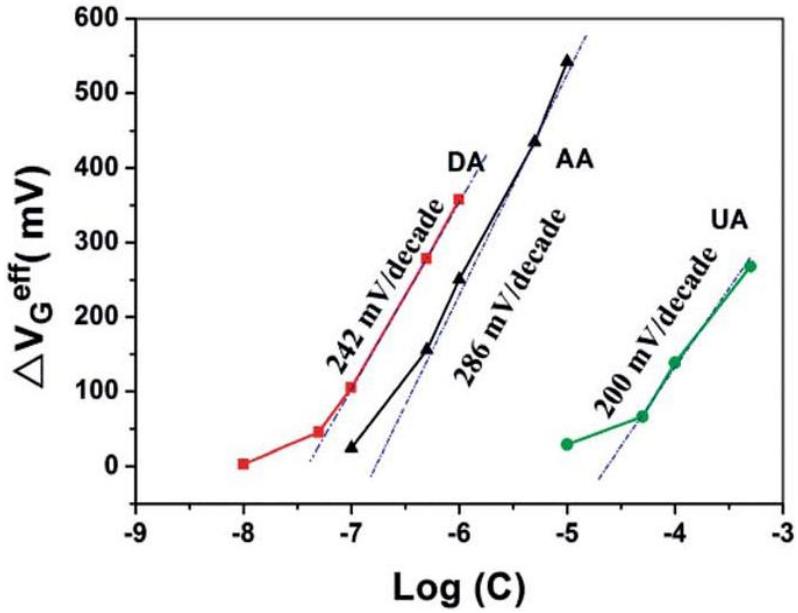

Figure 4.5 The change of effective gate voltage of the device as a function of analyte concentration. Curves: red for DA, black for AA and green for UA.

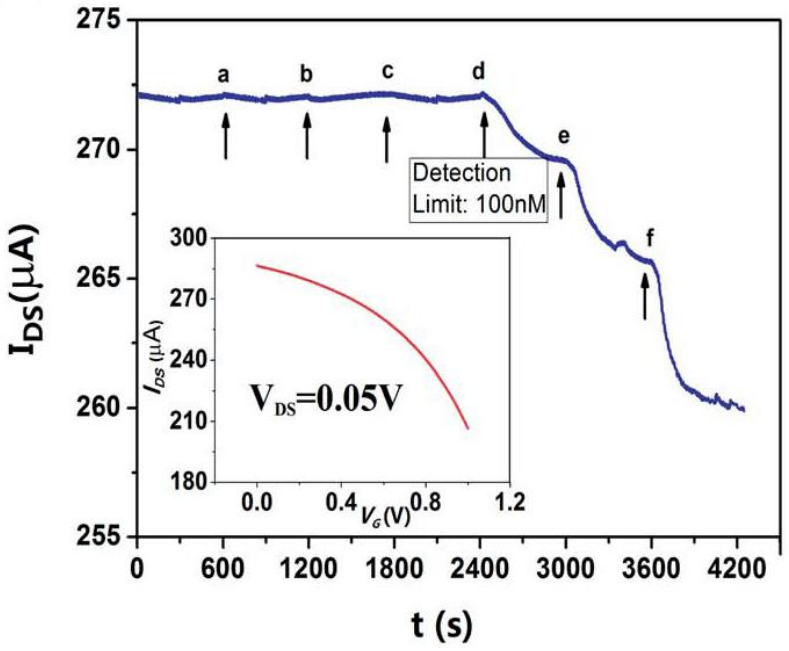

Figure 4.6 Response of the OECT with a Pt/CHIT gate electrode to additions of dopamine in PBS solution. From (a)–(f), the concentrations of glucose are 1, 10, 50, 100, 500 and 1000 nM, respectively. Inset: transfer curve (I_{DS} *vs.* V_G) of the OECT.

4.3.2 OECTs with CHIT Modified Gate

It has been reported that the selectivity of OECTs can be significantly improved by modifying the Pt gate electrode with a thin layer of CHIT. Figure 4.6 shows the current response of the OECT to DA addition. The detection limit of the modified device to DA is about 100 nM, with the sensitivity lower than that of device with pure Pt gate electrode. However, the selectivity of device was much improved, the device show no response until 10^3 nM was added and no observable response even when the concentration of UA was as high as 100 mM. Figure 4.7 demonstrates the relationships between the changes of effective voltage and the concentrations of three analytes. Compared with the unmodified ones, the change of effective gate voltage response of the device to DA detection (146 mV per decade) was largely decreased. The device also shows a reduced voltage response to AA (130 mV per decade) addition. Therefore, the sensitivity of OECT-based dopamine sensor was decreased by modifying the gate electrode with CHIT, which could be attributed to factor that the CHIT film act as the mass diffusion blocking layer and severely prohibit the transfer of DA molecules towards the electroactive sites of Pt electrode [92]. Owing to the electrostatic effects between analytes and modified polymer films, the selectivity of the device was much improved. Since the isoelectric point (pKa) of CHIT (pKa =6.4) is lower than the pH value of PBS solution(pH 7.4), CHIT is in the anionic states within the PBS solution. Similarily, as the pKa values of AA and UA are 4.2 and 5.4, respectively, these electro-active interference elements would also in a negatively charged form in PBS solution. Therefore, AA and UA molecules would

undergo electrostatic repulsion effects near the CHIT film, which largely prohibits the transfer of AA and UA through the CHIT layer to Pt electrode [124]. Although the interference effects from UA is almost eliminated, AA could still induce a significant response of device with the fact that AA concentration is normally 100 times higher than DA concentration in the human samples.

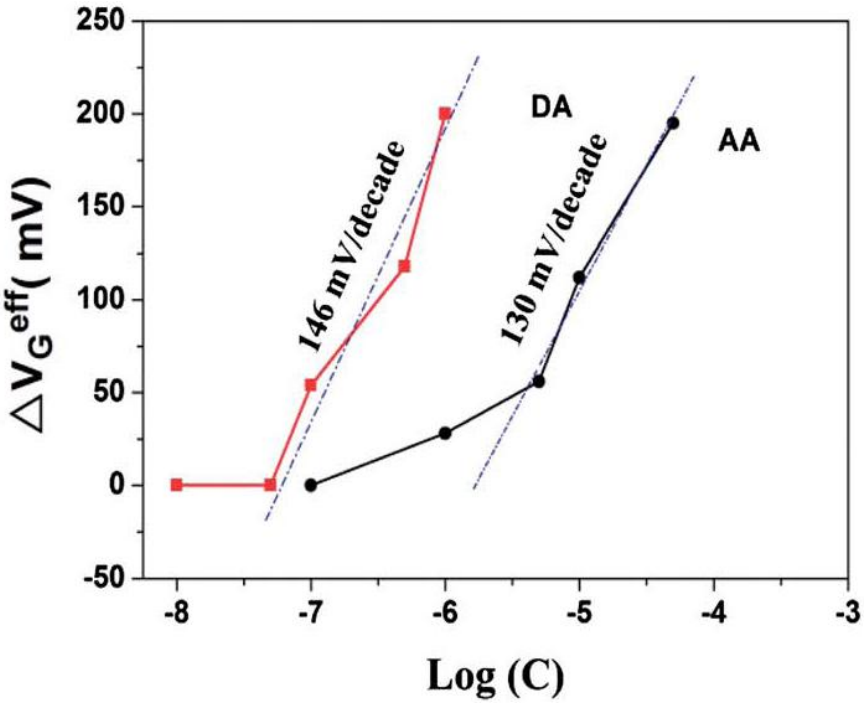

Figure 4.7 The change of effective gate voltage of the device as a function of analyte concentration. Curves: red for DA and black for AA.

4.3.3 OECTs with Nafion Modified Gate

As a perfluorinated ionomer, Nafion has been widely used as the electrode modification material to improve the performance of the device. The current responses of the device modified with 2.5% Nafion demonstrates the highest selectivity feature among the devices we have prepared. Figure 4.8 shows the response of the device to the addition of DA. The detection limit to DA is 50 nM, relatively little worse than that of the device with pure Pt electrode. The detection limit to AA and UA is about 10^4 nM, which is approximately three orders of magnitude higher than that of DA. Figure 4.9 shows the gate voltage changes as a function of three analytes concentration, among which DA addition induce the highest response. Similar to CHIT modified OECTs devices, the selectivity of device could be improved by the electrostatic effects in PBS solutions.

Nafion is a strong acid with a stable Teflon backbone and acidic sulfonic groups and is in a negatively charged form in PBS (pH= 7.4) solution [125], which could largely eliminate the interference effects from the anionic electro-active substances (AA and UA) because of the electrostatic repel interactions between the analytes and Nafion film. More importantly, the Nafion layer could also increase the surface concentration of DA (pKa=8.87, positively charged in PBS solution) via ion-exchange effects and electrostatic attraction interactions, both of which consequently improve the sensitivity and selectivity towards DA detection. The film thickness of Nafion layer dropped on gate electrode, which could be carefully controlled by the

concentration of Nafion solution, could strongly influence the performance of the device.

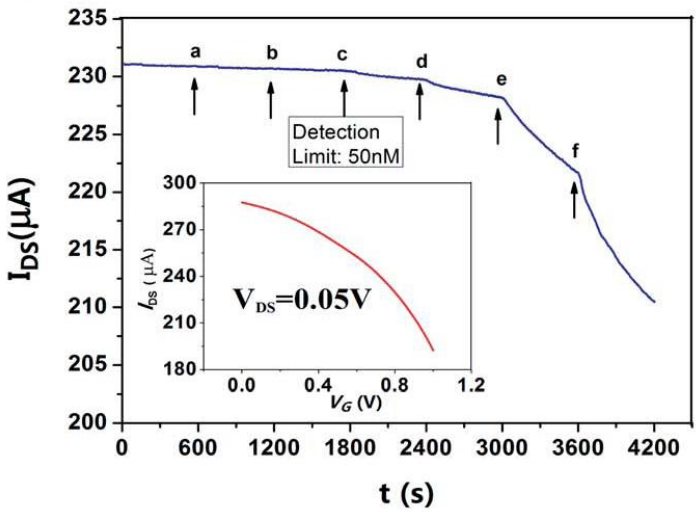

Figure 4.8 Response of an OECT with a Nafion (2.5%)/Pt gate electrode to additions of dopamine in PBS solution. From (a)–(f), the concentrations of dopamine are 1, 10, 50, 100, 500 and 1000 nM, respectively. Inset: transfer curve (I_{DS} vs. V_G) of the OECT.

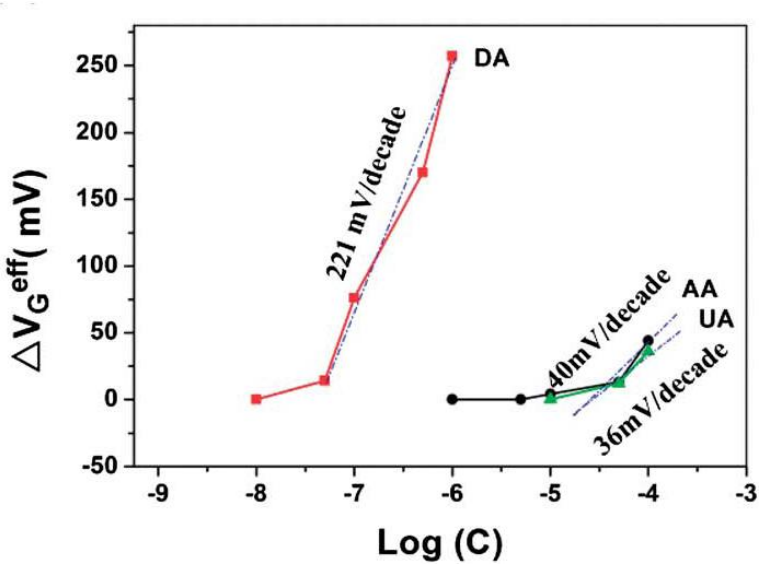

Figure 4.9 The change of effective gate voltage of the device as a function of analyte concentration. Curves: red for DA, black for AA and green for UA.

Table 4.1 Detection limit and the change of effective gate voltage (α) of the OECT-based sensors to the additions of DA, AA and UA

	DA		AA		UA	
Gate electrode	Detection limit (nM)	α_{DA} mV per decade	Detection limit (nM)	α_{AA} mV per decade	Detection limit (nM)	α_{UA} mV per decade
Pt	10	242	100	286	10^3	200
CHIT/Pt	100	146	10^3	130	Nil	Nil
CHIT–graphene/Pt	100	203	10^3	131	10^4	124
CHIT–rGO/Pt	100	99	10^3	74	Nil	Nil
Nafion (2.5%)/Pt	50	221	10^4	40	10^4	36
Nafion (1.0%)/Pt	50	200	10^4	82	10^4	38
Nafion (0.5%)/Pt	50	150	10^3	140	10^3	48
Nafion (2.5%)–graphene/Pt	50	211	10^4	171	5×10^3	74
Nafion (1.0%)–graphene/Pt	5	281	10^4	169	10^3	180
Nafion (0.5%)–graphene/Pt	10	251	5×10^3	187	10^4	119
Nafion (2.5%)–rGO/Pt	50	64	10^3	93	10^4	28
Nafion (1.0%)–rGO/Pt	100	123	500	189	5×10^4	62
Nafion (0.5%)–rGO/Pt	50	74	10^4	87	5×10^3	18

In this work, three different Nafion solution with the concentrations (2.5%, 1.0%, 0.5%) were used to modify the gate electrode and the device with 2.5% Nafion modified gate electrode exhibited the highest selectivity, as shown in Table 4.1. The effective gate voltage of 2.5% Nafion modified device changed 221 mV when the DA level was shifted for one decade, relatively smaller than the device with a pure Pt gate electrode (242 mV per decade). When the concentration of Nafion solution was decreased, the voltage change towards DA was reduced down to 150 mV per decade. In addition, the Nafion-modified devices demonstrated a degraded selectivity when the gate electrode was modified with a thinner Nafion layer. The 0.5% Nafion modified device showed a much lower selectivity in comparison with the 2.5% Nafion modified device. The device with 0.5% Nafion modified might not afford to provide sufficient electrostatic repulsion force to block the anionic based interference, inducing a much deteriorated selectivity. Therefore, the selectivity of OECTs devices

could be improved by modifying the gate electrode with Nafion or CHIT. However, the sensitivity of devices would be dramatically degraded because analytes molecules cannot transport freely through the modified layer to reach the reactive sites on Pt surface.

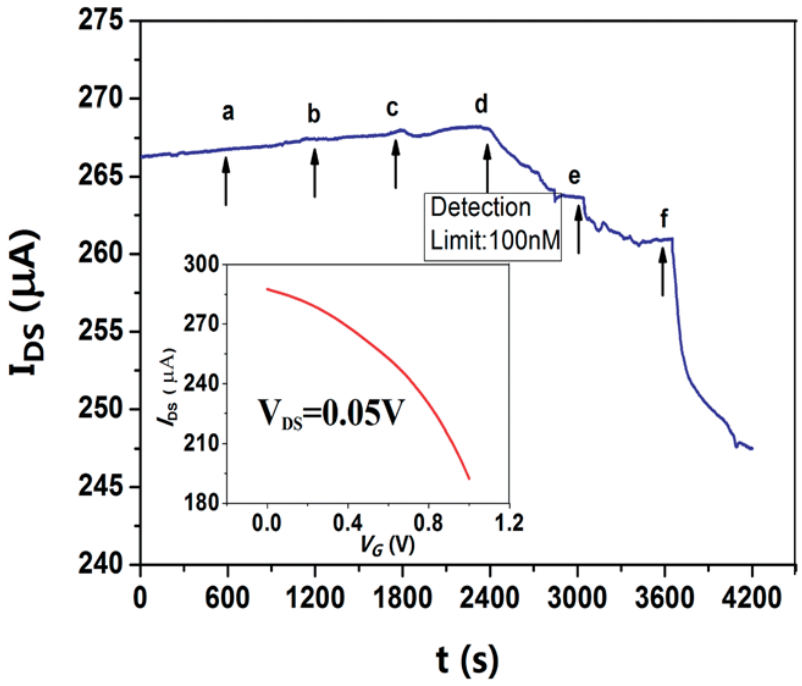

Figure 4.10 Response of the OECT with a CHIT–graphene/Pt gate electrode to additions of dopamine in PBS solution. From (a)–(f), the concentrations of glucose are 1, 10, 50, 100, 500 and 1000 nM, respectively. Inset: transfer curve (I_{DS} *vs.* V_G) of the OECT.

4.3.4 OECTs with CHIT and Graphene co-modified Gate

It has been reported that graphene material is a candidate material for the electrode modification to improve the sensitivity of conventional electrochemical sensors. Therefore, the performance of OECT based DA sensor is expected to be improved

by modifying the gate electrode with graphene materials. CHIT is an ideal material for the immobilization of graphene or rGO flakes onto gate electrodes, primarily due to its excellent film-forming features. Figure 4.10 shows the real-time current response of CHIT–graphene modified device to the additions of DA. The detection limit to DA is about 100 nM, which is approximately one order of magnitude higher than that of pure Pt gate electrode device. Compared with CHIT modified ones, the voltage response of device to three analytes is greatly improved. The improvement in voltage response of the device could be attributed the desirable properties of graphene. More importantly, the chemical prepared graphene flakes are two-dimensional(2-D) material with maximized size effects [126], which could significantly enhance the electrochemical reactivity and enlarge the active surface of electrode. As a result, the electron transfer process is greatly facilitated and the oxidation of the analytes is corresponding improved. In addition, the introduction of graphene flakes can improve the selectivity of device, as shown in Figure 4.11 Compared with the CHIT-modified OECT, the sensitivity to AA was reduced. Figure 4.12 is the SEM image shows the surface morphology of the CHIT–graphene flake composite film. The dark regions in the SEM image represent the uncovered parts of graphene flakes exposed to the air. Since the graphene flakes is electrochemical active and some may not be fully embedded within the CHIT film, electro-oxidation reaction can be directly catalyzed on the surface of graphene flakes without passing through the composite film. Different from AA, DA has a phenyl moiety in its molecular structure, which could help to form the p–p interaction formed between the 2-D planar hexagonal structure of graphene sheets and the

phenyl structure of DA. The intermolecular effect guarantees a feasible electron transfer [127] and thus improves the sensitivity to DA. Additionally, due to the weak p–p conjugation force with the graphene sheets, AA molecule is relatively inert on the surface of graphene sheets. rGO is also investigated for its versatility in sensing applications. Figure 13 shows the change of effective voltage *vs.* the analyte concentrations of the CHIT–rGO modified OECT. The response of device to DA is very low (90 mV per decade) and the selectivity is not improved either. As a result, the rGO is not as useful as the graphene flakes in the OECT based dopamine sensors, primarily due to the high electronic resistance of rGO sheets with oxygen-containing functional groups on the surface[128-130].

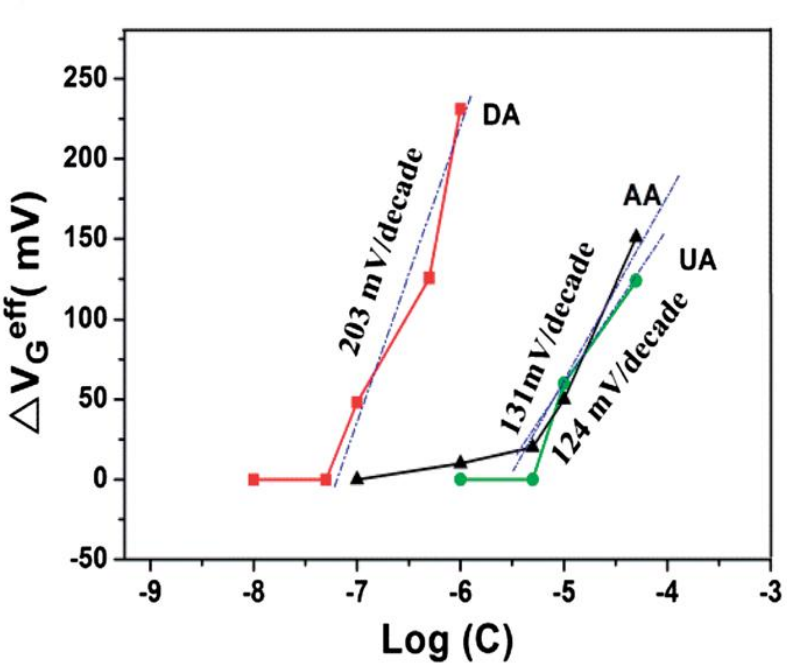

Figure 4.11 The change of effective gate voltage of the OECT with a CHIT–graphene/Pt gate electrode as a function of analyte concentration. Curves: red for DA, black for AA and green for UA.

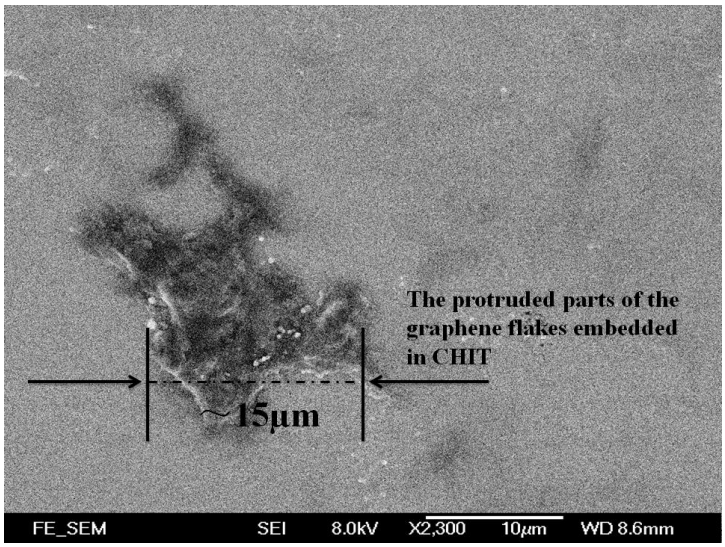

Figure 4.12 SEM image of a CHIT–graphene composite film on a Pt gate electrode.

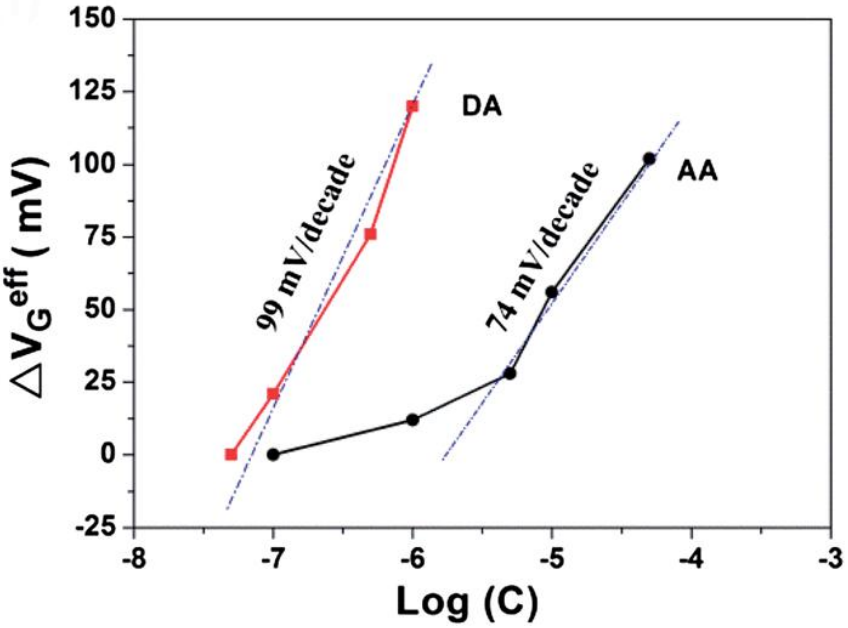

Figure 4.13 The change of effective gate voltage of the OECT with a CHIT–rGO/Pt gate electrode corresponding to different analytes. Curves: red for DA and black for AA.

4.3.5 OECTs with Nafion and Graphene co-modified Gate

Owing to the strong p–p interaction, graphene flakes tend to form irreversible agglomerates in solution, which could be effectively alleviated by the excellent dispersion ability of Nafion [131]. The performance of OECT devices modified with different Nafion (2.5%, 1.0%, 0.5%)–graphene composite film is systematically investigated. Figure 4.14 shows the response of an OECT modified with Nafion (1.0%)–graphene to the additions of DA, AA and UA, respectively. The modified device can detect DA down to 5 nM, which is more sensitive than the device solely modified with Nafion. The detection limits of AA and UA are 10 mM and 1 mM, respectively, approximately three orders of magnitude higher than that of DA. The large difference between the detection limit to DA and its electroactive interference indicates the high selectivity of graphene–Nafion co-modified device for the dopamine detection. The effective gate voltage change of device is about 281 mV for one decade analyte concentration. In addition, the device shows a stable response in a broad linear region from 5 nM to 1 mM DA. As discussed, the thickness of Nafion film is a key parameter for the high performance OECT based dopamine sensors. From table 4.1, Nafion (1.0%)– graphene co-modified devices demonstrated the highest sensitivity to DA among all fabricated devices. If the Nafion film is too thick, analytes can not freely pass through the modified layer and the charge transport process is also hindered, which in turn reduce the sensitivity of device. On the other hand, an insufficient thickness Nafion film may not be able to fully cover the electro-active surface of Pt electrode, inducing the enhanced electron-oxidation of

interferences (UA and AA) on the surface of gate electrode and a worse selectivity of the device. Nafion–rGO modified electrode is also investigated. Figure 4.15 shows the response of the Nafion (1.0%)–rGO modified device to three analytes. The detection limit to DA is about 50 nM, similar to that of the OECTs solely modified with Nafion. The voltage change to DA is 123 mV per decade, which is much lower than that of the device with graphene- modified ones. As the electric conductivity of rGO sheets is normally lower than that of graphene sheets, the charge transport in rGO sheets becomes more difficult, inducing a degraded response to the analytes. The selectivity of the devices is also reduced in comparison with the device modified with Nafion–graphene film. Therefore, rGO is not the prime candidate material for the modification of OECT-based DA sensors. The OECT with graphene flakes and Nafion co- modified shows high sensitivity and sufficient selectivity to dopamine detection in the real application. It has been reported that conventional electrochemical based dopamine sensors show the detection limits ranged tens of nM to several μM [122], which is few orders of magnitude higher than the OECT-based dopamine sensors. The OECT is actually acting as an amplifier that can significantly improve the response of signals induced by the reaction of analytes at gate electrode that is similar to the conventional electrochemical measurement. Because of the ultra-low dopamine level in human body (several nM) [132], the highly sensitive and selective OECT dopamine sensors hold great potential for the practical applications in future.

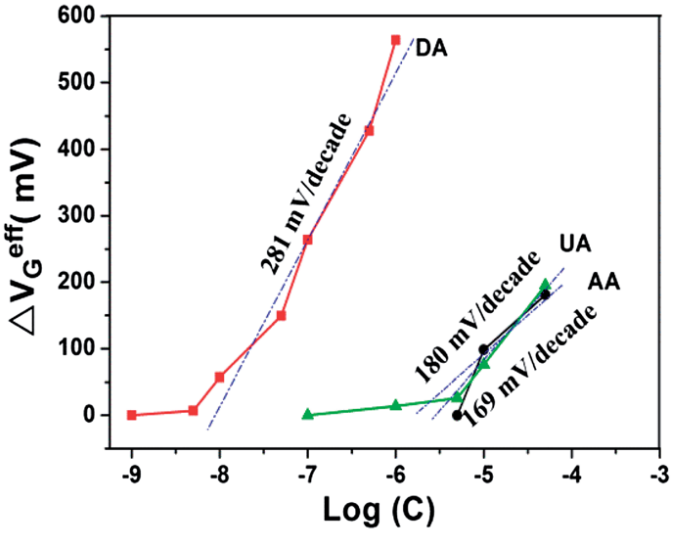

Figure 4.14 The change of effective gate voltage of the OECT with the Nafion (1.0%)–graphene/Pt gate electrode as a function of analyte concentration. Curves: red for DA, black for AA and green for UA.

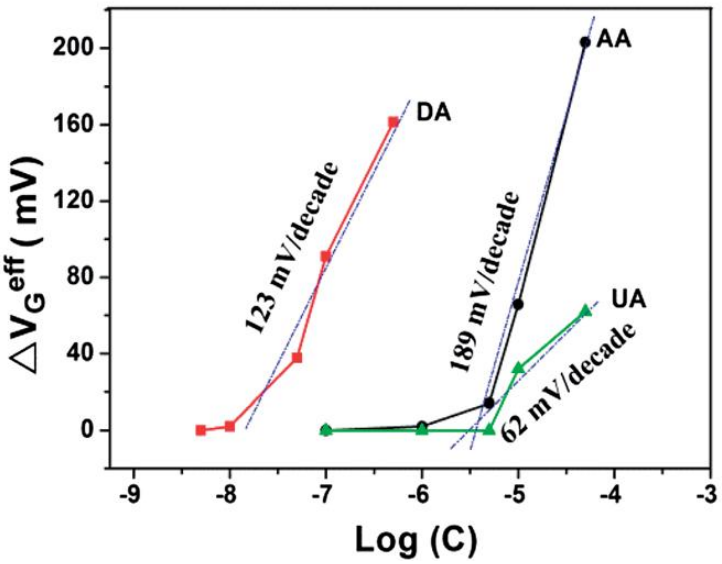

Figure 4.15 The change of effective gate voltage of the OECT with a Nafion (1.0%)–rGO/Pt gate electrode to different analytes. Curves: red for DA, black for AA and green for UA.

4.4 Summary

In summary, the sensitivity and selectivity of OECT-based DA sensors could be simultaneously improved by modifying the Pt gate electrodes with biocompatible polymers (CHIT or Nafion) and graphene-based nanomaterials (graphene or rGO flakes). Modified polymer films can improve the selectivity of device, primarily due to the different electrostatic interactions between the polymer films and the analytes. Graphene flakes were used to improve the sensitivity because of the excellent charge transport properties and high surface to volume ratio of graphene flakes. The devices modified with Nafion (1.0%)–graphene showed the detection limit down to 5 nM, a broad linear region from 5 nM to 1 mM and excellent selectivity to DA. The above results indicate that the OECT-based DA sensors are very promising for point-of-care medical applications in the future. More importantly, the OECTs devices could be easily fabricated by the solution processible process, making it particularly suitable for the disposable sensing applications.

Chapter 5 Multilayer Functionalized Enzyme Electrode for High Performance Uric Acid Sensor Based on Organic Electrochemical Transistors

In this chapter, organic electrochemical transistors with uricase functionalized gate electrodes are successfully fabricated and serve as the high-performance uric acid sensors for the first time. The Pt gate electrodes are modified with enzyme, semiconducting polymer (polyaniline) and graphene-based materials(graphene sheets and graphene oxide), which can simultaneously improve the sensitivity and selectivity of OECT devices. The sensor with UOx-GO /PANI/solution-based graphene/Pt gate electrode can detect uric acid down to 10 nM, which is approximately 4 orders of magnitude lower than that of conventional electrochemical UA sensors using the similar enzyme electrode. The devices show an excellent linearity in the range of 100 nM to 500 μM, covering the normal uric acid level in human sample. Error signals from most-common bio-active intereferents(e.g. glucose, dopamine and ascorbic acic) are largely reduced. The high performance of the devices can be ascribed to the optimized enzyme immobilization techniques. Adopting the same principle, the application of organic electrochemical transistors can be further explored by taking different gate electrode modification techniques.

5.1 Introduction

Uric acid (2,4,6-trihydroxypurine)is the excreted product of purine metabolism in human body. Abnormal uric acid level in body fluids is a good biomarker of several diseases, notably including gout, hyperuricemia, Lesch-Nyhan syndrome, and even cardiovascular disorder [133-135] . Therefore, fast and accurate determination of uric acid is of paramount importance in the diagnosis and treatment of diseases associated with the disordered urine metabolism. Pioneered in the late 19th century by Offer, uric acid analysis has engaged the full attention of the world. Various techniques, such as capillary electrophoresis– amperometry [136], spectrophotometry[137], high performance liquid chromatography (HPLC)[138], chemiluminescence [139] and fluorescence methods [140], etc., have been reported for the measurement of uric acid. However, these methods usually suffer from several drawbacks, including labor-intensive, expensive, time consuming and expert perform.

As an alternative, electrochemical based sensing methods have emerged as a viable way for the effective uric acid analysis due to its attracting properties such as simplicity, sensitivity, specificity, etc[141]. Electrochemical based sensing research is continually providing new insights into the field of uric acid analysis. For instance, Arora *et al* [142] demonstrated an enhanced electrochemical uric acid sensor using the uricase-immobilized electrodes. Glutaraldehyde acted as cross-linker was used to

covalently bind the enzyme to electrode. The enzyme electrodes exhibited a long-term stability and be able to detect uric acid level down to 100 μM. Interferants including excessive urea, ascorbic acid and cholesterol, displayed negligible effects on the reliable determination of uric acid.

Being an important type of organic thin film transistors (OTFTs), organic electrochemical transistors (OECTs) have emerged as the state of the art sensing platform for the realization of more applicable, versatile and robust electrochemical sensors[3]. Normally, OECTs is a three-terminal (source, drain and gate electrodes) device with a thin layer of organic material deposited on the channel area located between source and drain electrodes[57]. Poly(3,4-ethylenedioxythiophene) : poly(styrene sulfonate) (PEDOT: PSS) is the most-common material used in OECTs. Considering the inherent amplification capability of transistors, OECTs serve as the promising candidate used to bridge the gap between bio-chemical reaction and electronic signals. Potential uses of OECTs-based sensors virtually embrace a broad range of bio-chemical analytical tasks, ranging from pH through ions[45], lactate [73], glucose [124] and dopamine[72], to DNA[67], bacteria [71], protein[66], and cells[59], etc.

Typically, an electrochemical-based biosensor consist of two major elements: (i) an immobilization matrix, such as conducting polymers, nanomaterials and self-assembled monolayers(SAMs), etc., used to immobilize the bio-recognition elements(enzyme, antibody, DNA, etc.) on the working electrodes that enables

selective response to particular analytes; (ii) a physicochemical transducers used to deliver the complex biochemical reaction into a readable signal. The redox reaction occurred at the enzyme-modified electrodes thus can be electrochemically detected owing to the electrons transfer between the biomolecule redox site and the electrode. Therefore, enzyme-immobilization plays the critical role in the accurate measurement of uric acid. Several approaches have been developed to effectively immobilize the enzyme, including physical absorption, embedding, and covalent binding, etc,[143, 144]. Conducting polymers are extremely appealing and emerged as the effective matrix for enzyme immobilization[145]. Among various conducting polymers, polyanline (PANI) has attracted attention due to its desirable tunability, high stability and excellent electrochemical property. Kan *et al* [146]reported a polyaniline-uricase biosensor prepared with template process. The PANI template film with moderate cavities could effectively improve the loading of active uricase. Importantly, the modified PANI film can also improve the selectivity of device in uric acid detection. Jiang *et al* [147]fabricated a selective uricase biosensor based on polyaniline synthesized in ionic liquid at high pH. The results indicated that the well-known electroactive interferents have negligible effect on the effective current response. The device demonstrated a good linearity in the range of 1 μM to 1mM uric acid, and the detection limit to uric acid is as low as 1 μM.

Due to its unique properties, including high surface-to-volume ratio, outstanding electro-activity, and desirable tunablility, nanomaterial also serve as the promising candidate matrix material for effective enzyme immobilization. A notable attempt

was the introduction of graphene oxide (GO) onto the enzyme electrode[98]. Typically, highly efficient enzyme-modified electrode can be directly obtained by taking advantage of the covalent bonding between carboxyl acid groups of graphene oxide sheets and amines of enzymes. Therefore, GO is expected to have significant impacts for enzymatic biosensors.

Graphene, another kind of emerging 2-dimensional material, has engaged increasing attention recently. It has been reported that graphene holds great potential for optimized electrode modification in electrochemical sensing applications. Han *et al* [117]demonstrated that graphene could largely improve the electrocatalytic properties of modification layer in UA detection. Sun *et al* [141]also reported the significant role of graphene in the electrochemical detection of uric acid. The electrode co-modified by Pt nanoparticles and graphene demonstrated an excellent performance in UA analysis with a detection limit as low as 0.05 μM.

In this work, we integrate cross-linker or graphene-oxide with uricase to improve the performance of OECT-based UA sensors. Attempt to further enhance the responsibility of device, we also investigate the role of graphene in electrode modification. Modified Pt electrodes UOx-GO(cross-linker)/PANI/Pt and UOx-GO/PANI/Graphene/Pt were prepared and utilized as the gate electrodes of OECTs UA sensors. We found that these modification techniques could significantly improve the sensitivity and selectivity of the device. The OECTs sensors with optimized functional gate electrodes showed a UA detection limit as low as 10 nM,

approximately 4 orders of magnitudes than the conventional electrochemical methods using a similar modified electrode. The high sensitivity of OECT-based UA sensor guarantees a sufficient response to the trace amount of analyte in the highly diluted biological sample, in which the concentration of most interefering elements are diluted to a negligible level.

5.2 Fabrications and Measurements of OECTs

5.2.1. Materials

Uricase(UOx) (>3U mg^{-1}) was purchased from Worthington Biochemical Corporation and stored at -20 ℃. Glucose, dopamine, AA and UA were purchased from Sigma-Aldrich Co. Polyaniline (PANI) (5 wt. %,dispersion in xylene), Phosphate buffered saline (PBS) solution (pH 7.4), and PEDOT:PSS aqueous solution were purchased from Sigma-Aldrich Co.and stored at 4 ℃. The cross-linker glutaraldehyde solution (Grade II, 25% in H_2O) from Sigma-Aldrich Co. was used as received. Graphene and graphene oxide(GO) used as received were prepared by the chemical methods reported before. For purpose use, polyaniline solution was diluted to 0.5% by using the xylene, glutaraldehyde solution was diluted to 1% by using the de-ionized water. UOx solution (～50 U/ml) was prepared by the PBS solution. Glutaraldehyde-UOx mixed solution was prepared by adding 2 volumes UOx solution to 1 volume glutaraldehyde solution and then the mixed solution was sonicated for 5 mins. GO-UOx mixed solution was prepared by mixing 1 volume GO with 1 volume UOx solution and followed by 5 mins sonication.

5.2.2 Device Fabrication

Figure 5.1 shows the schematic structure of the OECT-based uric acid sensor using PEDOT: PSS as the active layer. Glass slides and flexible polyethylene terephthalate (PET) substrates were used as the substrates in the fabrication of devices. Patterned Ti/Pt (thickness: ～10 nm/100nm) source, drain and gate electrodes were deposited on substrates by RF magnetron sputtering through a shadow mask. The thin Ti layer was served as the adhesion layer for Pt electrodes. The width to length ration of the channel was 6.0 mm/0.2mm. For the fabrication of devices, the substrates with patterned electrodes were rinsed throughoutly with acetone, 2-propanol and DI-water. Attempt to improve the adhesion of the PEDOT: PSS layer, the substrates were treated with oxygen plasma for several minutes(5 mins for glass substrates, 3 mins for PET substrates). Then the thin PEDOT: PSS layer with a thickness approximately 80 nm was spin-coated on the patterned channel area. Finally, these devices were moved to the glove box filled with high purity N_2 for thermal annealing (200 ℃, 1h).

For the fabrication of high performance uric acid sensors, the Pt gate electrodes of OECT devices were modified with PANI, graphene oxide(GO)/cross-linker, graphene and uricase. In preparation of UOx-Glutaraldehyde /PANI/Pt functionalized electrodes, 5μl diluted PANI solution was firstly drop casted to fully cover the Pt electrode and dried at 4 ℃ in refrigerator, then 10μl glutaraldehyde – UOx mixed solution was dropped on the surface of the dried PANI layer. The

modified electrode was kept in refrigerator for 12 h to be solidified. UOx-GO/PANI/Pt and UOx-GO-/PANI/(CVD or solution)graphene/Pt functionalized electrodes were prepared by the similar approach. Before characterization, the modified gate electrodes were rinsed with DI-water to remove the unanchored residues.

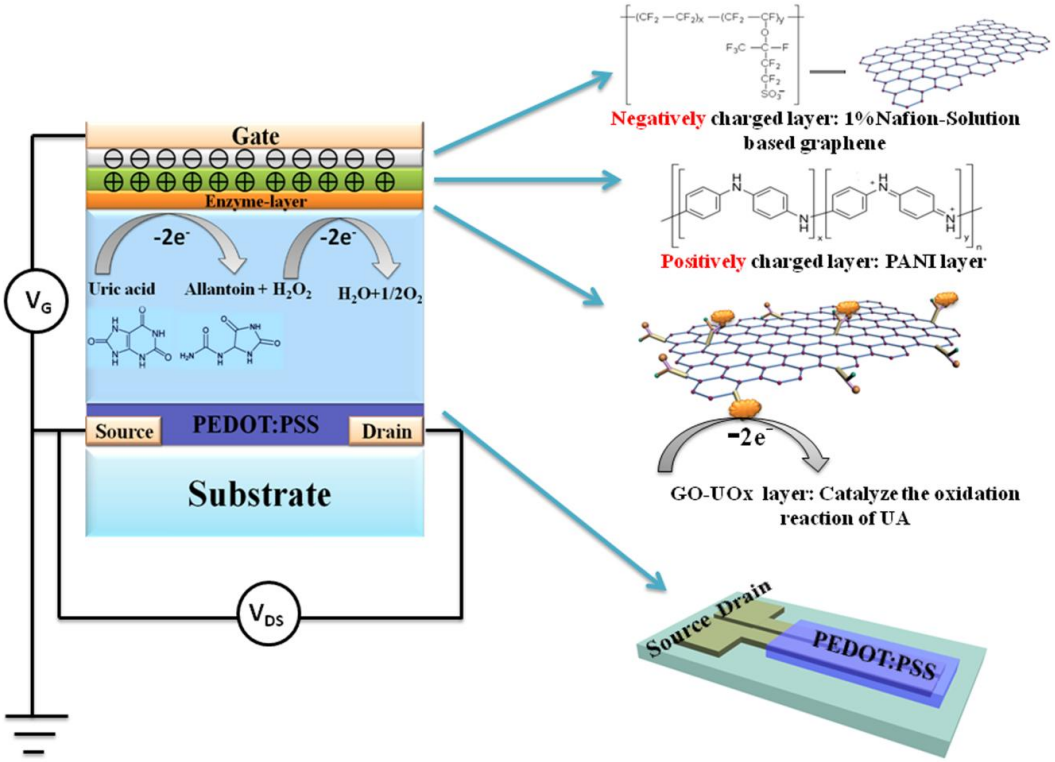

Figure 5.1 Schematic pictures of the OECT-based UA sensor. The electro-oxidation of uric acid occurs at the surface of the modified enzyme gate electrode.

5.2.3 Device Characterization

PARSTAT 2273 electrochemical integrated test system (Princeton Applied Research, USA) was used for the cyclic voltammetry (CV) and amperometric measurements of OECT devices. Individually modified gate electrodes immersed in the stirred PBS solution were employed as the working electrodes. In these measurements, an Ag/AgCl (sat. KCl) electrode and a Pt foil served as the reference electrode and counter electrode respectively. The amperometric i-t curve was obtained by a consecutive addition of uric acid solution into bulk PBS solution at fix time. The electrical measurements of OECT based uric acid sensors were conducted with Keithley source meters (Keithley 2400). The three electrodes of devices were connected to two Keithley 2400 meters controlled by a Labview program. For transfer characteristic, V_{DS} was fixed at 0.05V, channel current (I_{DS}) was measured as a function of V_g. In the measurements of response of modified devices to various analytes in electrolyte, V_{DS} was fixed at 0.05V, V_g was fixed at 0.4V.

5.2.4 Working Principle of OECT-based UA Sensors

PEDOT:PSS is the most-widely used p-type organic semiconductors in OECT-based sensors[60]. PEDOT:PSS demonstrates a wide range of conductivity due to the varied doping level of counter ions. Under the effect of a positive gate voltage, cations in electrolyte can be injected into PEDOT:PSS active layer[45]. The migration of cations can be regarded as a de-doping process that reduces the density of hole and thus reduce the electric conductivity of deposited polymer layer. Details

on the de-doping process can be found using the following electrochemical reaction[148]:

$$n(PEDOT^+:PSS^-) + Mn^+ + ne^- \underset{\text{Oxidation}}{\overset{\text{Reduction}}{\rightleftharpoons}} nPEDOT_0 + Mn^+:nPSS^- \quad (5.1)$$

where Mn^+ represents cation from electrolyte, n is the number of charge of cation, e- is an electron. The injection of Mn^+ to the active layer facilitates the reduction of oxidized $PEDOT^+$ to neutral state ($PEDOT^0$), leading to a decreased conductance of the channel.

According to eqn 5.1, the doping level of conducting polymer is quantitatively determined by applied effective gate voltage. Therefore, the channel current I_{DS} of active layer in an OECT device can be given [3, 39]:

$$I_{DS} = \frac{q\mu p_0 tW}{LV_p}\left(V_p - V_g^{eff} + \frac{V_{DS}}{2}\right)V_{DS}, \quad \left(|V_{DS}| << \left|Vp - V_g^{eff}\right|\right)$$

$$V_p = qp_0 t/c_i \quad (5.2)$$

$$V_g^{eff} = V_G + V_{off\,set},$$

where q is electronic charge of the carrier, p_0 is the initial hole density in active layer, μ is the mobility of hole, t is the thickness of organic thin film, V_p is the pinch-off voltage, V_g^{eff} is the applied effective gate voltage, and V_{offset} is an offset voltage related to analytes, W and L are the width and length of channel, respectively. c_i is the effective capacitance per unit area of the OECT, for simplicity, a constant value is assumed for c_i.

The underlying operation mechanism of an OECT-based uric acid sensor can be attributed to the varied interfacial potential drops at the interface of electrolyte/gate or electrolyte/semiconductor. In measurements, H_2O_2 is generated by the bio-catalyzed reaction of uric acid demonstrated in Figure 5.1. H_2O_2 undergo further oxidation and shuttle two electrons to the gate electrode. The electron flow induces a Faradaic current at the gate electrode and decreases the potential drop at the gate/electrolyte interface. Accordingly, the variations of chemical potential (ΔV_G) at the electrolyte/gate interface demonstrate a logarithmic dependence on the concentration of H_2O_2 and can be described in the Nernst equation form [39]:

$$E_{Nernst}=E_0+\frac{kT}{ne}\ln\left(\frac{[Ox]}{[Red]}\right)\Rightarrow \Delta E_{Gate/Electrolyte}=\frac{kT}{2e}\ln[H_2O_2]+\text{constant A} \qquad (5.3)$$

where k is Boltzmann's constant, e is charge, T is temperature and [H_2O_2] is the concentration of H_2O_2.Since the measurement is performed in the PBS buffer solution in the lab atmosphere , the concentration of [H] and [O_2] are assumed to be a constant value. As a result, the constant A in eqn 5.3 represent the integrated result of the E_0, [H] and [O_2] in the Nernst equation.

It has been reported that V_{offset} in eqn 5.3 originates from the ΔV_G described by Nernst equation and is multiplied by the factor of $(1+\gamma)$, γ is the ratio between the capacitance of gate and the capacitance of channel. Therefore, V_g^{eff} can be expressed using the form:

$$V_g^{eff}=V_g+(1+\gamma)\frac{kT}{2e}\ln[H_2O_2]+\text{constant B} \qquad (5.4)$$

Thus, the changed interfacial potential drops can modulate the effective gate voltage applied on device. According to the reaction, the concentration of H_2O_2 is proportional related to the concentration of UA, therefore the above mentioned equation can be further transformed into following simplified form:

$$V_g^{eff} = \alpha_{UA} \ln[UA] + \text{constant C} \quad (5.5)$$

Where [UA] is the concentration of the uric acid, constant α_{UA} is the slope of the fitted curve, constant C is related to other factors.

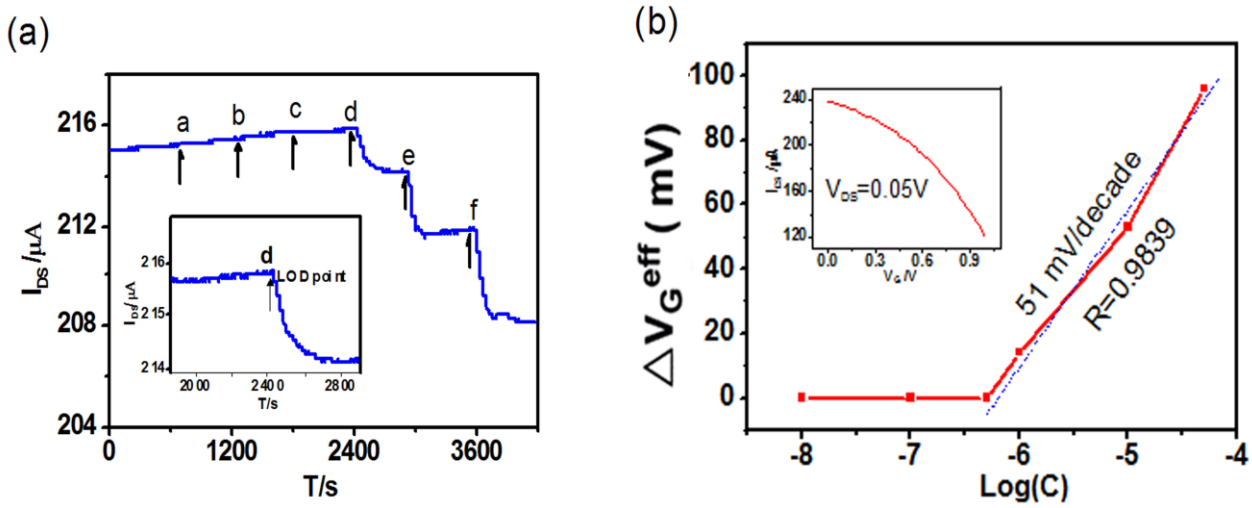

Figure 5.2 (a) Response of the OECT with pure Pt gate electrode to additions of UA in PBS solution. From a-f, the concentrations of UA are 10, 100, 500, and 1000nM, 10 and 50μM, respectively. Inset: Enlarged LOD point at d. (b) The change of effective gate voltage of the device as functions of UA concentrations. Inset: transfer curve (IDS vs VG) of the OECT.

5.3 High Performance of OECT-based UA sensors

5.3.1 High Sensitivity of the OECT-based UA sensors

Optimized enzyme electrodes for UA detection have been extensively investigated. Various enzyme immobilization approaches, either physically or chemically, have been used to immobilize the uricase onto the surface of gate electrode. Figure 5.2a shows the current response of unmodified OECTs device to UA and Figure 5.2b is the dependence of ΔV_g^{eff} as a function of UA concentration using pure Pt working electrode. The device showed no detectable I_{DS} change until 1 μM UA is added. The variation of effective gate voltage(ΔV_g^{eff}) is about 51mV/decade. As a result, the unmodified device demonstrated a low sensitivity even poorer than that of the conventional electrochemical sensors. Since the detection system is free of enzyme, the modulation of I_{DS} is induced by the oxidation of uric acid catalyzed by the highly efficient catalytic platinum electrode.

Attempt to improve the performance of UA sensors, the uricase(enzyme) is immobilized onto the working electrodes. Low detection limit, or low limit of detection(LOD), as indicated previously that the corresponding signal to noise ratio should be larger than 3 (S/N > 3), is used to evaluate the sensitivity of sensor device[72, 149]. The device using the UOx/PANI/Pt gate electrode demonstrates a low detection limit down to 300 nM and varied 143 mV for one decade, which is nearly three times larger than that of unmodified devices. The functional electrode was prepared by immersing the PANI/Pt electrode into the UOx solution for 4h in 4℃. Therefore, the enzyme was physically absorbed onto the surface of PANI layer.

The improvement in sensitivity can be attributed to the integration of uricase into the OECT sensors. As shown in Figure 5.1, uricase can lower the activation energy of UA oxidation and thus significantly accelerate the catalytic reaction. Since the PANI is in the form of highly conductive emeraldine salt[150], the sandwiched conductive polymer layer can effective shuttle the electrons between the redox center of enzyme and Pt gate electrode and induce large I_{DS} changes. Although uricase demonstrate impressively high sensitivity and selectivity to the UA oxidation reaction, the improvement in performance of enzyme electrode based on the physically absorption scheme is quite limited, which can be attributed to the week adhesion force between the enzyme and PANI layer. The week van der Waals forces occasional with limited hydrogen bonds in absorption is unable to provide high stability for the long-time operation in solution.

Interestingly, chemical methods involve with covalent bonding has emerged as the promising approach for the enhanced enzyme immobilization[151]. Figure 5.3a and Figure 5.3b demonstrate the UA-dependent responses of the device using UOx-glutaraldehyde/PANI/Pt functionalized electrodes. This kind device shows a much improved sensitivity, with a low detection limit down to 30 nM. The ΔV_g^{eff} shift per decade is 130mV and is much larger than that of the device using the pure Pt gate electrode. The significantly improved sensitivity is relied on the optimized enzyme electrodes. Glutaraldehyde, a small-weight organic compound with functional groups at both ends, is one of the most-commonly used cross-linker in chemistry. Highly efficient and stable enzyme-electrode for UA detection can be

achieved by taking advantage of the covalent bonding between the functional groups of glutaraldehyde, PANI and protein of enzyme.

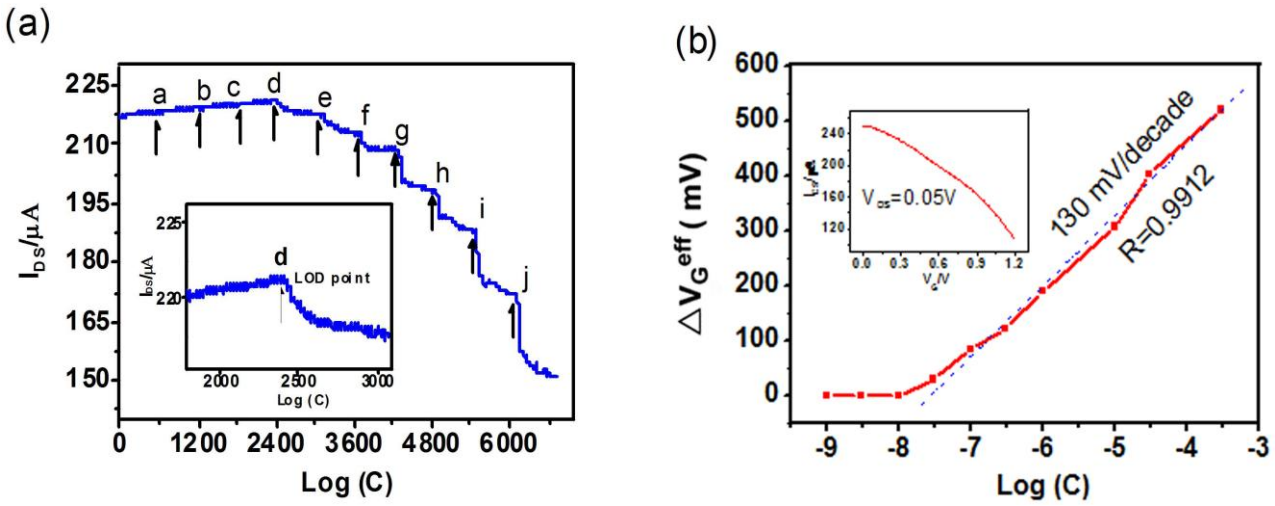

Figure 5.3 (a) Response of the OECT with glutaraldehyde -UOx/PANI/Pt functionalized electrodes gate electrode to additions of UA in PBS solution. From a-j, the concentrations of UA are 1,3,10, 30,100,300 and 1000nM, 10 30 and 500μM, respectively. Inset: Enlarged LOD point at d. (b) The change of effective gate voltage of the device as functions of UA concentrations. Inset: transfer curve (IDS vs VG) of the OECT.

Due to its desirable properties, 2-dimensional nanomaterials have also emerged as the candidate matrix material for effective enzyme immobilization[152]. OECT-based UA sensors employing the UOx-GO/PANI/Pt functionalized electrodes demonstrated high performance in the detection of UA. The device with GO modified enzyme electrode could used to detect UA down to 10nM, approximately 4 orders of magnitude lower than that of conventional electrochemical UA sensor using a similar enzyme electrode and 3 orders of magnitude lower than that of comparative amperometric measurement of the enzyme electrode using the same

modification technique. The ΔV_g^{eff} shift per decade is increased to 165mV. The remarkable improved sensitivity can be ascribed to the introduction of GO into the functional electrodes for the efficient enzyme immobilization. GO is a 2-dimensional graphene sheet with oxygen-containing functional groups anchored on the surface of sheet. These functional groups can readily react with the amine groups of protein enzyme and the reactive moieties of conductive PANI layer, leading to an optimized enzyme immobilization via the effective chemical covalent bonding. In addition, the weak physical van der Waals forces between the benzene rings of PANI and GO sheets can also improve the enzyme anchoring effect on working electrode[153]. Therefore, GO is a high performance material for the enzyme immobilization in UA detection. Figure 5.4 shows the ΔV_g^{eff} shifts of the devices using different kinds enzyme electrodes when 100 μM uric acid is added. Three identical electrodes are fabricated for each condition. Error bar shows the standard deviation of the ΔV_g^{eff} shifts for the three kind electrodes. The result indicates that the device using the UOx-GO/PANI/Pt modified electrodes demonstrate the largest ΔV_g^{eff} shifts when designed amount of UA is added. In sum, GO plays a critical role in enzyme immobilization for UA detection and demonstrate a much improved performance even better than that of the commonly-used cross-linker.

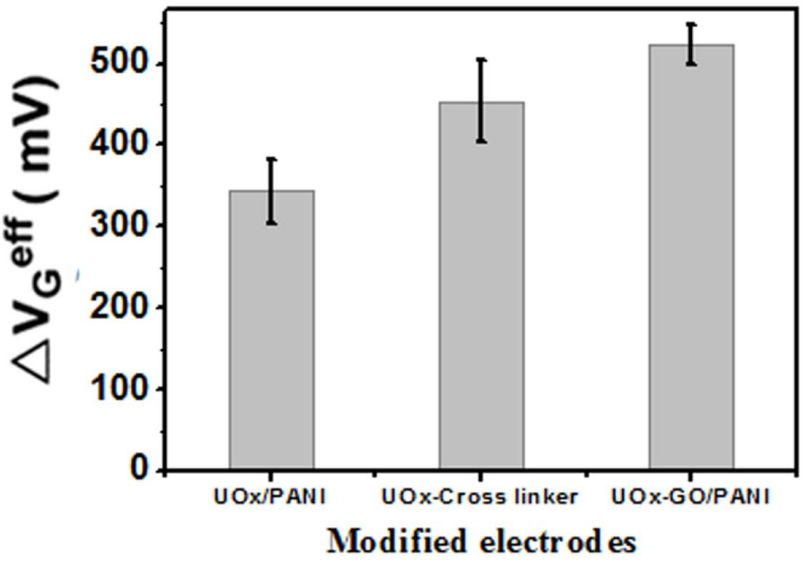

Figure 5.4 ΔV_g^{eff} shifts of the devices using different kinds enzyme electrodes when 100 μM uric acid was added. 1: UOx/PANI/Pt 2:UOx-Cross linker/PANI/Pt 3:UOx-GO/PANI/Pt.

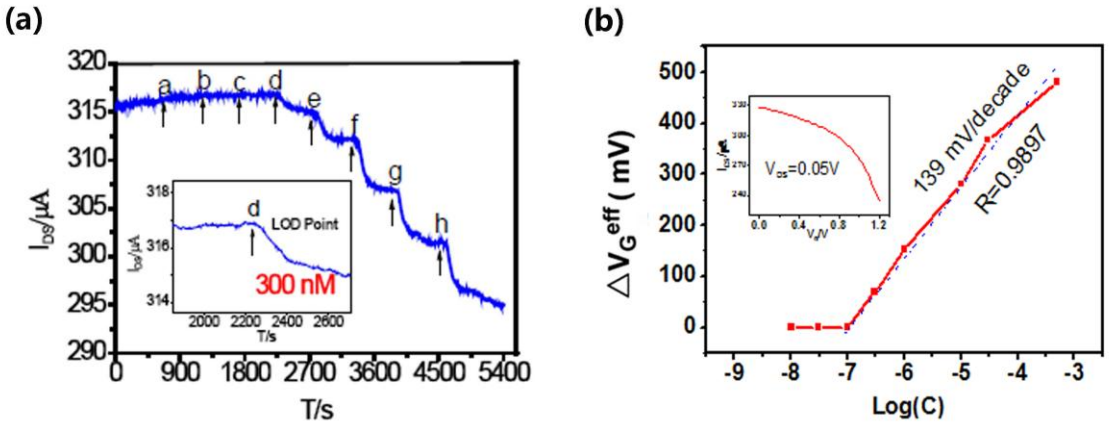

Figure 5.5 (a) Response of the OECT with UOx-GO /PANI/CVD-based graphene/Pt functionalized electrodes gate electrode to additions of UA in PBS solution. From a-h, the concentrations of UA are 10, 30,100,300 and 1000nM, 10, 30 and 500μM, respectively. Inset: Enlarged LOD point at d. (b) The change of effective gate voltage of the device as functions of UA concentrations. Inset: transfer curve (I_{DS} vs V_G) of the OECT. Inset: transfer curve (IDS vs VG) of the OECT.

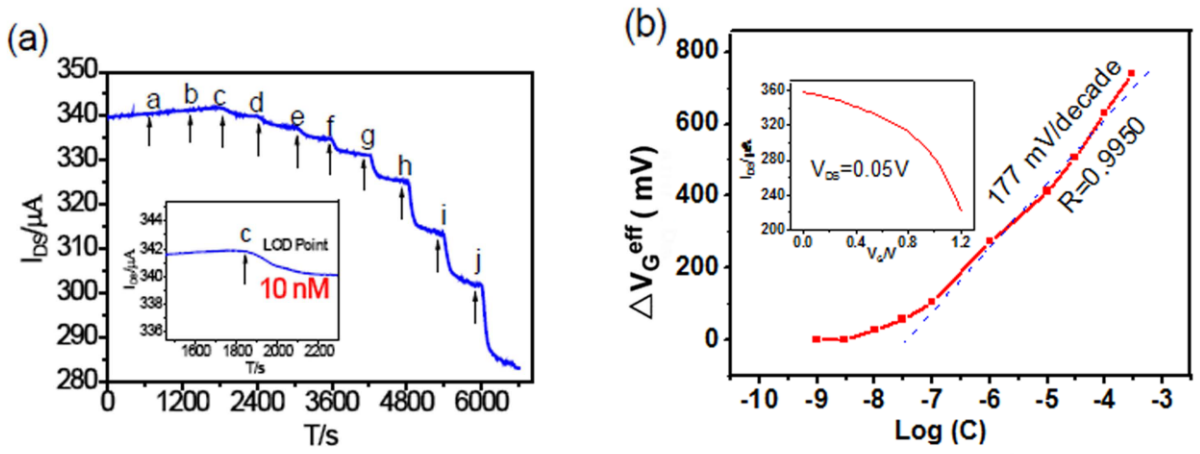

Figure 5.6 (a) Response of the OECT with UOx-GO /PANI/solution-based graphene/Pt functionalized enzyme electrode to additions of UA. From a-j, the concentrations of UA are 1,3,10, 30, 100 and 1000 nM, 10, 30,100 and 500μM, respectively. Inset: Enlarged LOD point at c. (b) The change of effective gate voltage of the device as functions of UA concentrations.

Owing to its attracting properties, graphene has engaged increasing attention and hold great potential in the electrochemical-based sensing applications. Figure 5.5 demonstrates the performance of the device with UOx-GO /PANI/CVD-based graphene/Pt modified gate electrode and Figure 5.6 shows the UA-dependent responses of the device with UOx-GO /PANI/solution-based graphene/Pt modified gate electrode. The low detection limit of CVD-based graphene modified device is about 300 nM, which is much poorer than that of device with solution-based graphene modified gate electrode. The OECT UA sensor with UOx-GO /PANI/solution-based graphene/Pt modified gate electrode shows an ultra-low UA detection limit down to 10 nM and a high ΔV_g^{eff} shift up to 177 mV/decade. More importantly, this kind device shows an excellent linearity (R=0.99501)ranging from

100 nM to 500 μM. Since the normal level of uric acid in human body is in the range of 100 to 450μM, this type OECT-based UA sensor enables the direct measurement of UA in human sample with a satisfactory response time approximately less than 50 s. In sum, UOx-GO /PANI/solution-based graphene/Pt modified enzyme electrode shows the best performance among all fabricated enzyme electrodes.

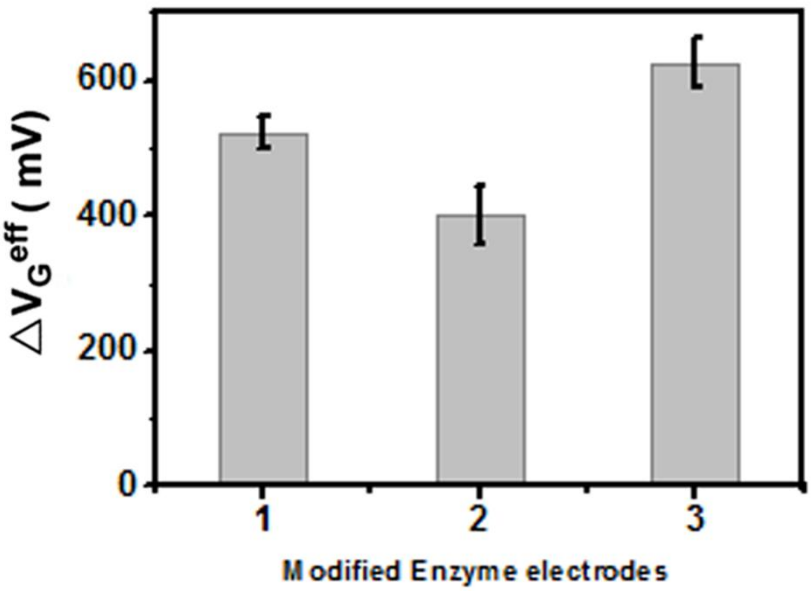

Figure 5.7 $\triangle V_g^{eff}$ shifts of the devices using different kinds enzyme electrodes when 100 μM uric acid was added. 1: UOx-GO/PANI/Pt 2: UOx-GO/PANI/CVD-graphene/Pt 3:UOx-GO/PANI/solution-graphene/Pt.

The impressive high performance of UOx-GO /PANI/solution-based graphene/Pt modified enzyme electrode can be ascribed to the unique role of graphene[154, 155]. Graphene sheets have a remarkably electron mobility at room temperate, which can readily facilitate the transportation of the electrons generated in the oxidation of

peroxide. In addition, the introduction of solution-based graphene can enhance the electrocatalytic activity of the modified enzyme electrode and thus improve the rate of bio-catalyzed reaction. However, CVD-based graphene sheet modified device shows limited improvements in UA measurements. In the preparation of CVD-based graphene modified device, a whole CVD-grown graphene sheet(about 5mm×5mm) was transferred to fully cover the Pt gate electrode. Therefore, the generated hydrogen peroxide unable to reach the Pt surface directly and the rate of oxidation reaction catalyzed by the highly catalytic-active Pt electrode would be significantly prohibited. Figure 5.7 demonstrates the 100 μM UA induced response of the device with UOx-GO /PANI/ Pt, UOx-GO /PANI/CVD-based graphene/Pt and UOx-GO /PANI/solution-based graphene/Pt modified enzyme electrodes, respectively. The experiments shows that UOx-GO /PANI/solution-based graphene/Pt enzyme electrodes demonstrate the largest response (ΔV_g^{eff} shift≈626mV) among these three type enzyme electrodes when 100μM UA is added. While CVD based enzyme electrode shows a performance(ΔV_g^{eff} shift≈400mV) even poorer than that of the enzyme electrode without graphene modification(ΔV_g^{eff} shift≈523mV). Therefore, introduction of solution-based graphene into the modified enzyme electrode can improve the performance of sensor device while CVD-based graphene can deteriorate the performance of sensor device in UA measurements.

More importantly, those modified enzyme electrodes demonstrated high stability in characterization and storage process. Under the effect of applied gate voltage, channel current reached a stable constant value within a short time. The high stability

of device in the liquid electrolyte can be attributed to the attracting properties of the deposited PEDOT: PSS layer covering the channel. PEDOT: PSS is a degenerately doped semiconducting material widely used in the organic electronic[149, 156]. Stable solid PEDOT: PSS film can be formed using necessary processing processes (e.g. drying, annealing and post-annealing, etc.) and demonstrates reliable electronic properties in liquid solutions. The stability of organic semiconducting layer can be further enhanced by adding the cross-linker to organic material to optimize the morphology in film-forming. Therefore, the device can be reused for many times regarding its high stability. It also interesting to note that after two weeks storage in refrigerator(4 ℃), the device still remain an excellent performance without any significant degradation.

For comparative study, we also perform the electrochemical characterization of UOx-GO /PANI/solution-based graphene/Pt enzyme electrodes using the conventional cyclic voltammograms and amperometric measurements. Figure 5.8 shows the electrochemical performance of UOx-GO /PANI/solution-based graphene/Pt enzyme electrode in pure PBS solution(Line I) and PBS solution containing 100 μM UA (Line II). The functionalized electrode shows no visible redox in pure PBS solution while demonstrates an obvious redox peak in PBS solution containing 100 μM UA *vs* Ag/AgCl. The redox peak of line II is located at 0.42V, which is corresponded to the oxidation of hydrogen peroxide generated by the catalyzed UA reaction[72]. Figure 5.9 is the amperometric response of device upon the continuous addition of UA. The measurement system demonstrate no

detectable signal until 3 μM UA is added, which is much poorer than that of OECT-based UA sensor using the same kind modified enzyme electrode (10 nM). Typically, OECT-based sensor is consist of a sensor can selectivity detect the target event and an amplifier that can significantly enhance the induced signals. The variation of interfacial drops induced by analytes can modulate the effective gate voltage applied on device and remarkably change the channel current up to several orders of magnitude. Therefore, transistor-based UA sensors show a much higher sensitivity in comparison with the conventional electrochemical-based techniques.

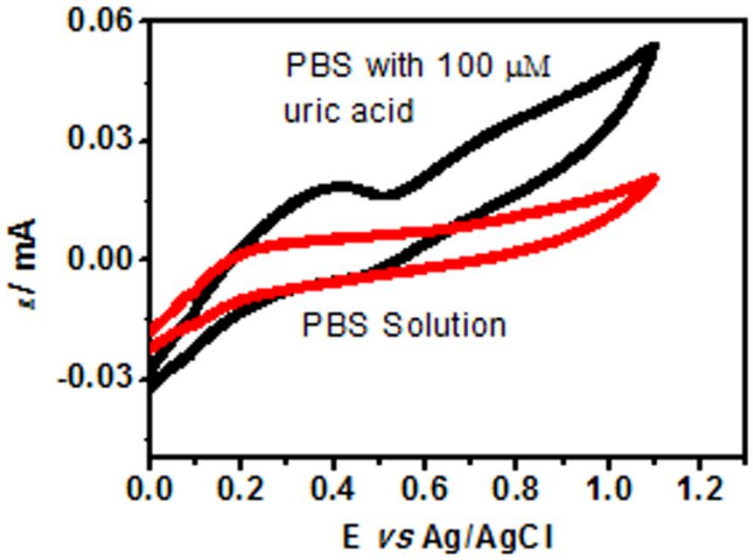

Figure 5.8 The cyclic voltammograms of the UOx-GO /PANI/solution-based graphene/Pt functionalized enzyme electrode in PBS solution(Red Curve) and in PBS solution with 100 μM UA.

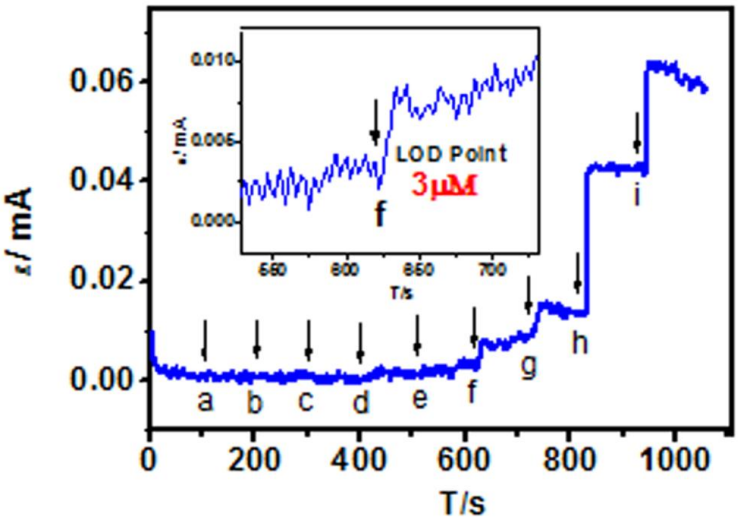

Figure 5.9 Amperometric responses of the UOx-GO /PANI/solution-based graphene/Pt functionalized enzyme electrode in PBS solution to the addition of UA. a-i: 1, 10, 30, 100 and 1000 nM, 3, 10,100 and 500μM, respectively. Inset: Enlarged LOD point at f.

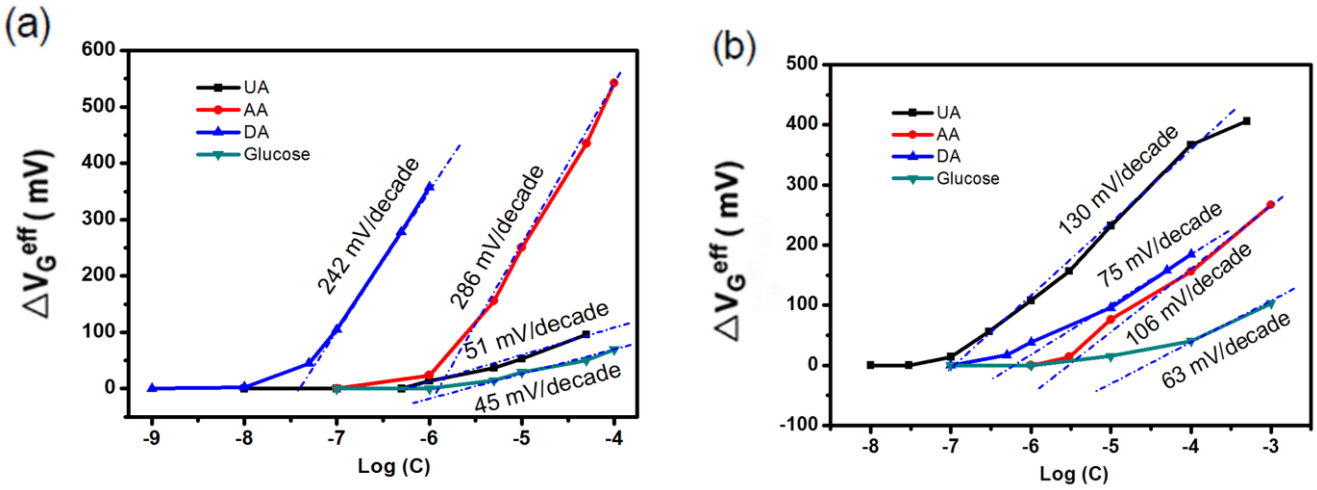

Figure 5.10 (a) The change of effective gate voltage of the device with pure Pt gate electrode as functions of three intereferent analytes(AA , DA and glucose). (b)The change of effective gate voltage of the device with UOx-GO /PANI/solution-based graphene/Pt functionalized enzyme electrode as functions of three intereferent analytes(AA , DA and glucose).

5.3.2 High Selectivity of the OECT-based UA sensors

Selectivity is a key parameter for the sensing applications[149, 157]. Human body fluids is a complex biological system containing a plethora of interferents, such as glucose, ascorbic acid(AA) and dopamine, that can cause significant error signals. Figure 5.10 shows the response of device to three most-common interferents(e.g. glucose, AA and dopamine). Figure 5.10a demonstrates the performance of the unmodified device, while Figure 5.10b unveils the result of the device with UOx-GO /PANI/solution-based graphene/Pt functionalized enzyme electrodes. The unmodified device shows no obvious response until 1 μM glucose is added and shift about 47mV per decade(Figure 5.10a), which is similar to that of device with functionalized electrodes(Figure 5.10b**,** glucose detection limit 3μM, 41mV/decade). The low sensitivity and responsibility of both type devices can be attributed to the low reaction rate of glucose oxidation. Since no glucose oxidase is added, this enzyme-canalized reaction is strongly prohibited and induces very limited interfacial potential drops that can modulate the channel current. Therefore, the interference signal from glucose is negligible. Curve II in both Figure 5.10a and Figure 5.10b demonstrate AA-dependent ΔV_g^{eff} shifts of devices. The device with pure Pt gate electrode begins to show response to AA at 1 μM and possess a large ΔV_g^{eff} shift up to 286mV/decade. The modified enzyme electrodes, interestingly, can reduce the interferencing response from AA. The dropped PANI layer cover the Pt electrode serve as barrier layer that can prevent the direct interactions between Pt electrode and AA molecules. Dopamine induced responses are demonstrated in both Figure 5.10a and Figure 5.10b. Device with pure Pt electrode can detect dopamine as low as

5 nM and changes 242mV for one decade. While the device with UOx-GO /PANI/solution-based graphene/Pt functionalized gate electrodes show no response until 50 nM dopamine is added, which is about one order of magnitude higher than that of device with pure Pt electrode. The much reduced ΔV_g^{eff} shift value (67 mV/decade) can be explained by the repel interactions between dopamine molecules and PANI film. PANI film covers the surface of Pt electrode is in H^+ protonated emeraldine salt form, which can strongly repel the positively charged dopamine molecules and thus significantly reduce the chemical-oxidation reaction of dopamine inducing the error signals. Considering the extremely low concentration of dopamine (several nM) in human body, the interferents induced by dopamine is very low when modified enzyme electrodes are adopted in UA measurements. In sum, OECT device with enzyme/conducting polymer/graphene co-modified enzyme electrodes serve as the viable platform for high selectivity detection of UA

5.3.3 Device on Flexible Substrate

OECT-based devices can be easily fabricated on flexible substrates, which is essential for the practical sensing applications in living systems. Figure 5.11a shows the pictures of flexible device bent up and down. Figure 5.11b demonstrates the performance of device fabricated on the flexible PET substrate using the UOx-GO /PANI/solution-based graphene/Pt functionalized gate electrodes. The low detection limit of flexible sensor to UA is 100 nM, which is about one order of magnitude higher than that the best-performed device fabricated on glass substrate using the same functionalized gate electrodes. The slope of curve ΔV_g^{eff} shift *vs* UA

concentration is reduced to 140mV/decade. The slightly degraded performance of flexible device can be ascribed to the different fabrication conditions in device preparation. For glass substrate based device, the annealing condition in PEDOT: PSS film-forming process is performed at 200 ℃ in the glove box with high purity N_2. However, for the PET based device, the annealing temperature is 120 ℃. Difference in annealing temperature will result in a different morphology of semiconducting polymer layer and thus a distinct electrical property of organic semiconductor film. It has been reported that temperature above 160 ℃ was needed for the optimized film of PEDOT: PSS[158]. Therefore, flexible PET device annealed at 120 ℃ demonstrated a relatively reduced performance in comparison with its counterparts fabricated on glass substrate. However, regarding the high sensitivity of PET-based UA sensor, flexible OECT device still holds great potential for the real UA detection in human sample.

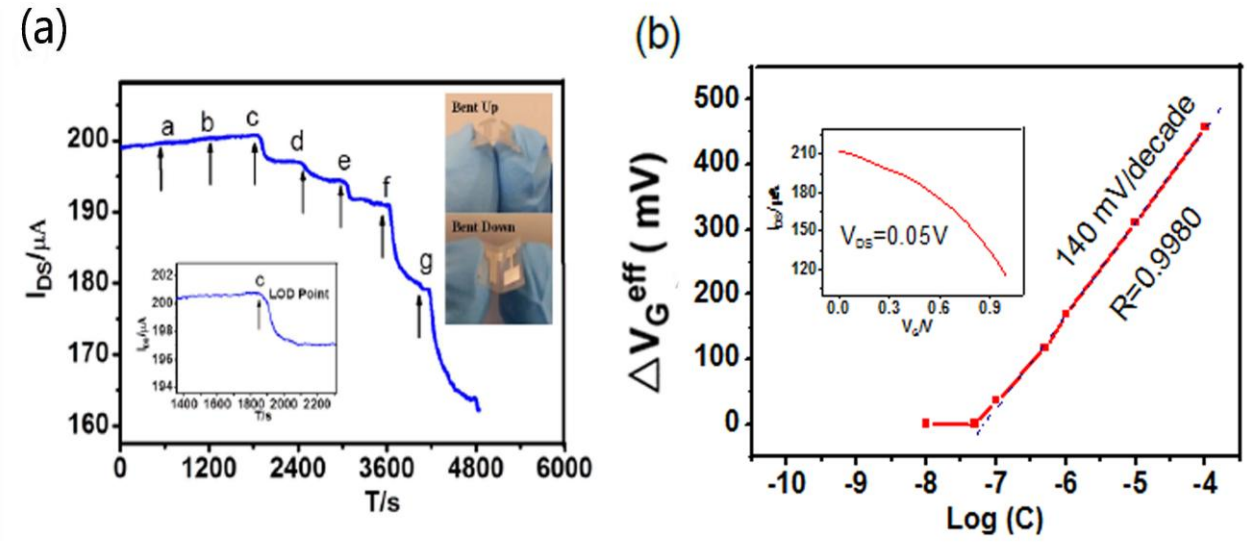

Figure 5.11 (a) Response of the OECT with UOx-GO /PANI/CVD-based graphene/Pt functionalized electrodes gate electrode based on the flexible PET to additions of UA in PBS solution. From a-g, the concentrations of dopamine are 10, 50,100,500 and 1000nM, 10 and 100μM, respectively. Inset: Enlarged LOD point at c(Left), pictures shows the device bent up and down(Right). (b)The change of effective gate voltage of the device with UOx-GO /PANI/solution-based graphene/Pt functionalized enzyme electrode as functions of UA concentrations. Inset: transfer curve (I_{DS} vs V_G) of the OECT.

5.4 Summary

In summary, OECTs with functionalized enzyme electrodes demonstrated high performance in UA detection. The enzyme was successfully immobilized onto the surface of Pt gate electrodes via the physical or chemical schemes. The device with UOx-GO /PANI/solution-based graphene/Pt modified electrode changed 177mV/decade and demonstrated a detection limit as low as 10 nM, which was three orders of magnitude lower than that of amperometric measurement using the same functionalized enzyme electrodes. The much improved sensitivity of OECT-based UA sensor was the combined result of the significant inherent signal amplifying capability and the optimized enzyme immobilization techniques. Therefore, OECT device with functionalized gate electrodes serve as a viable platform for the high-performance chemical and biological sensors.

Chapter 6 Conclusions and Future Outlook

6.1. Conclusions

In summary, the performances of organic electrochemical transistors (OECT) based glucose sensors were systematically investigated. The sensitivity of OECT sensors could be significantly increased by co-modifying the gate electrodes with graphene nano-materials(graphene or reduced graphene oxide (rGO)) and glucose oxidase. The functionalized devices were sensitive enough to detect glucose level down to 10 nM, which was two orders of magnitude better than that of device without graphene modification. The optimized device showed a linear response to a wide range glucose concentration from 10 nM to 1 mM, covering the physiological glucose range in human saliva. The selectivity of the devices was systematically studied for the first time. The sensitivity of OECT glucose sensors could be dramatically improved by modifying the gate electrodes with biocompatible polymers, including chitosan and Nafion. The interfering effect from uric acid and L-ascorbic acid was mostly blocked. Therefore, high performance OECT-based glucose sensors can be realized by modifying the gate electrodes.

Then OECTs were successfully fabricated as highly sensitive and selective dopamine sensors. The selectivity of OECT-based dopamine sensors was significantly

improved by coating biocompatible polymer Nafion or chitosan on the surfaces of gate electrodes. The interference induced by uric acid and ascorbic acid was effectively eliminated. In addition, the sensitivity of OECT devices was improved by graphene flakes co-modified on the gate electrodes. The detection limit of the devices to dopamine was down to 5 nM, which was much lower than that of conventional electrochemical methods.

Finally, OECTs with uricase functionalized gate electrodes were successfully fabricated and served as the high-performance uric acid sensors for the first time. The Pt gate electrodes were modified with enzyme, semiconducting polymer (polyaniline) and graphene-based materials(graphene sheets and graphene oxide), which could simultaneously improve the sensitivity and selectivity of the UA sensors. The sensor with UOx-GO /PANI/solution-based graphene/Pt gate electrode could detect uric acid down to 10 nM, which was approximately 4 orders of magnitude lower than that of the conventional electrochemical UA sensors using the similar enzyme electrodes. The devices showed an excellent linearity in the range of 100 nM to 500 μM, covering the normal uric acid level in human sample. Signals from most-common bio-active intereferents(e.g. glucose, dopamine and ascorbic acic) were largely reduced. The high performance of the devices could be ascribed to the optimized enzyme immobilization techniques. Adopting the same principle, the application of OECTs could be further explored by taking different gate electrode modification techniques.

6.2. Future Outlook

Owing to its versatile synthetic approaches, tunable electronic conductivity, solution processable fabrication methods, as well as excellent biocompatibility, organic semiconductors have been extensively used in the transistor-based sensors. Typically, PEDOT:PSS, poly(3-akylthiophene), pentacene, and polyaniline, etc., are the most common ones for OTFT sensing application. OTFT, particularly OECT-based devices, have been intensively investigated for various kinds of applications in chemical and biological sensors.

In the past few years, research on novel organic semiconducting materials for OTFT-based sensors have exponentially increased, various kinds of organic semiconducting materials with high carrier mobility and excellent stability have been synthesized and exploited in sensing applications. The next big leap will be the further improvement of these devices for real applications, which could be accomplished via two ways. The first one to improve the performance of the existing organic bioelectronics is to optimize the geometric features of devices or adopt new techniques in the devices fabrication processes. The second one is to explore new type of devices based on OTFT platform and further expand the biological application scope of these devices. In sum, from the personal perspective of us, the beautiful marriage between organic electronics and biology will be further developed to serve as the versatile toolbox for biological applications.

References

[1] D.D. Borole, U.R. Kapadi, P.P. Mahulikar, D.G. Hundiwale, Conducting polymers: an emerging field of biosensors, Designed Monomers & Polymers, 9(2006) 1-11.

[2] B. Adhikari, S. Majumdar, Polymers in sensor applications, Prog Polym Sci, 29(2004) 699-766.

[3] P. Lin, F. Yan, Organic thin-film transistors for chemical and biological sensing, Adv Mater, 24(2012) 34-51.

[4] C. Bartic, G. Borghs, Organic thin-film transistors as transducers for (bio) analytical applications, Analytical and Bioanalytical Chemistry, 384(2005) 354-365.

[5] B.C.-K.T. Stefan C. B. Mannsfeld, Randall M. Stoltenberg, Christopher V. H-H. Chen, Soumendra Barman, Beinn V. O. Muir, Anatoliy N. Sokolov, Colin Reese, Zhenan Bao, Highly sensitive flexible pressure sensors with microstructured rubber dielectric layers, Nat Mater, 9(2010) 859–864.

[6] R.M.O.a.G.G. Malliaras, Organic Electronics at the Interface with Biology, MRS Bull, 35(2010) 449-456.

[7] M. Berggren, A. Richter-Dahlfors, Organic Bioelectronics, Adv Mater, 19(2007) 3201-3213.

[8] L. Kergoat, B. Piro, M. Berggren, M.-C. Pham, A. Yassar, G. Horowitz, DNA detection with a water-gated organic field-effect transistor, Organic Electronics, 13(2012) 1-6.

[9] P. Lin, F. Yan, Organic thin-film transistors for chemical and biological sensing, Adv Mater, 24(2012) 34-51.

[10] D. Lakshmi, M.J. Whitcombe, F. Davis, I. Chianella, E.V. Piletska, A. Guerreiro, et al., Chimeric polymers formed from a monomer capable of free radical, oxidative and electrochemical polymerisation, Chem Commun (Camb), (2009) 2759-2761.

[11] S.C. Maria Daniela Angione, Maria Magliulo, Antonia Mallardi, Davide Altamura, Cinzia Giannini, Nicola Cioffi, Luigia Sabbatini, Emiliano Fratini, Piero Baglioni, Gaetano Scamarcio, Gerardo Palazzo, and Luisa Torsi, Interfacial electronic effects in functional biolayers integrated into organic field-effect transistors, Proc Nail Acad Sci USA, 109(2012) 6429–6434.

[12] L. Kergoat, B. Piro, M. Berggren, G. Horowitz, M.C. Pham, Advances in organic transistor-based biosensors: from organic electrochemical transistors to electrolyte-gated organic field-effect transistors, Anal Bioanal Chem, 402(2012) 1813-1826.

[13] T.K. David Nilsson, Per-Olof Svensson, Magnus Berggren, An all-organic sensor–transistor based on a novel electrochemical transducer concept printed electrochemical sensors on paper, Sens Actuators B Chem, 86(2002) 193-197.

[14] C. Liao, F. Yan, Organic Semiconductors in Organic Thin-Film Transistor-Based Chemical and Biological Sensors, PolymRev, 53(2013) 352-406.

[15] S. Cotrone, D. Cafagna, S. Cometa, E. De Giglio, M. Magliulo, L. Torsi, et al., Microcantilevers and organic transistors: two promising classes of label-free

biosensing devices which can be integrated in electronic circuits, Anal Bioanal Chem, 402(2012) 1799-1811.

[16] E.J.L. Hideki Shirakawa, Alan G. MacDiarmid, Chwan K. Chiang and Alan J. Heeger, Synthesis of electrically conducting organic polymers halogen derivatives of polyacetylene(CH)x, J Chem Soc, Chem Commun, (1977) 578-580.

[17] A.M. Fabio Silvestri, Mirko Seri , Choongik Kim, Tobin J. Marks, Antonio Facchetti, Aldo Taticchi Solution-processable low-molecular weight extended arylacetylenes versatile p-type semiconductors for field-effect transistors and bulk heterojunction solar cells, J Am Chem Soc, 132(2010) 6108–6123.

[18] J.L. Zhike Liu , Zhen-Hua Sun , Guoan Tai , Shu-Ping Lau , Feng Yan The application of highly doped single-layer graphene as the top electrodes of semitransparent organic solar cells, ACS Nano, 6(2011) 810–818.

[19] S.A.V. C. W. Tang, Organic electroluminescent diodes, Appl Phys Lett, 51(1987) 913-915.

[20] G. Horowitz, Organic field-effect transistors, Adv Mater, 10(1998) 365–377.

[21] M.E.R. Anatoliy N. Sokolov, Zhenan Bao, Fabrication of low-cost electronic biosensors, MaterToday 12(2009) 12–20.

[22] S. Liu, W.M. Wang, A.L. Briseno, S.C.B. Mannsfeld, Z. Bao, Controlled Deposition of Crystalline Organic Semiconductors for Field-Effect-Transistor Applications, Advanced Materials, 21(2009) 1217-1232.

[23] J.D. Myers, J. Xue, Organic Semiconductors and their Applications in Photovoltaic Devices, Polymer Reviews, 52(2012) 1-37.

[24] B. de Boer, A. Facchetti, Semiconducting Polymeric Materials, Polym Rev

48(2008) 423-431.

[25] Y. Lin, Y. Li, X. Zhan, Small molecule semiconductors for high-efficiency organic photovoltaics, Chemical Society reviews, 41(2012) 4245-4272.

[26] Y. Wen, Y. Liu, Y. Guo, G. Yu, W. Hu, Experimental techniques for the fabrication and characterization of organic thin films for field-effect transistors, Chem Rev, 111(2011) 3358-3406.

[27] W. Wu, Y. Liu, D. Zhu, Pi-conjugated molecules with fused rings for organic field-effect transistors: design, synthesis and applications, Chem Soc Rev, 39(2010) 1489-1502.

[28] J. Rivnay, R.M. Owens, G.G. Malliaras, The Rise of Organic Bioelectronics, Chem Mater, 26(2014) 679-685.

[29] S. Gunes, H. Neugebauer, N.S. Sariciftci, Conjugated polymer-based organic solar cells, Chem Rev, 107(2007) 1324-1338.

[30] H. Sirringhaus, High-Resolution Inkjet Printing of All-Polymer Transistor Circuits, Science, 290(2000) 2123-2126.

[31] G. Latessa, F. Brunetti, A. Reale, G. Saggio, A. Di Carlo, Piezoresistive behaviour of flexible PEDOT:PSS based sensors, Sensors and Actuators B: Chemical, 139(2009) 304-309.

[32] J.C. Scott, L.D. Bozano, Nonvolatile Memory Elements Based on Organic Materials, Advanced Materials, 19(2007) 1452-1463.

[33] M.K. A. M. Nardes, R. A. J. Janssen, J. A. M. Bastiaansen, N. M. M. Kiggen, B. M. W. Langeveld, A. J. J. M. van Breemen, M. M. de Kok, Microscopic

understanding of the anisotropic conductivity of PEDOT: PSS thin films, Adv Mater, 19(2007) 1196–1200.

[34] Z.U.K. Olga Bubnova, Abdellah Malti, Slawomir Braun, Mats Fahlman, Magnus Berggren , Xavier Crispin, Optimization of the thermoelectric figure of merit in the conducting polymer poly (3, 4-ethylenedioxythiophene), Nat Mater, 10(2011) 429–433.

[35] K.G.N. E.T. Kang, K.L. Tan, Polyaniline: A polymer with many interesting intrinsic redox states, Prog Polym Sci, 23(1998) 277–324.

[36] A.F. Diaz, Castillo, Juan I., A polymer electrode with variable conductivity: polypyrrole, J Chem Soc, Chemical Communications, (1980) 397-398.

[37] J.R. A. Yassar , F. Garnier, Conductivity and conjugation length in poly(3-methylthiophene) thin films, Macromolecules, 22(1989) 804–809.

[38] D.A. Bernards, G.G. Malliaras, Steady-State and Transient Behavior of Organic Electrochemical Transistors, Advanced Functional Materials, 17(2007) 3538-3544.

[39] D.A. Bernards, D.J. Macaya, M. Nikolou, J.A. DeFranco, S. Takamatsu, G.G. Malliaras, Enzymatic sensing with organic electrochemical transistors, Journal of Materials Chemistry, 18(2008) 116-120.

[40] F. Cicoira, M. Sessolo, O. Yaghmazadeh, J.A. DeFranco, S.Y. Yang, G.G. Malliaras, Influence of device geometry on sensor characteristics of planar organic electrochemical transistors, Adv Mater, 22(2010) 1012-1016.

[41] K.D. Kreuer, On the development of proton conducting materials for technological applications, Solid State Ionics 97(1997) 1–15.

[42] R.F. M. Berggren, J. Bobacka, P. -O. Svensson, D. Nilsson, O. Larsson, A. Ivaska, Organic Semiconductors in Sensor Applications: Springer Berlin Heidelberg; 2008.

[43] D.A. Bernards, G.G. Malliaras, G.E.S. Toombes, S.M. Gruner, Gating of an organic transistor through a bilayer lipid membrane with ion channels, Applied Physics Letters, 89(2006) 053505.

[44] Z. Mousavi, A. Ekholm, J. Bobacka, A. Ivaska, Ion-Selective Organic Electrochemical Junction Transistors Based on Poly(3,4-ethylenedioxythiophene) Doped with Poly(styrene sulfonate), Electroanalysis, 21(2009) 472-479.

[45] P. Lin, F. Yan, H.L. Chan, Ion-sensitive properties of organic electrochemical transistors, ACS Appl Mater Interfaces, 2(2010) 1637-1641.

[46] G. Tarabella, C. Santato, S.Y. Yang, S. Iannotta, G.G. Malliaras, F. Cicoira, Effect of the gate electrode on the response of organic electrochemical transistors, Applied Physics Letters, 97(2010) 123304.

[47] G. Tarabella, G. Nanda, M. Villani, N. Coppedè, R. Mosca, G.G. Malliaras, et al., Organic electrochemical transistors monitoring micelle formation, Chemical Science, 3(2012) 3432-3435.

[48] G. Tarabella, M. Villani, D. Calestani, R. Mosca, S. Iannotta, A. Zappettini, et al., A single cotton fiber organic electrochemical transistor for liquid electrolyte saline sensing, Journal of Materials Chemistry, 22(2012) 23830-23834.

[49] T. Toccoli, E. Borga, H. Blond, D. Maniglio, L. Minati, C. Fasoli, et al., Polyelectrolytes-coated gold nanoparticles detection by PEDOT:PSS electrochemical transistors, Organic Electronics, 13(2012) 1716-1721.

[50] Z.T. Zhu, J.T. Mabeck, C. Zhu, N.C. Cady, C.A. Batt, G.G. Malliaras, A simple poly(3,4-ethylene dioxythiophene)/poly(styrene sulfonic acid) transistor for glucose sensing at neutral pH, Chem Commun (Camb), (2004) 1556-1557.

[51] D.J. Macaya, M. Nikolou, S. Takamatsu, J.T. Mabeck, R.M. Owens, G.G. Malliaras, Simple glucose sensors with micromolar sensitivity based on organic electrochemical transistors, Sensors and Actuators B: Chemical, 123(2007) 374-378.

[52] N.Y. Shim, D.A. Bernards, D.J. Macaya, J.A. Defranco, M. Nikolou, R.M. Owens, et al., All-plastic electrochemical transistor for glucose sensing using a ferrocene mediator, Sensors (Basel), 9(2009) 9896-9902.

[53] S.K. Kanakamedala, H.T. Alshakhouri, M. Agarwal, M.A. DeCoster, A simple polymer based electrochemical transistor for micromolar glucose sensing, Sensors and Actuators B: Chemical, 157(2011) 92-97.

[54] S.Y. Yang, F. Cicoira, R. Byrne, F. Benito-Lopez, D. Diamond, R.M. Owens, et al., Electrochemical transistors with ionic liquids for enzymatic sensing, Chem Commun (Camb), 46(2010) 7972-7974.

[55] J.T. Mabeck, J.A. DeFranco, D.A. Bernards, G.G. Malliaras, S. Hocdé, C.J. Chase, Microfluidic gating of an organic electrochemical transistor, Applied Physics Letters, 87(2005) 013503.

[56] S.Y. Yang, J.A. Defranco, Y.A. Sylvester, T.J. Gobert, D.J. Macaya, R.M. Owens, et al., Integration of a surface-directed microfluidic system with an organic electrochemical transistor array for multi-analyte biosensors, Lab Chip, 9(2009) 704-708.

[57] H. Tang, F. Yan, P. Lin, J. Xu, H.L.W. Chan, Highly Sensitive Glucose Biosensors Based on Organic Electrochemical Transistors Using Platinum Gate Electrodes Modified with Enzyme and Nanomaterials, Advanced Functional Materials, 21(2011) 2264-2272.

[58] F. Patolsky, B.P. Timko, G. Yu, Y. Fang, A.B. Greytak, G. Zheng, et al., Detection, stimulation, and inhibition of neuronal signals with high-density nanowire transistor arrays, Science, 313(2006) 1100-1104.

[59] P. Lin, F. Yan, J. Yu, H.L. Chan, M. Yang, The application of organic electrochemical transistors in cell-based biosensors, Adv Mater, 22(2010) 3655-3660.

[60] M. Zhang, P. Lin, M. Yang, F. Yan, Fabrication of organic electrochemical transistor arrays for biosensing, Biochim Biophys Acta, 1830(2013) 4402-4406.

[61] D.F. Balkovetz, J. Katz, Bacterial invasion by a paracellular route: divide and conquer, Microbes and Infection, 5(2003) 613-619.

[62] L.H. Jimison, S.A. Tria, D. Khodagholy, M. Gurfinkel, E. Lanzarini, A. Hama, et al., Measurement of barrier tissue integrity with an organic electrochemical transistor, Adv Mater, 24(2012) 5919-5923.

[63] S.A. Tria, L.H. Jimison, A. Hama, M. Bongo, R.M. Owens, Validation of the organic electrochemical transistor for in vitro toxicology, Biochim Biophys Acta, 1830(2013) 4381-4390.

[64] M.H. Bolin, K. Svennersten, D. Nilsson, A. Sawatdee, E.W.H. Jager, A. Richter-Dahlfors, et al., Active Control of Epithelial Cell-Density Gradients Grown Along the Channel of an Organic Electrochemical Transistor, Advanced Materials, 21(2009) 4379-4382.

[65] K. Krishnamoorthy, R.S. Gokhale, A.Q. Contractor, A. Kumar, Novel label-free DNA sensors based on poly(3,4-ethylenedioxythiophene), Chem Commun (Camb), (2004) 820-821.

[66] M. Kanungo, D.N. Srivastava, A. Kumar, A.Q. Contractor, Conductimetric immunosensor based on poly(3,4-ethylenedioxythiophene), Chemical Communications, (2002) 680-681.

[67] P. Lin, X. Luo, I.M. Hsing, F. Yan, Organic electrochemical transistors integrated in flexible microfluidic systems and used for label-free DNA sensing, Adv Mater, 23(2011) 4035-4040.

[68] G.D.S. R. B. Dabke, A. Dhanabalan, R. Lal, A. Q. Contractor, An Ion-Activated Molecular Electronic Device, Anal Chem, 69(1997) 724–727.

[69] D.J. Kim, N.E. Lee, J.S. Park, I.J. Park, J.G. Kim, H.J. Cho, Organic electrochemical transistor based immunosensor for prostate specific antigen (PSA) detection using gold nanoparticles for signal amplification, Biosens Bioelectron, 25(2010) 2477-2482.

[70] M.K. Yaron S, A reverse transcriptase - polymerase chain reaction assay for detection of viable Escherichia coli O157: H7 investigation of specific target genes, J Appl Microbiol 92(2002) 633-640.

[71] R.-X. He, M. Zhang, F. Tan, P.H.M. Leung, X.-Z. Zhao, H.L.W. Chan, et al., Detection of bacteria with organic electrochemical transistors, Journal of Materials Chemistry, 22(2012) 22072-22076.

[72] H. Tang, P. Lin, H.L. Chan, F. Yan, Highly sensitive dopamine biosensors based on organic electrochemical transistors, Biosens Bioelectron, 26(2011) 4559-4563.

[73] D. Khodagholy, V.F. Curto, K.J. Fraser, M. Gurfinkel, R. Byrne, D. Diamond, et al., Organic electrochemical transistor incorporating an ionogel as a solid state electrolyte for lactate sensing, Journal of Materials Chemistry, 22(2012) 4440-4443.

[74] V.P. Torchilin, Recent advances with liposomes as pharmaceutical carriers, Nat Rev Drug Discov, 4(2005) 145-160.

[75] G. Tarabella, A.G. Balducci, N. Coppede, S. Marasso, P. D'Angelo, S. Barbieri, et al., Liposome sensing and monitoring by organic electrochemical transistors integrated in microfluidics, Biochim Biophys Acta, 1830(2013) 4374-4380.

[76] D.W.S. J. G. Wagner, C. P. Quinn, T. F. Fleming, B.Bernacky,and A. Heller, Continuous amperometric monitoring of glucose in a brittle diabetic chimpanzee with a miniature subcutaneous electrode, Proc Natl Acad Sci USA, 95(1998) 6379-6382.

[77] H. Tang, F. Yan, Q. Tai, H.L. Chan, The improvement of glucose bioelectrocatalytic properties of platinum electrodes modified with electrospun TiO2 nanofibers, Biosens Bioelectron, 25(2010) 1646-1651.

[78] M.R. AN Sokolov, Z Bao, Fabrication of low-cost electronic biosensors, Mater Today, 12(2009) 12–20.

[79] G.P.K. Henry S. White , Mark S. Wrighton, Chemical derivatization of an array of three gold microelectrodes with polypyrrole fabrication of a molecule-based transistor, J Am Chem Soc, 106(1984) 5375–5377.

[80] P.F.M. J. Huang, J.S. Wilson, A.J. de Mello, J. C. de Mello andD. D. C. Bradley, Investigation of the Effects of Doping and Post-Deposition Treatments on the Conductivity, Morphology, and Work Function of Poly(3,4-ethylenedioxythiophene)/Poly(styrene sulfonate) Films, Adv Funct Mater, 15(2005) 290–296.

[81] M.S.W. J. W. Thackeray Chemically responsive microelectrochemical devices based on platinized poly(3-methylthiophene) variation in conductivity with variation in hydrogen, oxygen, or pH in aqueous solution, J Phys Chem, 90(1986) 6674-6679.

[82] T. Kuila, S. Bose, P. Khanra, A.K. Mishra, N.H. Kim, J.H. Lee, Recent advances in graphene-based biosensors, Biosens Bioelectron, 26(2011) 4637-4648.

[83] X. Kang, J. Wang, H. Wu, I.A. Aksay, J. Liu, Y. Lin, Glucose oxidase-graphene-chitosan modified electrode for direct electrochemistry and glucose sensing, Biosens Bioelectron, 25(2009) 901-905.

[84] H. Wu, J. Wang, X. Kang, C. Wang, D. Wang, J. Liu, et al., Glucose biosensor based on immobilization of glucose oxidase in platinum nanoparticles/graphene/chitosan nanocomposite film, Talanta, 80(2009) 403-406.

[85] C. Shan, H. Yang, D. Han, Q. Zhang, A. Ivaska, L. Niu, Graphene/AuNPs/chitosan nanocomposites film for glucose biosensing, Biosens Bioelectron, 25(2010) 1070-1074.

[86] K. Zhou, Y. Zhu, X. Yang, C. Li, Electrocatalytic Oxidation of Glucose by the Glucose Oxidase Immobilized in Graphene-Au-Nafion Biocomposite, Electroanalysis, 22(2010) 259-264.

[87] Y. Song, K. Qu, C. Zhao, J. Ren, X. Qu, Graphene oxide: intrinsic peroxidase catalytic activity and its application to glucose detection, Adv Mater, 22(2010) 2206-2210.

[88] Y. Liu, D. Yu, C. Zeng, Z. Miao, L. Dai, Biocompatible graphene oxide-based glucose biosensors, Langmuir, 26(2010) 6158-6160.

[89] K.M. John P. Lowry , Satea S. El Atrash , Adrienne Duff , Robert D. O'Neill, Characterization of Glucose Oxidase-Modified Poly(phenylenediamine)-Coated Electrodes in vitro and in vivo: Homogeneous Interference by Ascorbic Acid in Hydrogen Peroxide Detection, Anal Chem, 66(1994) 1754–1761.

[90] S.H. Lim, J. Wei, J. Lin, Q. Li, J. Kuayou, A glucose biosensor based on electrodeposition of palladium nanoparticles and glucose oxidase onto Nafion-solubilized carbon nanotube electrode, Biosens Bioelectron, 20(2005) 2341-2346.

[91] M.M. Joseph Wang , Yuehe Lin, Solubilization of Carbon Nanotubes by Nafion toward the Preparation of Amperometric Biosensors, J Am Chem Soc, 125(2003) 2408–2409.

[92] M. Yang, Y. Yang, B. Liu, G. Shen, R. Yu, Amperometric glucose biosensor based on chitosan with improved selectivity and stability, Sensors and Actuators B: Chemical, 101(2004) 269-276.

[93] H. Chang, G. Wang, A. Yang, X. Tao, X. Liu, Y. Shen, et al., A Transparent, Flexible, Low-Temperature, and Solution-Processible Graphene Composite Electrode, Advanced Functional Materials, 20(2010) 2893-2902.

[94] H. Chang, Z. Sun, Q. Yuan, F. Ding, X. Tao, F. Yan, et al., Thin film field-effect phototransistors from bandgap-tunable, solution-processed, few-layer reduced graphene oxide films, Adv Mater, 22(2010) 4872-4876.

[95] H. Chang, Z. Sun, K.Y. Ho, X. Tao, F. Yan, W.M. Kwok, et al., A highly sensitive ultraviolet sensor based on a facile in situ solution-grown ZnO nanorod/graphene heterostructure, Nanoscale, 3(2011) 258-264.

[96] C. Su, C. Zhang, G. Lu, C. Ma, Nonenzymatic Electrochemical Glucose Sensor Based on Pt Nanoparticles/Mesoporous Carbon Matrix, Electroanalysis, 22(2010) 1901-1905.

[97] M. Rinaudo, Chitin and chitosan: Properties and applications, Progress in Polymer Science, 31(2006) 603-632.

[98] J. Zhang, F. Zhang, H. Yang, X. Huang, H. Liu, S. Guo, Graphene oxide as a matrix for enzyme immobilization, Langmuir, 26(2010) 6083-6085.

[99] M.M. Masaki Yamaguchi, Yoshio Kano, Noninvasively measuring blood glucose using saliva, IEEE Een Med Biol, 17(1998) 59 - 63.

[100] R.M. Wightman, J.A. Jankowski, R.T. Kennedy, K.T. Kawagoe, T.J. Schroeder, D.J. Leszczyszyn, et al., Temporally Resolved Catecholamine Spikes Correspond to Single Vesicle Release from Individual Chromaffin Cells, P Natl Acad Sci USA, 88(1991) 10754-10758.

[101] C. Opazo, X. Huang, R.A. Cherny, R.D. Moir, A.E. Roher, A.R. White, et al., Metalloenzyme-like activity of Alzheimer's disease beta-amyloid. Cu-dependent catalytic conversion of dopamine, cholesterol, and biological reducing agents to neurotoxic H(2)O(2), J Biol Chem, 277(2002) 40302-40308.

[102] S. Ikemoto, Dopamine reward circuitry: two projection systems from the ventral midbrain to the nucleus accumbens-olfactory tubercle complex, Brain Res Rev, 56(2007) 27-78.

[103] J.D. Cohen, D. Servan-Schreiber, Context, cortex, and dopamine: a connectionist approach to behavior and biology in schizophrenia, Psychol Rev, 99(1992) 45-77.

[104] Z.D. Peterson, D.C. Collins, C.R. Bowerbank, M.L. Lee, S.W. Graves, Determination of catecholamines and metanephrines in urine by capillary electrophoresis-electrospray ionization-time-of-flight mass spectrometry, Journal of chromatography B, Analytical technologies in the biomedical and life sciences, 776(2002) 221-229.

[105] K. Hashizume, A. Yamatodani, T. Ogihara, Free and total dopamine in human plasma effects of posture, age and some pathophysiological conditions, Hypertens Res, 18(1995) S205-207.

[106] S.R. Laviolette, Dopamine modulation of emotional processing in cortical and subcortical neural circuits: evidence for a final common pathway in schizophrenia?, Schizophr Bull, 33(2007) 971-981.

[107] E. Szantai, A. Szilagyi, A. Guttman, M. Sasvari-Szekely, Z. Ronai, Genotyping and haplotyping of the dopamine D4 receptor gene by capillary electrophoresis, Journal of Chromatography A, 1053(2004) 241-245.

[108] K.E. Hubbard, A. Wells, T.S. Owens, M. Tagen, C.H. Fraga, C.F. Stewart, Determination of dopamine, serotonin, and their metabolites in pediatric

cerebrospinal fluid by isocratic high performance liquid chromatography coupled with electrochemical detection, Biomed Chromatogr, 24(2010) 626-631.

[109] H. Chen, R. Li, L. Lin, G. Guo, J.M. Lin, Determination of L-ascorbic acid in human serum by chemiluminescence based on hydrogen peroxide-sodium hydrogen carbonate-CdSe/CdS quantum dots system, Talanta, 81(2010) 1688-1696.

[110] S.J. Clarke, C.A. Hollmann, Z. Zhang, D. Suffern, S.E. Bradforth, N.M. Dimitrijevic, et al., Photophysics of dopamine-modified quantum dots and effects on biological systems, Nat Mater, 5(2006) 409-417.

[111] S.R. Ali, R.R. Parajuli, Y. Balogun, Y. Ma, H. He, A Nonoxidative Electrochemical Sensor Based on a Self-Doped Polyaniline/Carbon Nanotube Composite for Sensitive and Selective Detection of the Neurotransmitter Dopamine: A Review, Sensors, 8(2008) 8423-8452.

[112] D.M. Franck Malem Self-assembled monolayers in electroanalytical chemistry: application of .omega.-mercapto carboxylic acid monolayers for the electrochemical detection of dopamine in the presence of a high concentration of ascorbic acid, Anal Chem, 65(1993) 37–41.

[113] J. Li, Z. Sun, F. Yan, Solution processable low-voltage organic thin film transistors with high-k relaxor ferroelectric polymer as gate insulator, Adv Mater, 24(2012) 88-93.

[114] P. Lin, F. Yan, H.L. Chan, Improvement of the tunable wettability property of poly(3-alkylthiophene) films, Langmuir, 25(2009) 7465-7470.

[115] F. Yan, S.M. Mok, J. Yu, H.L. Chan, M. Yang, Label-free DNA sensor based on organic thin film transistors, Biosens Bioelectron, 24(2009) 1241-1245.

[116] W.B. Nowall, W.G. Kuhr, Electrocatalytic surface for the oxidation of NADH and other anionic molecules of biological significance, Analytical chemistry, 67(1995) 3583-3588.

[117] D. Han, T. Han, C. Shan, A. Ivaska, L. Niu, Simultaneous Determination of Ascorbic Acid, Dopamine and Uric Acid with Chitosan-Graphene Modified Electrode, Electroanalysis, 22(2010) 2001-2008.

[118] H.S. Wang, T.H. Li, W.L. Jia, H.Y. Xu, Highly selective and sensitive determination of dopamine using a Nafion/carbon nanotubes coated poly(3-methylthiophene) modified electrode, Biosens Bioelectron, 22(2006) 664-669.

[119] M. Pumera, A. Ambrosi, A. Bonanni, E.L.K. Chng, H.L. Poh, Graphene for electrochemical sensing and biosensing, TrAC Trends in Analytical Chemistry, 29(2010) 954-965.

[120] L. Wu, L. Feng, J. Ren, X. Qu, Electrochemical detection of dopamine using porphyrin-functionalized graphene, Biosens Bioelectron, 34(2012) 57-62.

[121] S.F. Hou, M.L. Kasner, S.J. Su, K. Patel, R. Cuellari, Highly Sensitive and Selective Dopamine Biosensor Fabricated with Silanized Graphene, J Phys Chem C, 114(2010) 14915-14921.

[122] M. Liu, L. Wang, J. Deng, Q. Chen, Y. Li, Y. Zhang, et al., Highly sensitive and selective dopamine biosensor based on a phenylethynyl ferrocene/graphene nanocomposite modified electrode, Analyst, 137(2012) 4577-4583.

[123] Y. Bao, J. Song, Y. Mao, D. Han, F. Yang, L. Niu, et al., Graphene Oxide-Templated Polyaniline Microsheets toward Simultaneous Electrochemical Determination of AA/DA/UA, Electroanalysis, 23(2011) 878-884.

[124] C. Liao, M. Zhang, L. Niu, Z. Zheng, F. Yan, Highly selective and sensitive glucose sensors based on organic electrochemical transistors with graphene-modified gate electrodes, Journal of Materials Chemistry B, 1(2013) 3820-3829.

[125] R.M. KA Mauritz, State of Understanding of Nafion, Chem Rev, 104(2004) 4535-4585.

[126] C.N. Rao, A.K. Sood, K.S. Subrahmanyam, A. Govindaraj, Graphene: the new two-dimensional nanomaterial, Angew Chem Int Ed Engl, 48(2009) 7752-7777.

[127] Y. Wang, Y. Li, L. Tang, J. Lu, J. Li, Application of graphene-modified electrode for selective detection of dopamine, Electrochemistry Communications, 11(2009) 889-892.

[128] R.X. He, P. Lin, Z.K. Liu, H.W. Zhu, X.Z. Zhao, H.L. Chan, et al., Solution-gated graphene field effect transistors integrated in microfluidic systems and used for flow velocity detection, Nano letters, 12(2012) 1404-1409.

[129] F. Yan, Zhang, M., Li, J., Solution-gated graphene transistors for chemical and biological sensors, Adv Healthc Mater, 3(2014) 313-331.

[130] R.T.W. Cristina Gómez-Navarro , Alexander M. Bittner , Matteo Scolari , Alf Mews , Marko Burghard , Klaus Kern, Electronic Transport Properties of Individual Chemically Reduced Graphene Oxide Sheets, Nano Lett, 7(2007) 3499–3503.

[131] Y. Liu, L. Gao, J. Sun, Y. Wang, J. Zhang, Stable Nafion-functionalized graphene dispersions for transparent conducting films, Nanotechnology, 20(2009) 465605.

[132] Y.A. Hashizume K, Ogihara T., Free and Total Dopamine in Human Plasma Effects of Posture, Age and Some Pathophysiological Conditions, Hypertens Res, Suppl 1(1995) S205-S207.

[133] H.H. Takahiko Nakagawa , Sergey Zharikov , Katherine R. Tuttle , Robert A. Short , Olena Glushakova , Xiaosen Ouyang , Daniel I. Feig , Edward R. Block , Jaime Herrera-Acosta , Jawaharlal M. Patel , Richard J. Johnson, A causal role for uric acid in fructose-induced metabolic syndrome, American Journal of Physiology - Renal Physiology, 290(2006) F625-F631.

[134] F.M.R. W N Kelley, J F Henderson, J E Seegmiller, A specific enzyme defect in gout associated with overproduction of uric acid, Proc Natl Acad Sci U S A, 57(1967) 1735–1739.

[135] D.H. Kang, A Role for Uric Acid in the Progression of Renal Disease, Journal of the American Society of Nephrology, 13(2002) 2888-2897.

[136] L.H. Dan-Ke Xu, Zi-Man Li, Hong-Yuan Chen, Identification and quantitative determination of uric acid in human urine and plasma by capillary electrophoresis with amperometric detection, J Chromatogr B Biomed Appl, 694(1997) 461–466.

[137] D.L. Rocha, F.R.P. Rocha, A flow-based procedure with solenoid micro-pumps for the spectrophotometric determination of uric acid in urine, Microchemical Journal, 94(2010) 53-59.

[138] J. Perello, P. Sanchis, F. Grases, Determination of uric acid in urine, saliva and calcium oxalate renal calculi by high-performance liquid chromatography/mass spectrometry, Journal of chromatography B, Analytical technologies in the biomedical and life sciences, 824(2005) 175-180.

[139] A.G.V. Dachun Yao, Nicholaos P Evmiridis, Microdialysis sampling and monitoring of uric acid in vivo by a chemiluminescence reaction and an enzyme on immobilized chitosan support membrane, Analytica Chimica Acta, 478(2003) 23–30.

[140] A.G.V. Dachun Yao, Nicholaos P. Evmiridis, Monitoring reactive oxygen species in vivo using microdialysis sampling and chemiluminescence detection as an alternative global method for determination of total antioxidant capacity, Analytica Chimica Acta, 467(2002) 133–144.

[141] C.L. Sun, H.H. Lee, J.M. Yang, C.C. Wu, The simultaneous electrochemical detection of ascorbic acid, dopamine, and uric acid using graphene/size-selected Pt nanocomposites, Biosensors & bioelectronics, 26(2011) 3450-3455.

[142] K. Arora, G. Sumana, V. Saxena, R.K. Gupta, S.K. Gupta, J.V. Yakhmi, et al., Improved performance of polyaniline-uricase biosensor, Analytica chimica acta, 594(2007) 17-23.

[143] R.A. Sheldon, Enzyme Immobilization: The Quest for Optimum Performance, Advanced Synthesis & Catalysis, 349(2007) 1289-1307.

[144] U.T. Bornscheuer, Immobilizing enzymes: how to create more suitable biocatalysts, Angew Chem Int Ed Engl, 42(2003) 3336-3337.

[145] B.D. Malhotra, A. Chaubey, S.P. Singh, Prospects of conducting polymers in biosensors, Analytica chimica acta, 578(2006) 59-74.

[146] J. Kan, X. Pan, C. Chen, Polyaniline-uricase biosensor prepared with template process, Biosensors & bioelectronics, 19(2004) 1635-1640.

[147] Y. Jiang, A. Wang, J. Kan, Selective uricase biosensor based on polyaniline synthesized in ionic liquid, Sensors and Actuators B: Chemical, 124(2007) 529-534.

[148] N.R. D. Nilsson, M. Berggren, R. Forchheimer, Electrochemical Logic Circuits, Advanced Materials, 17(2005) 353-358.

[149] N.J. Ronkainen, H.B. Halsall, W.R. Heineman, Electrochemical biosensors, Chem Soc Rev, 39(2010) 1747-1763.

[150] J.M.W. Younan Xia , Alan G. MacDiarmid , Arthur J. Epstein, Camphorsulfonic Acid Fully Doped Polyaniline Emeraldine Salt Conformations in Different Solvents Studied by an Ultraviolet Visible Near-Infrared Spectroscopic Method, Chem Mater, 7(1995) 443–445.

[151] E. Taqieddin, M. Amiji, Enzyme immobilization in novel alginate–chitosan core-shell microcapsules, Biomaterials, 25(2004) 1937-1945.

[152] S. Kochmann, T. Hirsch, O.S. Wolfbeis, Graphenes in chemical sensors and biosensors, TrAC Trends in Analytical Chemistry, 39(2012) 87-113.

[153] X. Yan, J. Chen, J. Yang, Q. Xue, P. Miele, Fabrication of free-standing, electrochemically active, and biocompatible graphene oxide-polyaniline and graphene-polyaniline hybrid papers, ACS applied materials & interfaces, 2(2010) 2521-2529.

[154] S. Wu, Q. He, C. Tan, Y. Wang, H. Zhang, Graphene-based electrochemical sensors, Small, 9(2013) 1160-1172.

[155] Y. Shao, J. Wang, H. Wu, J. Liu, I.A. Aksay, Y. Lin, Graphene Based Electrochemical Sensors and Biosensors: A Review, Electroanalysis, 22(2010) 1027-1036.

[156] J.H.J. J.Y. Kim, D.E. Lee, J. Joo, Enhancement of electrical conductivity of poly(3,4-ethylenedioxythiophene)/poly(4-styrenesulfonate) by a change of solvents, Synthetic Metals, 126(2002) 311–316.

[157] A.P. Turner, Biosensors: sense and sensibility, Chemical Society reviews, 42(2013) 3184-3196.

[158] Y. Kim, A. Ballantyne, J. Nelson, D. Bradley, Effects of thickness and thermal annealing of the PEDOT:PSS layer on the performance of polymer solar cells, Organic Electronics, 10(2009) 205-209.